

Dynamic Timber

A Practice Oriented Seismic Analysis Workflow for Tall Timber
Structures with Variable Parameters

Annebel van der Meulen

MSc. Architecture, Urbanism, and Building Sciences - Building Technology

Mentors: Simona Bianchi, Michela Turrin

Abstract

For a long time, timber has taken the backseat to steel and concrete for largescale structures, but due to sustainability interests many developments have been made to improve its less desirable qualities. With the introduction of engineered wood products, large timber sections required for fire resistant design became economical and the timber structural behavior became more reliable. However, there are still many challenges when it comes to the seismic design of tall timber structures. Current modelling strategies are time-consuming to implement, provide inconsistent results, and do not account for the passive parameters which impact the seismic behavior of the structure throughout its lifetime. Since timber is a natural material, it is subject to varying levels of moisture content which impacts its stiffness. Furthermore, given the lightweightedness of timber structures (compared to concrete or steel alternatives), any changes to the mass distribution of the structure drastically changes its dynamic response.

This research project develops a computational workflow for the seismic analysis of tall timber structures which integrates the seismic analysis model seamlessly into the main design workflow, simplifies the process for setting the parameters in a semi component-level model for seismic analysis, includes a lifetime analysis option which considers the variables which impact the structural performance of the structure over time, and provides the engineer with component-level data over time. Python class objects are used to develop this computational workflow inside of the Grasshopper environment for Rhino, using the OpenSeesPy library for analysis. It follows the analysis standards provided by the (recent drafts of the) Eurocodes and supporting research papers. It has been developed to align with the most prominent tall timber construction types, as defined through the literature review. The analysis script utilizes the modelling strategy put forth by Rinaldi et al. (2021) to determine the effective stiffness of a cross-laminated timber wall, and its implementation was validated with a comparative analysis to the results of that research. The implementation of the full workflow and its impact on the design process is demonstrated through a case study, with results confirming the importance of including lifetime variables for analysis. This research increases the timeframe of analysis that the engineer can perform on tall timber structures such that the initial structural design can be informed by future predicted events, allowing for more resistant designs.

Keywords: tall timber structures, variable mass, variable stiffness, computational workflow, seismic analysis, life-time analysis

Contents

1	Background	5
1.1	Why Timber?	5
1.2	Challenges and Limitations with Tall Timber Structures	6
2	Research Design	8
2.1	Ensuring Research Validity	8
2.2	Problem Statement	10
2.3	Research Questions	10
2.4	Research Methodology	11
3	Problem Investigation	12
3.1	Trends in Tall Timber	12
3.2	Seismic Design of Tall CLT Structures	13
3.3	Experimental Data & Calculation Strategies	21
3.4	Variable Parameters	23
3.4.1	Time-based Parameters	23
3.4.2	Event-based Parameters	26
3.5	Validation Strategies	27
3.6	Results from Problem Investigation	28
4	Solution Design	29
4.1	Defining the Scope	29
4.1.1	Software Environment	29
4.1.2	Construction Type	30
4.1.3	Material and Component Database	31
4.1.4	Seismic Analysis Parameters Input	31
4.1.5	Variable Parameters	31
4.2	Computational Workflow	32
4.2.1	Materials and Component Database	33
4.2.2	Modelling the Structure	33
4.2.3	Analysis	33
4.3	Validation Design	34
5	Implementation	34
5.1	Materials and Components Database	35
5.2	Model Generation	36

5.3	Analysis	38
5.3.1	Static Linear Analysis	38
5.3.2	Lifetime Analysis	39
5.4	Outputting Data to Excel	40
5.5	Other User Features	40
5.6	Evaluation of Implementation	41
5.6.1	Comparative Study of FE Modelling Strategy	41
5.6.2	Case Study of Implementation	42
6	Conclusions and Reflection	44
7	Resources	46
8	Appendix	50

1 Background

1.1 Why Timber?

Timber structures have numerous benefits for not only the planet but also the individual. Various studies have concluded that if a forest is responsibly managed, wood is a carbon-neutral material (Laguarda Mall et al. 2015). This is due to the carbon sequestration process where photosynthesis turns carbon dioxide into biomass. According to Puettmann et al. (2005), each cubic meter of wood stores around 1.10 tons of CO₂. Additionally, the usage of natural materials within buildings has been related to improved health in building occupants (Foster et al. 2020), owing to a biophilic response in which people equate natural materials with experiencing nature itself.

For millennia, timber has been the preferred building material as it was affordable, plentiful, and had an impressive strength-to-weight ratio. It wasn't until the inclusion of stricter regulations for structural design that timber began to become impractical for large-scale structures, leaving the market to steel and concrete. While wood can be exceedingly strong, it has inherent structural heterogeneity due to its anisotropy and deformations. Design specifications often require engineers to design to the lower fifth percentile of a material's tested strength, hence timber constructions are frequently not designed to their full potential (Foster & Ramage, 2020). Furthermore, the intrinsic combustibility of wood presents another issue. While larger sections of timber can protect the core with their natural charring ability, they are difficult to dry out uniformly, resulting in warping and cracking. Furthermore, large sections of solid sawn timber must be sourced from large trees, making the material less economical and sustainable.

To address these issues, researchers began looking for a way to produce large cross sections of timber

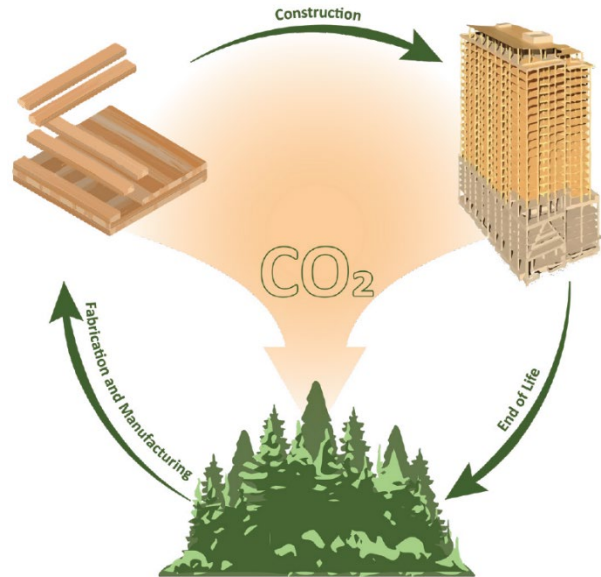


Figure 1.1 Life cycle of cross-laminated timber for responsibly managed forests

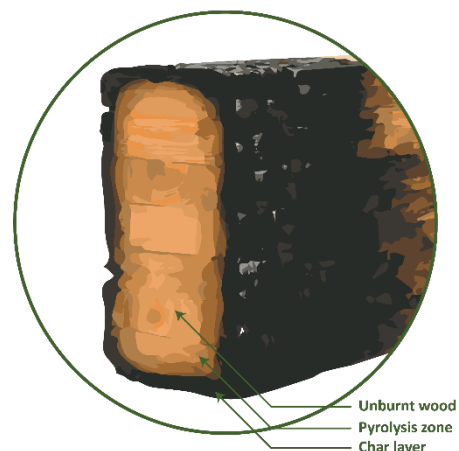


Figure 1.2 Diagram showing charring nature of timber

economically. Since design standards only allow engineers to utilize the lower fifth percentile of tested strength values, designing timber with more homogeneity will boost design strength (Foster & Ramage, 2020). Mass timber products employ a range of tactics to reduce material variability, mostly centered around the idea of using smaller pieces to build up large sections. Glue laminated timber (glulam) glues solid sawn lumber pieces on top of and parallel to each other to build up large cross-sections. This became an economical timber option for long-span uniaxial bending applications

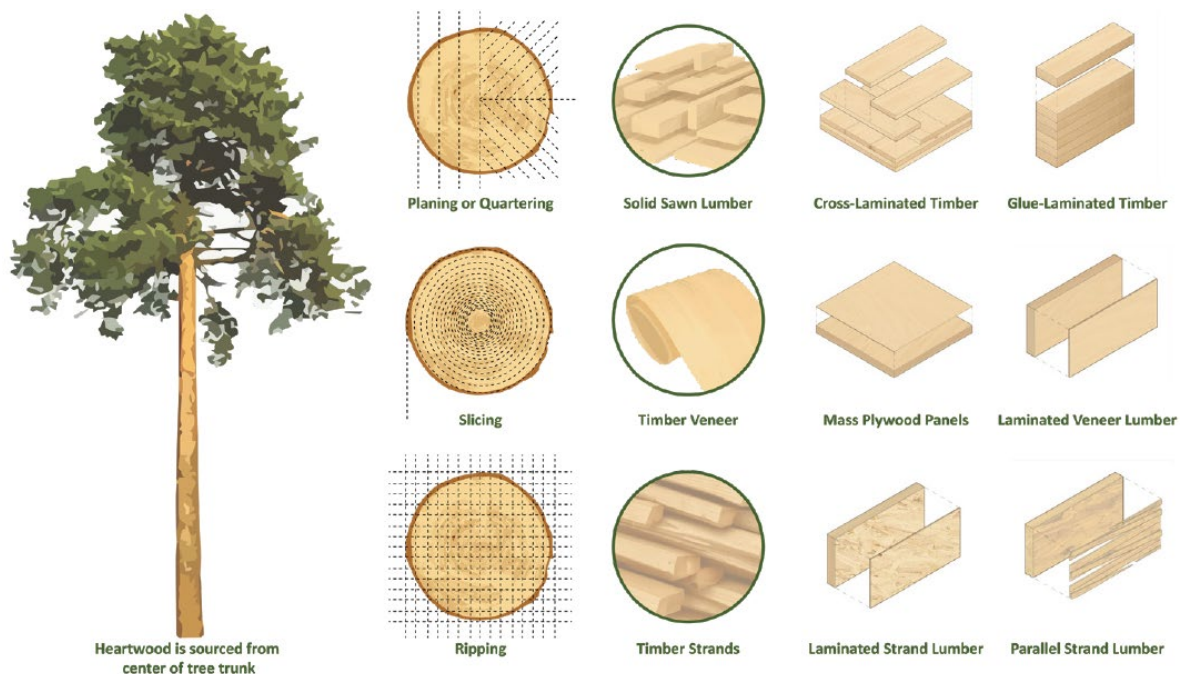


Figure 1.3 Example of various engineered wood products

like beams, trusses, and tall columns subjected to buckling. Cross laminated timber (CLT) glues solid sawn lumber pieces in layers perpendicular to each other to create mass timber panels capable of resisting loads in two directions. This product is suitable for large (two-way) spanning floors and load bearing (shear) wall applications. Other common products include parallel strand lumber (PSL), laminated veneer lumber (LVL), and mass plywood panels (MPP).

1.2 Challenges and Limitations with Tall Timber Structures

With these mass timber products on the market, large-scale timber structures were once again feasible, economical, and safer than ever. So, what's the hold-up? Gonzalez et al. performed a wholistic review of the advancements and limitations of multi-story timber structures by reviewing 266 research articles on the topic (2022). It was determined that cross-laminated timber products have been developed to the point where they are considered both an economically and environmentally sustainable alternative to

equivalent steel and concrete structures. However, there is still a large lack of knowledge and trust in the materials over time, particularly when considering fire risk, dynamic loads, and moisture.

Unfortunately, the vision of timber structures up in flames had been burned into the public's minds. To address this, research on how fire spreads through a mass timber structure is required to inform both the standards for structural design and the computational modelling methods used to predict fire behavior. Current fire modeling methodologies for timber structures only include compartment

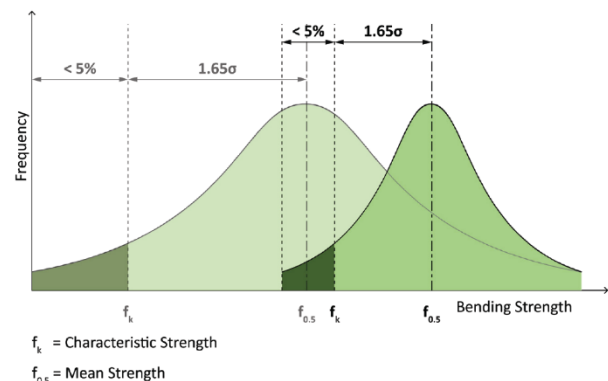


Figure 1.4 Diagram showing of how changing the distribution of tested values improves the design strength of the material

fires, which begin in one room (compartment) of the building that is thermally divided from the next (Mitchell et al. 2022). Philion et al. (2022) devised a modelling strategy for open plan timber structures to explain the behavior of each member in the room under various heat fluxes, flame spread rates, and extinction rates; more data is needed to improve the modelling accuracy. Mitchell et al. (2022) also emphasizes the importance of large-scale tests to establish timber performance in the presence of fire, so that these models are more realistic.

How these multistory timber structures behave under lateral and cyclic loading conditions is also not well understood. While recent research has greatly focused on the seismic design and behavior of multi-story buildings (particularly at the connections), there is still a large knowledge gap in how the interaction between components contributes to the global behavior of the structures (Gonzalez et al. 2022). Furthermore, practice-oriented modelling strategies for seismic analysis are few and often limited in applicability because of the specific testing data required to accurately calibrate them (Pozza et al. 2017). An additional level of complication is that the lightweightedness

and susceptibility to deterioration of timber structures make the system susceptible to changes in mass and stiffness, and consequently seismic behavior (Yan et al. 2023). For example, if the occupancy and thus the interior finishings changes, the impact on the weight distribution of a timber structure is far greater than it would have been on a heavier steel or concrete structure. The stiffness could change too, either due to deterioration of the material or if the connections are retrofitted in the future. This means that even after the engineer successfully models the seismic behavior of the tall timber structure, the model will likely be out of date shortly after construction.

An ever-present variable which impacts the mechanical properties of timber is moisture. Timber is inherently hygroscopic, so water will absorb and evaporate depending on relative humidity and temperature. The material volume changes as moisture enters and exits the wood, resulting in induced stresses and degradation within the timber. Engineered wood products exhibit increased variability in their response to moisture due to the rearrangement of the lamella structure, and physical changes to the wood can impact glue integrity between layers. The moisture

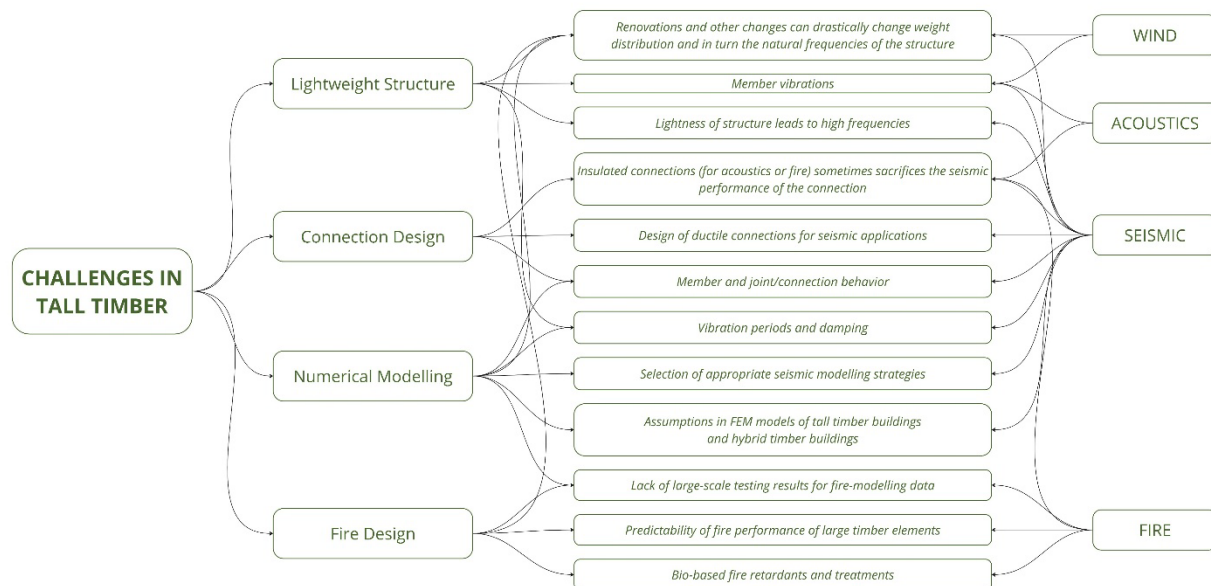


Figure 1.5 Common challenges with tall timber structures

content of the timber when it arrives to site, the weather conditions of when the timber was installed and exposed, the interaction between timber and curing concrete, the humidity within the building once operating, and the façade and foundational detailing all impact how the timber will deteriorate overtime due to moisture penetration (Schmidt and Riggio 2019).

2 Research Design

2.1 Ensuring Research Validity

To ensure that the design, implementation, and presentation of this engineering research is valid, the conceptual framework laid out by Wiering and Heerkens (2006) will be utilized. This paper separated research problems into knowledge problems and world problems. A knowledge problem is that which addresses a lack of knowledge about the world, existing in the researcher's mind. If this knowledge problem is then investigated and presented via the research cycle described in this study, the results can be

considered valid. A world problem is a difference between the way that the world is and the way that the researcher thinks that it should be; this is usually where an engineering problem lies. The engineering cycle can be used to investigate and validate the results of this type of research problem.

In the case of this present research, the problem being investigated is a world problem. To properly address this world problem, the following five concepts must be defined:

- 1) **Phenomena:** the entity of the problem that will be addressed
- 2) **Norms:** the desired values, goals, what we want the phenomena to achieve
- 3) **Relationships** between norms and phenomena: this is achieved with indicators or criteria
- 4) **Stakeholders:** defining the stakeholders will define the norms and their relationships to the phenomena

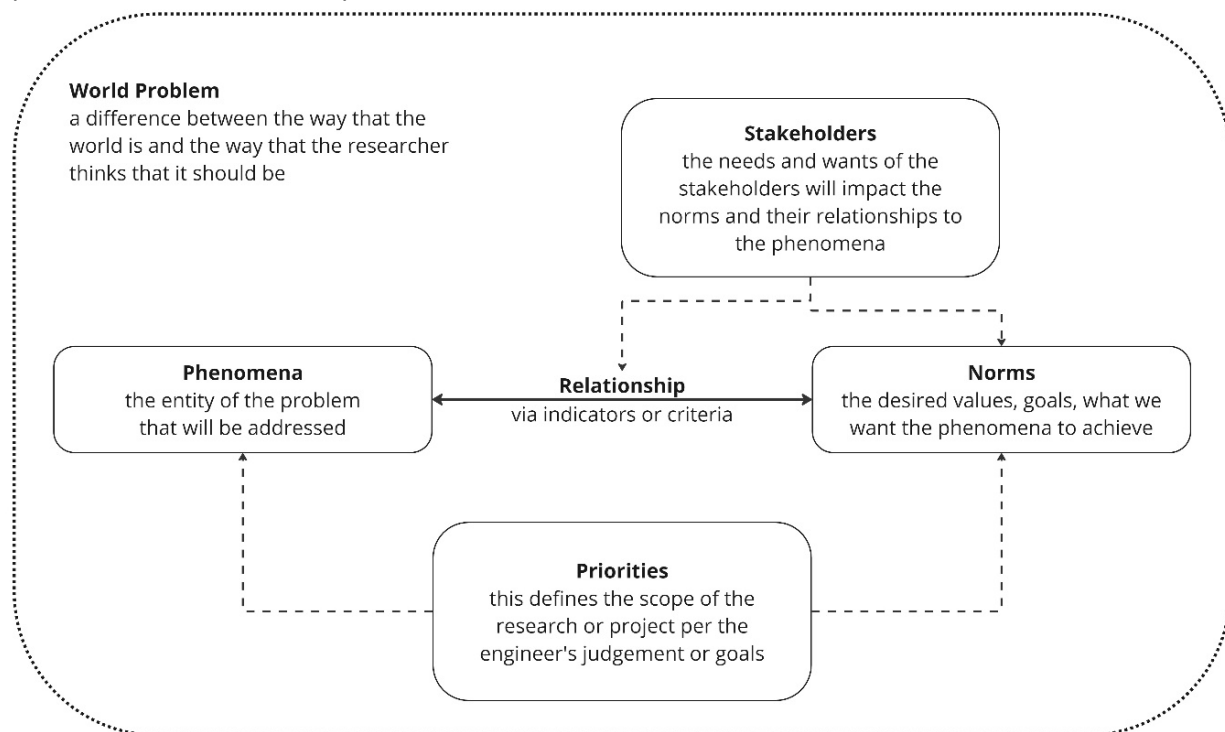


Figure 2.1 World problem definition and parameters

- 5) **Priorities:** defining the scope per the engineer's judgement or goals

To solve a world problem, the engineer will often also need to address some knowledge problems before getting started. To properly address these knowledge problems, the following five concepts must be defined:

- 1) **Phenomena:** which phenomena are to be observed
- 2) **Variables:** the measurable properties of these phenomena
- 3) **Relationships** among variables: casual or statistical
- 4) **Research questions:** the knowledge problem is operationalized into research questions, often with related sub-questions
- 5) **Priorities:** the priorities of the researcher should be clearly defined

These parameters, if not already known, will be defined via the problem investigation stage of the research cycle. This involves understanding the problem itself by answering the who, what, where, why, and how we want to know this information. After the problem is well understood, the research

design will state what is to be observed through research and how. Referring to the research questions, it can be decided how these questions might be answered, such as via literature review, laboratory work, or case studies. A measure of validity must be determined in the next stage, to ensure that the research work described in the research design phase is valid. Three kinds of validity are typically used for research questions:

- **Construct validity:** have the concepts being researched been appropriately operationalized into observable variables?
- **Internal validity:** are the claims being made directly from observations?
- **External validity:** are the claims being made about the research population valid to be generalized to the entire population?

Once a validity measure has been defined for each research method, the research is conducted and the results are evaluated to determine if the research questions have been answered satisfactorily.

To begin the engineering cycle, the engineer needs to identify the causal relationships between the

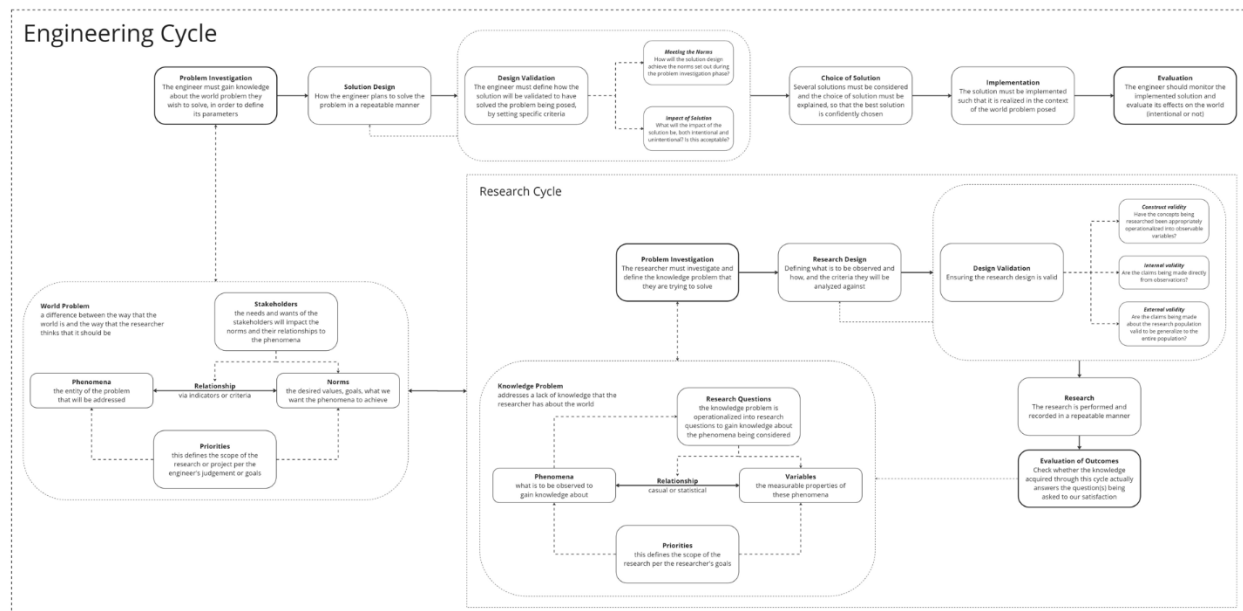


Figure 2.2 Diagram of the engineering cycle

defined norms and phenomena. Once this is defined, the engineer can begin designing a solution. Through this, they must identify the source of the solution (whether it is borrowed, adapted, or totally new) and the specifications of the solution (within what scope the solution is designed for). The design validation phase of the engineering cycle is purely defining the criteria that the solution must meet to be considered successfully solving the world problem being addressed. For example, if the problem is that current simulation strategies take too long to run, the design validation might be that the solution design completes the simulation faster than other methods. The choice of the solution must be addressed as well, in terms of why this solution method was chosen over other alternatives available, such that this solution can be determined as the best solution for the problem being addressed. Finally, the solution must be implemented, and the implementation must be evaluated.

The relevance of the solution to the world problem (likely supported by knowledge problems) must be discussed by addressing three key points: the novelty of the solution, its applicability to current practices, and its contribution to current knowledge. If the engineering research conducted is designed, implemented, and presented as described above, the research can be considered valid and thus can be used by future researchers to build upon.

2.2 Problem Statement

Current practice-oriented seismic design and analysis methods for tall timber structures do not provide sufficient data for how various components behave over the structure's lifetime. To achieve this, a (semi)component-level modelling approach is required so that the impact of stiffness and mass changes on the components can be analyzed. However, the experimental data used to calibrate this kind of model is construction

specific, and a cohesive database of current results does not exist. Furthermore, the seismic analysis of the structure is typically done in an environment separate from the main design workflow.

The above points can be summarized in the following problem statement which is addressed by the present research:

Current practice-oriented seismic analysis methods for tall timber structures are isolated from the main design process, complex to implement, and do not consider variability of parameters over the structure's lifetime.

2.3 Research Questions

The problem investigation stage of the engineering cycle is used to answer the knowledge problems required to begin the solution design of the world problem. The world problem being addressed in this research can be operationalized into the following question:

How can a practice-oriented computational workflow for the seismic analysis of tall timber structures be streamlined and integrated into the main design workflow while accounting for variability in the structure over time?

The following supporting research questions will also be investigated via literature review to inform the main research question:

- 1) What are the trends in tall timber construction?
- 2) What are the existing (practice-oriented) methods for designing tall timber structures under seismic loads and what are their limitations?
- 3) Which variable phenomena impact the structure's seismic performance over time?

The following questions will be investigated via computational design:

- 4) How can a practice-oriented seismic model utilize (semi)component-level experimental data?
- 5) How can these variable phenomena over the structure's lifetime be integrated into the initial analysis?

The following question will be investigated via a comparative analysis:

- 6) How does the developed modelling strategy and its results compare to that of previous researchers?

The following question will be investigated via a case study:

- 7) What is the impact of variable phenomena on the seismic behavior of the tall timber structure?
- 8) How does this computational workflow impact the analysis process and decision making of the engineer?

2.4 Research Methodology

The above research questions will be answered with four different research methods: a literature review, computational design, comparative analysis, and a case study.

Literature Review

Problem investigation was completed via a literature review, utilizing a snowballing method. It began by reviewing other current wholistic literature studies for trends in tall timber construction around the world and the current research areas. These papers included a wholistic review of tall timber structures (Gonzalez et al. 2022), a literature review to determine main design considerations in tall timber structures (Ilgin 2023), and a review of the seismic behavior of tall cross-laminated timber structures (Izzi et al. 2018). This provided a good overview of what the field currently looks like, providing this research with key terms to be used when narrowing the scope. It

also provided a list of credible resources to begin diving deeper into specific areas of research.

Through this initial literature review, the trends, existing practice-oriented seismic modelling methods, and phenomena which impact the stiffness and mass of tall timber structures were identified. This informed the scope and goals of the project. This initial literature informed the scope and goals of the project, serving as the basis for the more specific literature review that was then conducted throughout the solution design and implantation phases of the research. This included collecting experimental data and identifying factors to be used for the seismic analysis.

Computational Design

Computational design methods were used to develop a computational workflow for a practice-oriented model for the seismic analysis of tall timber structures. The workflow utilizes a modular approach to break the several steps of the analysis into smaller chunks, which can be rearranged according to the engineer's needs for analysis. This also allows for the integration of future developments in the workflow, so that a future user can add upon the workflow to their preference. These modules have different isolated functions, including extracting information from the database, building the wall, floor, and structure class objects for analysis, conducting the static linear analysis, copying and modifying the structure based on lifetime variables, and outputting the relevant data into a usable format for post-processing.

Comparative Analysis

A comparative analysis is conducted to test the accuracy of the modelling strategy used to calculate the effective wall stiffness. This is completed with a direct comparison to the results of the modelling strategy which it is based on (Rinaldi et al. 2021). The mesh size was calibrated to most closely match the results of the study.

Case Study

A case study will be modelled with this computational workflow to demonstrate its capabilities. If an existing structure is utilized as the case study model, then the results of the lifetime analysis of the structure could be compared to the current state of the structure. It will have to be investigated whether an appropriate structure exists for such a comparison, while still demonstrating the other aspects of the tool.

3 Problem Investigation

Problem investigation was completed via a literature review. It began by reviewing other current wholistic literature studies for trends in tall timber construction around the world and the current research areas. These papers included a wholistic review of tall timber structures (Gonzalez et al. 2022), a literature review to determine main design considerations in tall timber structures (Ilgin 2023), and a review of the seismic behavior of tall cross-laminated timber structures (Izzi et al. 2018). This provided a good overview of what the field currently looks like, providing the research with key terms and a narrowing of the scope. It also provided a list of credible resources to begin diving deeper into specific areas of research.

3.1 Trends in Tall Timber

For the purposes of this research, a tall timber structure is over eight stories tall and has both its primary vertical and lateral structural components made entirely out of timber (excluding the concrete podium, which as of this study all tall timber structures included). This definition is adopted from Hüseyin Emre Ilgin, who conducted a wholistic review of trends in timber construction through 49 case studies from all around the world (Ilgin 2023). It was determined that thanks to its well managed forests, 56% of tall timber structures are in Europe (primarily in Nordic nations). Nearly two-thirds of tall timber structures are designed for

residential functions because the structural system creates divisions appropriate for residential use. A centralized core accounted for 63% of the timber structures, providing efficient load distribution and equidistance egress routes. Two-thirds of timber structures are designed with a prismatic form such that it is simple to construct, efficient in space usage, and cost-effective. Most tall timber structures were timber-concrete composite structures thanks to the inclusion of a concrete core to minimize wind sways. In seismic zones, timber-steel composites were most prevalent. Most interestingly though, in Europe full timber structures were preferred (reminder, every tall timber structure investigated has a concrete podium). Finally, the preferred structural system was the shear frame system. This marries the rigid frame system with the shear wall system, where the rigid frame limits deflections in the upper levels while the shear walls limits deflections in the lower levels.

Through this study, it was also determined that out of all the engineered wood products on the market, cross-laminated timber (CLT) was the most prominent in production (Ilgin 2023). This was due to its low carbon emission, high thermal insulation value, and exceptional structural stability and capacity for in-plane and out-of-plane loads. Today, CLT is cost-competitive and more environmentally sustainable than traditional materials in many markets (Gonzalez 2022). However, most building standards do not have prescribed guidelines for tall timber structures yet (Ilgin 2023). The Canadian standard CSA O86:19 (Engineering design in wood) was the first structural code to introduce instructions for the seismic design of CLT buildings, as well as other engineered wood products, as of 2019 (Izzi et al. 2018). The most recent draft of the Eurocode has standards for design of tall timber structures, but these are not yet approved. Furthermore, when compared to experimental research, the guidelines for the seismic design of CLT structures significantly overestimate the stiffness of connections when compared to



Figure 3.1 The scope of the workflow to be developed

experimental data (Pozza 2017). Thus, engineers must rely on the experimental values for design of tall CLT structures, and as the production of CLT becomes more regulated these experimental results become more plentiful and applicable.

Defining the Scope for Further Research

The above research defines the scope for researching the more detailed questions. Since cross-laminated timber (CLT) is the most prominent mass timber product on the market, this material is the focus of seismic design research. Studies which follow the Eurocode standards are prioritized since most tall timber construction is occurring in Europe. However, since the Eurocodes do not have an approved standard which considers engineered wood products, a large portion of the literature review will need to focus on collecting experimental results and understanding the experimental strategies used. While concrete cores and concrete podiums were the trend, the interaction between the concrete elements and CLT walls was not further investigated due to added complexity and workload. Free form timber structures and non-centralized core plans are out of scope for this project, as these are less common and would require more specific research than is available. A deeper investigation into existing knowledge on

the structural behavior and modelling strategies of shear-frame systems began but soon revealed that this structural system would be too complex to simulate within the context of the project. Thus, the shear wall system was instead researched in further depth to be used within the computational workflow.

3.2 Seismic Design of Tall CLT Structures

As was briefly summarized in the introduction to this paper, several research topics exist for the seismic application of tall timber structures, but all primarily focus on the material strength and durability of timber (Ilgin 2023). For the seismic analysis of tall timber structures, most advancements have been made in the understanding of the behavior of structural panel elements, the effectiveness of different hybrid systems, structural modelling and experimental tests, and connection design (Gonzalez 2022). Connection design is its own research topic but has significant cross-over with the topic of seismic design. Relevant advancements include panel-to-panel connections, the connections of hybrid building designs, the durability and protection of the timber at the connection, and the performance of connections during and after fire events

(Gonzalez 2022). So far, the biggest limitation of these two categories has been properly modelling structural interactions between components at the connections such that its impact on the global response of the structure is captured (Gonzalez 2022).

Finite Element Method

CLT structures can be modelled via the finite element method where the timber panels are assumed to behave elastically (linear behavior) and the connections behave plastically, accounting for the non-linear behavior of the structure (Izzi et al. 2018). The finite element method (FEM) is used to obtain approximate solutions of equations governing a continuous system by splitting the body being analyzed into a collection of small elements, a process called discretization. There are hundreds of element types, and the best one to use will depend on the problem being solved and the desired output. However, they can be split into three different types as line (1D), surface (2D), or solid (3D) elements (The Efficient Engineer 2021). Furthermore, these elements can then be modelled with only nodes at the ends of the element edges (linear or first-order elements) or with additional nodes at the middle of the edges (quadratic or second-order elements). These elements are then connected via their nodes to create the finite element mesh.

The nodes within the finite element mesh must then be defined with their degrees of freedom,

stored in a vector list of all degrees of freedom. A vector list of the same length must also be created with the parameters which is impacting on these degrees of freedom (such as force or heat). A matrix then defines the resistance that the nodes have to the impacting parameter. For example, when using the FEM for a structural analysis, Hooke's law is used to define these relationships where the acting force is equal to the stiffness multiplied by the displacement of the element:

$$F = -kx$$

Where:

F = force

k = stiffness

x = displacement

For a finite element analysis (FEA) of a structural element, the element will be discretized and then the nodes, their deflections, and their stiffnesses would be defined as:

$$\{f\} = [K]\{u\}$$

Where:

$\{f\}$ = force vector

$[K]$ = stiffness matrix

$\{u\}$ = displacement vector

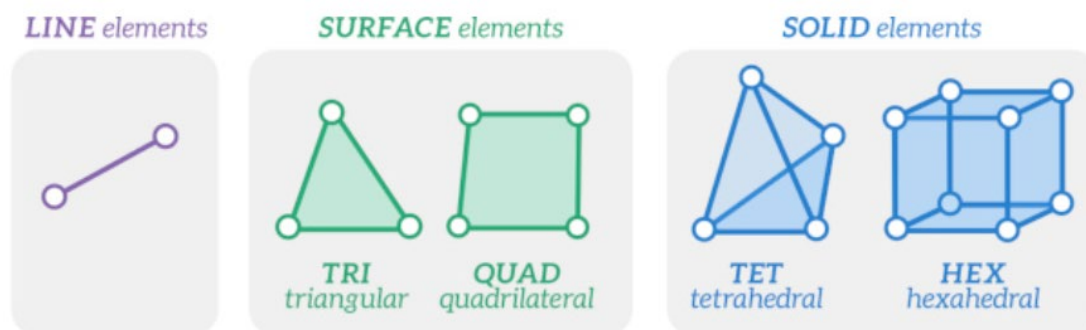


Figure 3.2 Examples of finite element types (Source: YouTube, The Efficient Engineer, 2021)

In this case, the displacement vector represents the degrees of freedom in the structure, the force vector represents the parameters impacting the structure, and the stiffness matrix represents the resistance the structure has to those forces.

Typically, the element stiffness matrices for different element types are defined in the FEA software being used – they don't need to be derived by the user. The element stiffness matrix for a specific element is derived from the equilibrium equations that govern the behavior of that element. Ideally the stiffnesses can be expressed in strong form with differential equations, which will yield an exact solution when solved with the direct method. However, for more complex problems, the equations will be expressed in weak form with integral equations, which will yield approximate solutions. This can be far simpler to solve than the direct method though, either via the variational method or the Galerkin method of weighted residuals and thus can be preferable for large problems. Once the stiffnesses for each element is defined, the element stiffness matrices must then be constructed based on the element connectivity to each node. Then, these element matrices can be constructed into the global stiffness matrix $[K]$ to represent the stiffness of the entire structure, and the global FEM equation can be constructed.

The global FEM equation describes the relationship between the forces and moments acting on all the nodes in the mesh, the degree of freedom (ie. displacements or rotations) at all nodes in the mesh, and the global stiffness matrix. All known nodal forces and boundary conditions must be inputted into the force vector and displacement vector, respectively, before beginning to solve, including zeros. The next step is to solve the equation, which can be done directly by inverting the global stiffness matrix if the model is not too large or sparse (lots of zeros). Otherwise, iterative methods are more practical, where the displacement vector is approximated iteratively

until the difference between the calculated forces and the actual forces is minimized (perhaps via the conjugate gradient method). To summarize, the finite element method for structural analysis consists of these steps:

- 1) **Defining the Problem:** The problem is defined, which includes defining the body being analyzed, its material properties, and the loads and boundary conditions acting on it.
- 2) **Discretization:** The body is discretized as a collection of nodes and elements to create a mesh.
- 3) **Define the Element Stiffness Matrix:** For each element in the mesh an element stiffness matrix is defined that describes how the nodes of the element will displace for a set of applied loads.
- 4) **Assemble the Global Stiffness Matrix:** The element stiffness matrices for all the elements in the mesh are assembled to form a global stiffness matrix based on how the elements are connected.
- 5) **Define the Global FEM Equation:** The global FEM equation that describes how all the nodes in the model will displace for a set of applied loads is defined based on the global stiffness matrix.
- 6) **Solve:** The global FEM equation is solved using computational methods based on the applied loads and boundary conditions that have been defined. This provides the translations and rotations at each node of the mesh.
- 7) **Post-Processing and Validation:** Strains, stresses and other desired outputs can be determined based on the calculated nodal displacements.

Practice-Oriented Finite Element Modeling Strategies for CLT Structures

The most critical considerations influencing the design of the tall timber structure is the structural design and system, but the structural modelling

strategies are currently separated from the main design workflow. This is a limitation because the speed at which the design can come to fruition is greatly reduced due to constant back and forth between stakeholders (Gonzalez 2022). Current CLT structural behavior model results still greatly depend on the modelling approaches used; thus the findings are still unreliable for general applications. They require in-depth analysis, which is usually more easily done when separated from the main design workflow.

While there is not a standardized modelling strategy established yet, there are some common trends. It is generally understood that in CLT structures, the mechanical connections are designed to dissipate energy while the CLT panels behave elastically. The in-plane behavior of these panels is categorized as sliding, rocking, or panel deformation, and should be properly represented in the model as they each contribute to the structural deformation in different ways. The interaction between panels or with the foundation remains a challenging aspect of modelling CLT structures for seismic analysis, with phenomena such as friction, overstrength, or other second-order effects being difficult to capture. Furthermore, for the modelling of connections, the complex implementation of non-linear procedures and the need to input several mechanical

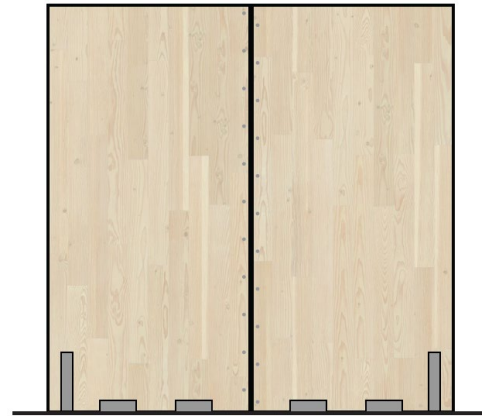


Figure 3.3 Multi-panel CLT wall construction

parameters make many current modelling strategies more suitable for research rather than for design and practice (Rinaldi et al. 2021).

Practice oriented finite element modelling strategies for CLT wall panels can be categorized as either the frame model approach or the 2D model approach. For the frame model (also known as a truss model), two horizontal line elements create a hinged frame to represent the perimeter of the CLT wall, and a diagonal truss link is used to represent the lateral stiffness of the panel due to bending and shear deformation (Rinaldi et al. 2021). The 2D model (or a surface model) models either the individual layers of the CLT panel with their appropriate orientations and material properties, or as one surface with equivalent mechanical properties (Rinaldi et al. 2021). As mentioned

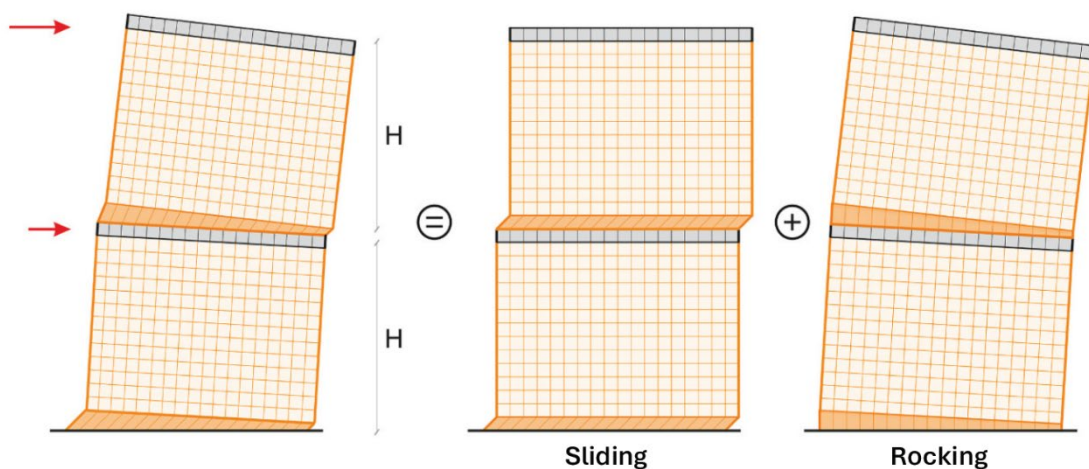


Figure 3.4 Combined deformation effects of CLT walls (Rinaldi et al. 2021)

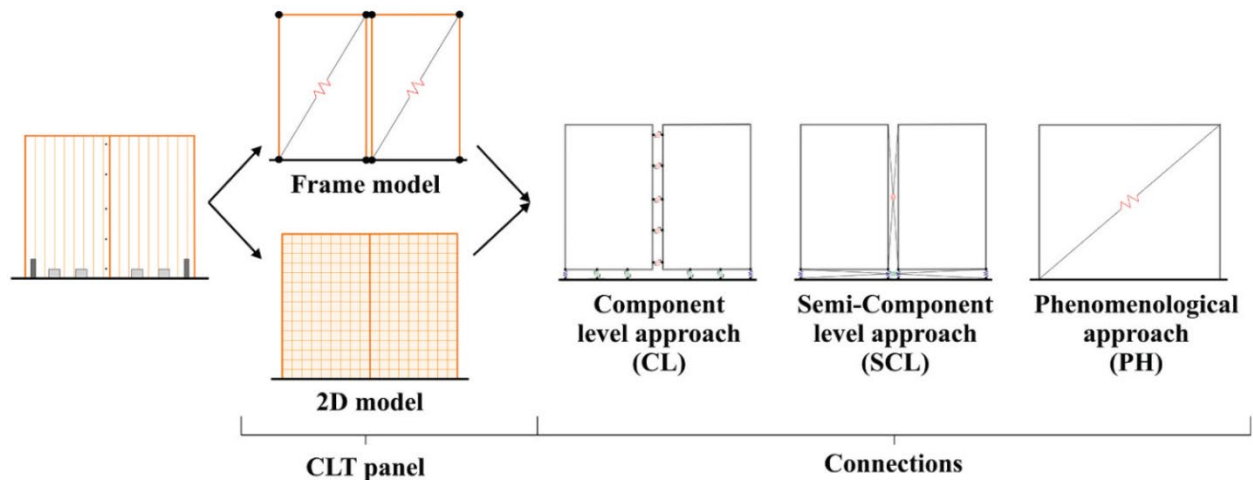


Figure 3.5 Summary of various modelling strategies for CLT walls (Rinaldi et al. 2021)

previously, the mechanical properties of the CLT panels must be either determined via reference equations or obtained from previous reference studies such as that performed by Bogensperger et al. (2016), Blass and Fellmoser (2004), or Flaig and Blass (2013).

Practice oriented finite element modelling strategies for the connections of CLT structures can be categorized as component level, semi-component level, or phenomenological

approaches. The component level approach utilizes an individual spring element for every connection (Rinaldi et al. 2021) to reproduce the structural response of each component within the structural system (Pozza et al. 2017). A semi-component level approach models the properties and deformation contribution of multiple connections of a wall into one single link element, which helps reduce computational power (Rindali et al. 2021). A phenomenological approach models only the CLT panels with adjusted mechanical

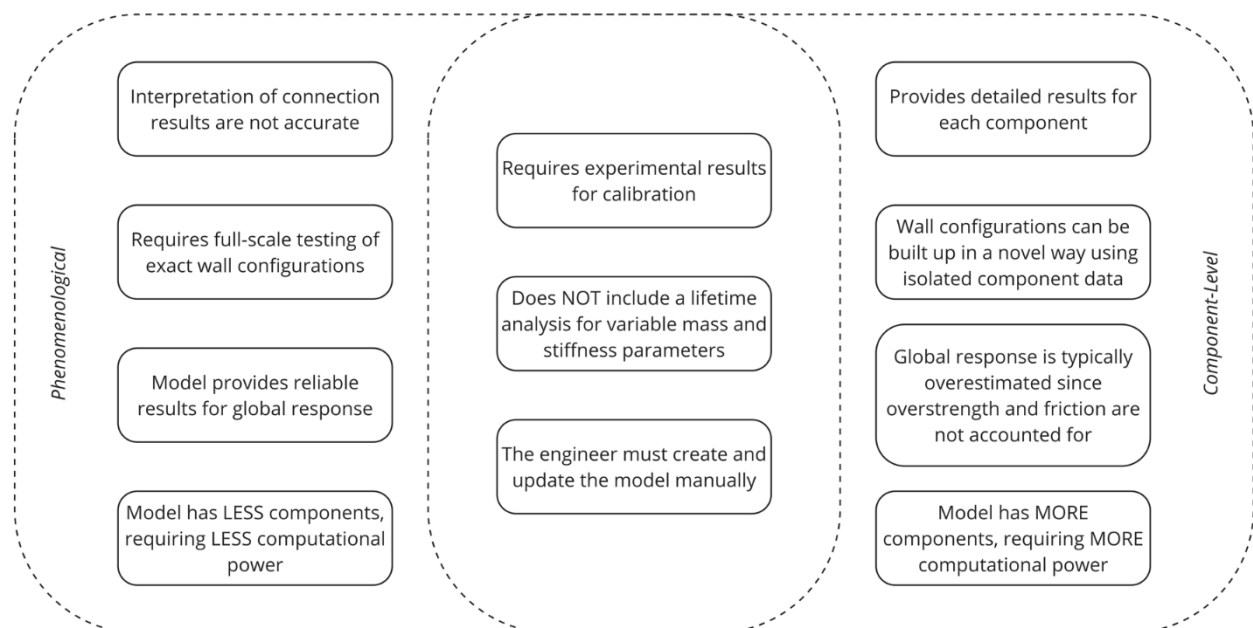


Figure 3.6 Comparison between phenomenological and component-level modelling approaches

properties which account for the effects from the connections.

The research conducted by Pozza et al. (2017) provides a thorough comparison between component-level and phenomenological modelling approaches for both linear and non-linear analysis strategies. Both modelling strategies require experimental data to calibrate the structural behavior of the model. The component-level approach utilizes isolated component test data to build its structural system, allowing the designer to create their desired wall configurations. However, this data neglects second order interaction and coupling effects which impact the global response of the CLT structure. The phenomenological approach accounts for global effects because it utilizes experimental data for wall configurations exactly matching that which is to be modelled, but this is quite limited for general modelling. A hybrid approach addresses the limitation of component-level modelling by calibrating the global response of a component-level model to the experimental data of a matching wall configuration, but this remains with the same limitation of the phenomenological approach.

To compare the modelling strategies under linear analysis, the phenomenological model was calibrated to match the displacements of the component model. This resulted in each model providing similar global results, but the uplift forces at connections was significantly overestimated by the phenomenological model. For non-linear analysis, the component and phenomenological models were both calibrated to match the experimental data for the components and global response (provided by Gavric et al. 2015). This was done by optimizing the parameters of the Pinching4 constitutive law to minimize the difference between the dissipated energy in the numerical models and the experimental data. The results suggested that a component modelling approach with biaxial forces (ie. shear and tension forces simultaneously acting on connections) and the phenomenological approach both were sufficient modelling strategies for non-linear analysis. However, the component approach did not account for overstrength or the coupling effects, thus the uplift deflections were consistently overestimated while base slips were overestimated for low amplitudes and underestimated for high amplitudes. Thus, the

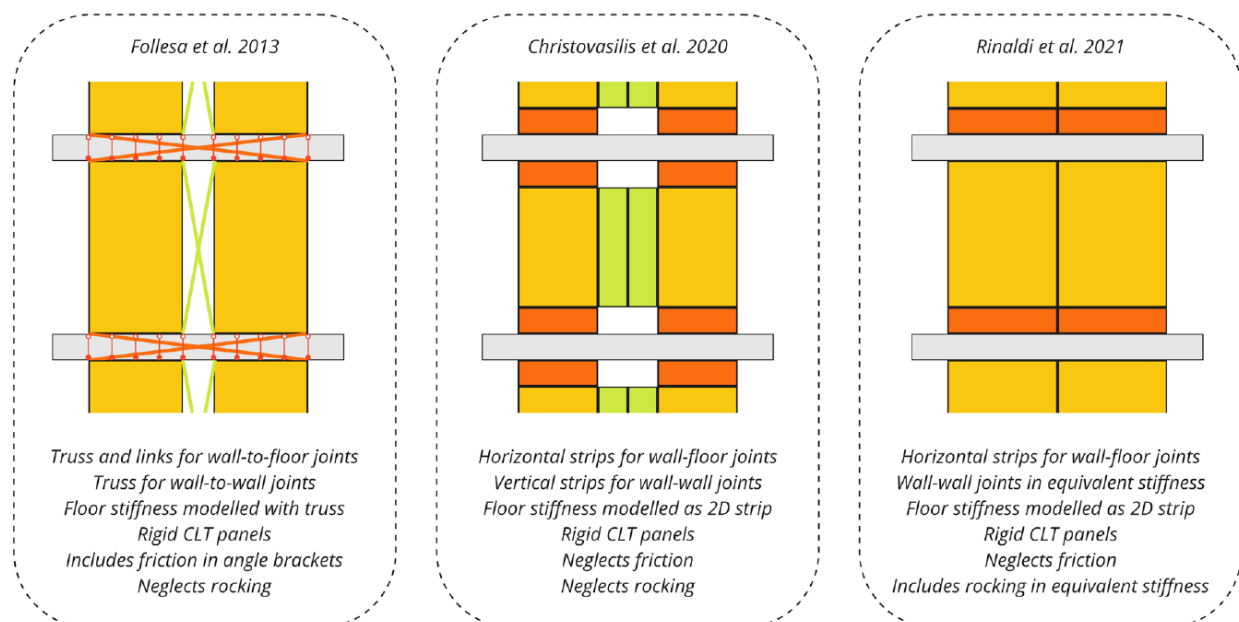


Figure 3.7 Comparison between proposed modelling strategies from previous researchers

inclusion of these factors is vital for accurate modelling.

The modelling strategy put forth by Rinaldi et al. in 2021 could be categorized as a semi-phenomenological modelling method for static linear analysis, in that it utilizes 2D elements rather than springs to model all the connections as one element. This is done by splitting the CLT wall panel horizontally some distance from the floor, creating a horizontal “connection” strip in which the connection properties can be represented. This strategy is an upgraded version of the modelling strategy put forth by Christovasilis et al. in 2020, which did not account for the deformation contribution from the rocking behavior of the CLT walls (Rinaldi et al. 2021). Comparing the lateral stiffnesses of both Rinaldi’s and Christovasilis’s model to a conventional component-level model, Rinaldi’s version produced deflections more like the conventional model, especially in cases without vertical loads where the rocking behavior of the wall is more likely activated (Rinaldi et al. 2021). Furthermore, this modelling strategy did not involve a calibration step and rather compared the model results of a wall configuration to a full-scale test of the same wall configuration provided by Gavric et al. (2015). The experimental results show intrinsic randomness, and the model results were similarly scattered and therefore the modelling strategy could be considered reasonably accurate, especially for multi-panel wall configurations (Rinaldi et al. 2021). More detailed information on this modelling strategy can be found in the Appendix.

Existing Finite Element Modelling Software

SAP2000 has been considered the state-of-the-art analytical modelling software since it was first introduced 30 years ago. It provides a versatile and intuitive user interface and provides the engineer with a wide range of analysis and design options. However, to integrate with design modelling software used by other roles in the project (such as REVIT or Rhino and Grasshopper), additional steps

must be taken with third-party software or plug-ins. Both Revit and Rhino/Grasshopper geometry can be converted into the Industry Foundation Classes (IFC) format, which can then be imported into SAP2000. For Revit, the model can be imported into ETABS and then saved as a SAP2000 model from there. Else, various plug-ins and supplements are an option. This back and forth between software spaces is time consuming and not ideal for a streamlined design process where the finite element analysis results highly impact the overall design of the structure. Especially if the goal is to analyze and adjust the design of the structure over a lifetime analysis. Thus, a plug-in which can be used in the same environment as the main design process could be beneficial.

FEM-Design, on the other hand, is highly integrated into the design software environment. It has an add-in for Revit which enables two-direction communication between Revit and FEM-Design, and an application programming interface (API) for Grasshopper, allowing for seamless integration. Furthermore, it has various design modules which can be used to solve material specific structural analysis problems, including timber design and CLT design. It also has many options for the seismic analysis of structures according to various building standards. However, the generation of the finite element model from general geometry is not automatic and must be created by the engineer prior to running analysis.

OpenSees, or the Open System for Earthquake Engineering Simulation, is an object-oriented, open-source software framework which allows users to create finite element computer models for simulating the structural response under earthquake loads. Originally developed by Francis Thomas McKenna as part of a doctoral degree at UC Berkeley in 1997, this software framework has remained opensource and free to use and expand upon to ensure the relevance and functionality of the framework. Previous object-oriented analysis frameworks would construct one single analysis

object to perform the analysis. OpenSees breaks down the analysis object into separate objects that are simpler to interpret and edit by the engineer. This modular approach offers great flexibility as the analysis type can be changed by changing any of the constructor objects and allows for extensive analyses to be performed with multiple subclasses. Though originally developed for C++, a library for python, OpenSeesPy, is now available.

Shear-frame system

For high-rise structures, most used structural systems include frame systems, shear wall systems, and a combination of the two called shear-frame systems (Wang 2020). Frame structures are less rigid and require large cross-sections for tall timber applications. Shear wall systems are more material efficient for tall timber applications but require the walls to be close together leaving little room for flexibility in the structure's floor plan. When combined in a hybrid system, the shear walls are far more rigid than the frame and thus act as the first line of defense against lateral loads. At the bottom of the structure, the shear walls deform less and help to constrain the deformation of the frame elements. Conversely, at the top of the

structure where the shear walls deform further, the frame can begin bearing some of the shear force as well. This combined effect utilizes the high ductility of the frame system and the high seismic performance of the shear wall only where it is advantageous, allowing for sparser use of shear walls and smaller frame elements in lower demand areas. It's important to note that for the frame and the shear wall to work together properly, the floor must be assumed to have infinite stiffness, ie. it should act as a rigid diaphragm (Wang 2020).

The load flow through the system needs to be well understood to accurately model this system. The gravity loads are transferred through the floor to the beams and columns of the frame. The shear walls are also load bearing walls, so gravity loads from the floor are also transferred directly to the walls where appropriate. The lateral loads flow through the system are a bit more complex to understand, as it depends on the overall deformation of the structure. As mentioned above, and the lower floors the lateral loads are accounted for nearly entirely by the shear walls, with some amount being shared with the columns of the frame at the upper floors. The exact

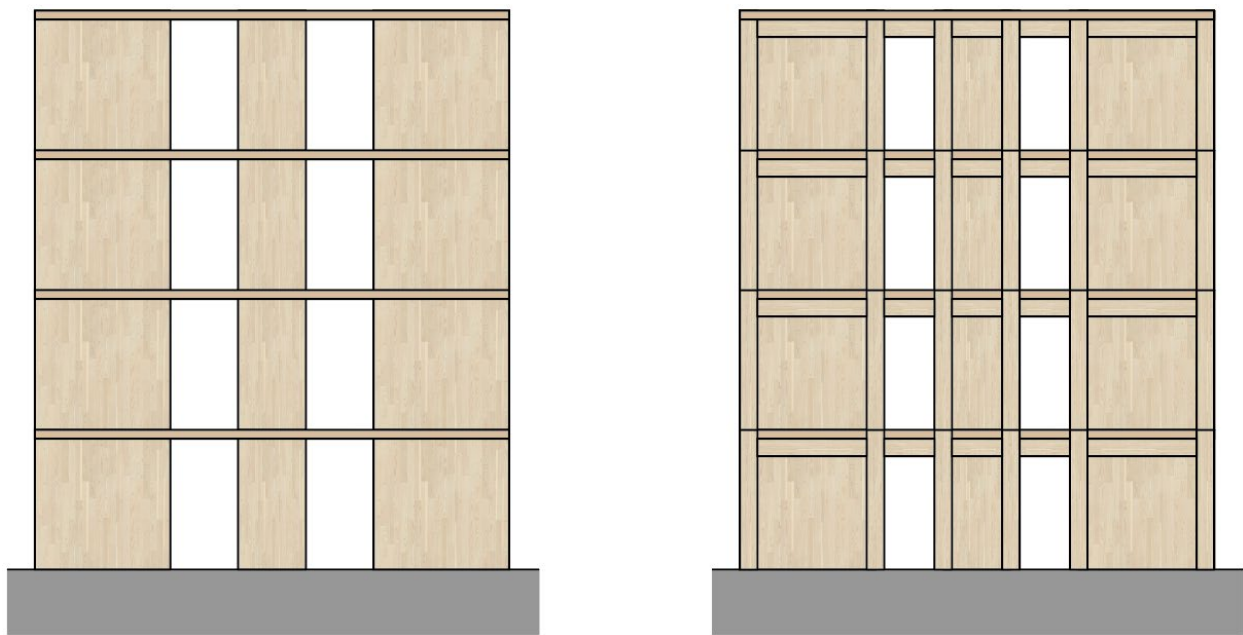


Figure 3.8 Shear wall (left) vs shear-frame (right) structural systems

distribution of these lateral loads have been studied by a few researchers. Xia et al. (2019) derived a set of equations to represent the element stiffness and mass matrices of such a system for both the shear walls and frame elements, considering the interaction effects of these two systems at their interfaces.

Shear Wall System

The shear wall system is a less efficient structural system for a timber high rise, but the load flow through the system is well understood. The CLT walls are designed for both gravity and lateral loads. The gravity loads are distributed to the wall panels via the structural floor system, spreading a distributed load over the top of the wall with magnitude relative to the tributary width of the wall. Where a CLT panel is not present, a beam or header will transfer the floor load to a nearby CLT panel as a point load. The lateral loads of the structure are distributed from the floors to the walls depending on the diaphragm behavior of the floor construction. Assuming a rigid diaphragm floor system, all walls will deflect the same distance at each level and thus the lateral loads will be distributed to the walls relative to their effective stiffness. In a flexible diaphragm system, the loads are distributed to the walls based on their proximity to other walls and their length. A steel or timber joist and beam floor system is typically considered a flexible diaphragm, while a concrete or timber panel system can be considered a rigid diaphragm.

3.3 Experimental Data & Calculation Strategies

CLT Mechanical Properties

Cross-laminated timber panels have unique mechanical properties that vary based on the loading direction (in- versus out-of-plane, and parallel to or against the grain of the outer layer). Blass and Fellmoser (2004) put forth a method of calculating the modulus of elasticity for each of

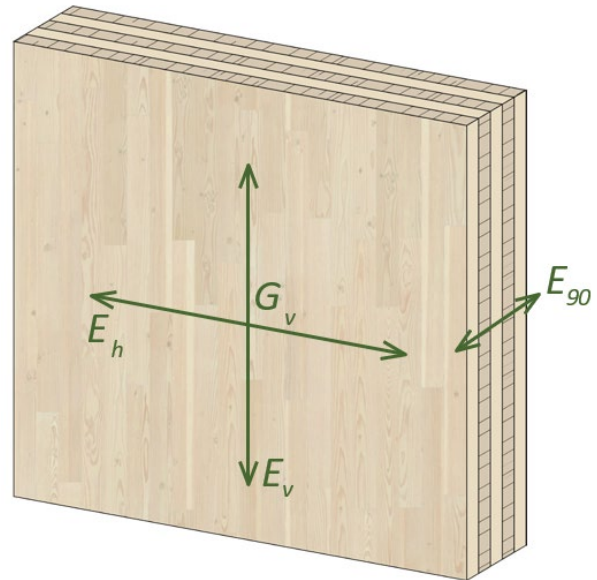


Figure 3.9 CLT panel and mechanical properties

these loading cases based on the material properties of the timber pieces which make up the panel. They then also proposed a classification system for these CLT panels that would summarize the four different stiffnesses under the four different loading situations. These are summarized in the tables below. This method for calculating the stiffness of the CLT panels has been tested repeatedly by various researchers against experimental values for CLT panels, and has been used in various analytical modelling verifications. A summary of this calculation can be found in the Appendix.

Similarly, the research done by Bogensperger et al. (2016) has been used to calculate the effective shear modulus of CLT panels. It was determined that if the timber boards in each layer were glued together along the narrow face, the shear stiffness of the CLT panel would be equivalent to that of the individual timber boards. If this is not the case, the effective shear stiffness for the CLT panel would be a ratio of that of the timber boards. This method has been referenced repeatedly by other researchers and has been tested and peer-reviewed thoroughly. An example of this calculation can be found in the Appendix.

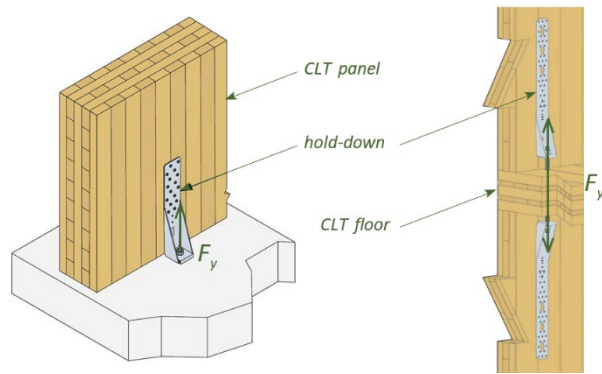


Figure 3.11 Diagrams of hold-downs (Source: Simpson Strong-Tie catalogue)

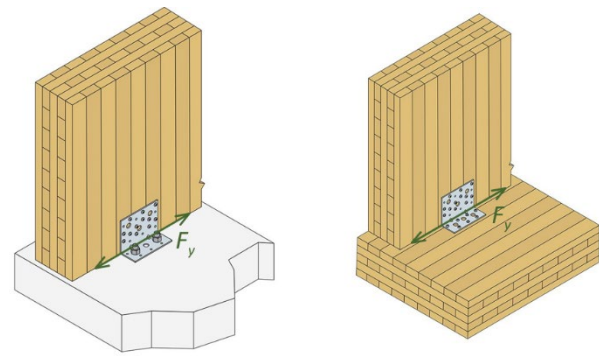


Figure 3.10 Diagrams of angle brackets (Source: Simpson Strong-Tie catalogue)

Another study was conducted to determine a calculation model for the shear strength and stiffness of CLT-beams. Compared to the solid or glue-laminated beam counterparts, the CLT-beam has several major advantages including high tensile strength in the perpendicular axis. Flaig and Blass (2013) conducted research to determine an analytical approach for determining the shear stiffness of such beams when loaded in plane.

Connections

The connection systems of CLT structures is quite complex to predict, as it largely depends on the orientation to the CLT panel, the load direction, the mechanical properties of the CLT panels, and the type of fasteners used. The value of the stiffness and strength of the component cannot be simply calculated but rather depends on isolated and in-situ experimental results. Gavric et al. (2015) performed several tests on hold-downs and angle brackets in-situ to determine the tensile and shear strength and stiffnesses. To maintain relevance within the research world, they tested the connections used in the three-story SOFIE building, as tested in 2006. This also allowed for direct comparisons to be made between the individual tests and the observed behavior of the full-scale shake table test. The same research team performed similar experimental tests on the screw connection details of the same SOFIE building. The results of this research have been referenced by many other studies to inform the expected

behavior of these specific connections. The values of the connections tested by Gavric et al. (2015) can be found in the appendix.

The strength of a connection depends on both the materials of the connection and the strength of the materials it is connecting. The connection component has its own yield strength dependent on the steel material and shape. For timber, hold-downs and brackets are typically screwed into the surface of the member. Since the strength of timber depends on a variety of factors (grain orientation, moisture content, species), the strength of the connection must be calculated or tested for each specific use case. Thus, as the engineer the independent yield strength of the connector and the strength of the fasteners in the timber (with withdrawal, shear, embedment) must be determined; the characteristic strength of the connection will be the lower of the two values.

Most building standards have calculation strategies for determining the characteristic strength of the fasteners in sawn timber and engineered timber members with reliable properties. However, because of its transverse directional layout, equations for determining the strength of connections into CLT members are not typically provided and instead rely on experimental testing. Several recent studies have been conducted to create a set of equations which predict the embedment strength of dowel-like fasteners into CLT members within a certain degree of accuracy.

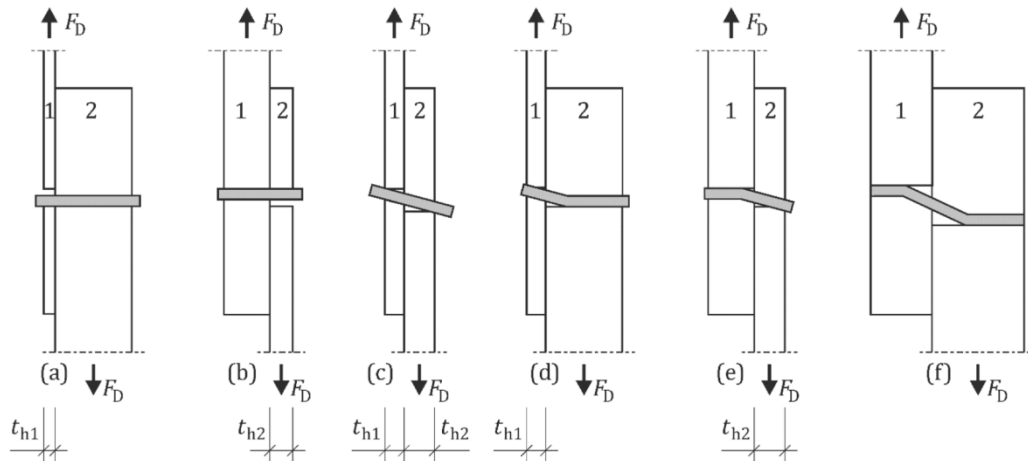


Figure 3.12 Failure modes of a dowel connecting two members (EN 1995)

Uibel and Blass (2013) conducted experimental tests on dowel-type fasteners in CLT panels loaded in various directions and developed some model equations. Kennedy et al. (2014) conducted over 1000 similar embedment strength tests on self-drilling and lag screws of various diameters into Canadian CLT to develop a nonlinear regression model for their strength. The two north American standards (NDS and CSA O86) for wood construction provide standard equations for the calculations of embedment strength in CLT members. These four models were used to predict the embedment strength of several connection configurations by Dong et al. (2020), and they were compared to the actual tested values to understand the trends of the model. This research team then worked to create a more reliable model for predicting the embedment strength of dowel-type fasteners in CLT panels based on the CLT wood density and the thickness ratio of the transverse layers to the total panel thickness. The equations for all these models can be found in the Appendix.

Once the embedment strength is determined, the strength of the connection between the steel plate of the connector and the CLT member can be determined. For a connection between two members, there are six possible failure modes that must be checked when determining the characteristic value of the dowel-effect contribution to the characteristic lateral resistance

of a single fastener in the considered connection (EN 1995). Additionally, a rope effect contribution may be considered in certain specific cases, but it is conservative to ignore this contribution. These equations from the Eurocode (EN 1995) are provided in the Appendix. The strength of the connection can then be solved via statics (using the equilibrium equations). An example of the calculation of a hold-down connection and an angle bracket connection can be found in the Appendix.

3.4 Variable Parameters

Timber is a natural and lightweight material, making it susceptible to changes in stiffness and structural mass distribution over time (Yan et al. 2023). One way to address this is to utilize semi-active tuned mass dampening systems, which can be tuned appropriately such that the behavior of the structure more closely aligns with the period and frequency it was designed for with sensors and user input data (Yan et al. 2023). Another perhaps less expensive option would be to model this as part of a life-cycle analysis of the structure, anticipating the changes to the material and planning for retrofits to achieve this same goal.

3.4.1 Time-based Parameters

Time-based parameters are ever-changing parameters which significantly impact the stiffness

or mass of the timber elements. The impact of a time-based parameter might be cyclical (such as wetting and drying) or compounding over time (such as deterioration). When analyzing the structure for time-based parameters, the goal is to determine the critical point(s) in time where the material stiffness or structural mass distribution changes enough to significantly impact the behavior of the structure for the design acceleration spectrum. The two such parameters that are being investigated are moisture content and biological deterioration.

Moisture

Timber is a porous and natural material which is subject to deterioration due to cyclical moisture infiltration over time. The way that the timber is protected from moisture during construction and throughout the lifetime of the structure influences its impact on the structural performance of the timber components and their connectors. There are currently no standards for regulating moisture management of timber during construction and little is understood about the effects of moisture exposure on the mechanical properties of cross-laminated timber structures. In 2019, a hygrothermal monitoring study tracked moisture performance of a CLT and glulam structure over the first six months of construction (Schmidt et al. 2019). It confirmed that the moisture distribution through the timber materials is largely dependent on the local conditions and construction detailing, with most locations being able to dry out to 16% moisture content quickly unless the detailing trapped moisture. Moisture-trapping details lead to permanent moisture infiltration in the interior plies, at which point it can become an ideal habitat for decay fungi and reduce the structural capacity of the timber components (Schmidt et al. 2019).

Moisture induced discontinuities mostly occur at the edges and connections where moisture fluctuation and accumulation are the greatest (Schmidt et al. 2019). In fact, heavily wetted CLT can dry out to acceptable moisture content levels

of less than 16% in under six months, unless moisture trapping conditions exist (Schmidt et al. 2019). Favorable construction factors which limit the risk of deterioration due to moisture exposure include constructing during the dry season, high levels of standardization and prefabrication, having the façade installed coincidentally with the timber walls, sheltering CLT floors, applying wax to end-grain and cuts outs, and utilizing a vapor permeable coating on all CLT surfaces. Predicting moisture damage is tricky. It involves understanding the risk factors which impact the likelihood of moisture damage to occur, as well as understanding the cyclical nature of the wetting and drying process. This relies on not only environmental factors, but also on the detailing of the connection of concern (a well-ventilated façade cavity versus ground contact details).

When moisture does penetrate the CLT panel, the swelling and shrinking of the cells stresses the timber and can significantly change the mechanical properties of the CLT panel. Udele et al. (2023) conducted extensive experimental research on this phenomenon on 4 different wood species 3-layer CLT layups with over 100 samples each. Particularly, they were curious how the wetting and redrying process (and exposure to fungal decay) impacted the mechanical properties of a typical perpendicular connection. 10 of the 100 samples of each wood type were designated as wetting and redrying controls so that the impact of moisture alone could be distinguished from the impact of fungal decay. They tested several mechanical properties after the samples had been successfully wetted to a moisture content of above 30% (the fiber saturation point) and redried, the results of which varied from species to species, but trends were clear. Overall, the peak load increased, while the stiffness, energy dissipation, and ductility significantly decreased when compared to the dry controls. This same research group conducted similar testing on the impact of moisture (and fungal decay) on the dowel bearing strength of dowel-type fasteners in CLT, finding a statistically



Figure 3.13 Moisture damage and fungal decay in angle bracket connection from Udele research (Udele et al. 2024)

significant decrease after wetting and redrying (Udele et al. 2024). The results of these studies are summarized in the Appendix.

Biological Deterioration

Biological deterioration is often a result of extended moisture exposure or saturation of the timber fibers. Comprehensive research has been done on decay growth to support performance-based service life design within different exposure conditions (Schmidt et al. 2019). The worst decay damage cases in North Europe are found in the floors and lower parts of walls, where water accumulates due to different reasons (Viitanen et al. 2010). This could be due to leaks or condensation trapped on the surfaces of the timber panels, which then run down to the base of the wall or sit on the floor. Mold growth can be modelled based on humidity, temperature, exposure time, and material type, and such tools can help provide a reliable prediction of the durability of the structure. These simulations require the moisture capacity and moisture transport properties of the material as factors.

Modelling the impact of fungal decay on the mechanical properties of CLT requires lots of testing, as it depends on various factors including exposure time, growth rate, fungal type, and fungal environment. Udele et al. (2023) conducted extensive experimental research on this phenomenon on 4 different wood species 3-layer

CLT layups with over 100 samples each. Particularly, they were curious how fungal decay impacted the mechanical properties of a typical perpendicular connection between two CLT panels. 10 of the 100 samples of each wood type were designated as wetting and redrying controls so that the impact of moisture alone could be distinguished from the impact of fungal decay. Another 80 samples of each wood type were exposed to one of two different brown rot fungi, either *Gloeophyllum trabeum* or *Rhodonia placenta*. The test samples were measured periodically for several mechanical and physical properties over the course of 40 weeks, and linear regression models were created to model these changes in properties over time. Each species had different results than one another, and sometimes even between the two fungi species, but the following overall conclusions could be made: peak load and energy dissipation at the connection significantly decreased, while stiffness and ductility could be attributed to the wetting and drying process rather than fungal decay.

Linear regression models of changes in these properties over time were created for each wood species when exposed to each fungal spore, they are summarized in the Appendix. Mass losses were also noted, ranging from 3-18%, but a linear regression could not model this to an acceptable confidence level. This same research group conducted similar testing on the impact of fungal decay on the dowel bearing strength of dowel-type fasteners in CLT, finding that prolonged fungal exposure directly decreases the dowel bearing strength of the CLT samples, but only significantly after 30 weeks of exposure (Udele et al. 2024). Similar linear regression models were again developed to represent these changes over time and can be found in the Appendix. The researchers also note that the conditions for their accelerated laboratory growth are not necessarily representative of real-world situations, referencing Wang et al. (2020) who suggests that three times

the exposure time is required for natural decay to produce similar impacts on mechanical properties.

3.4.2 Event-based Parameters

Event-based parameters are single points in time where an event occurs which impacts the stiffness or mass of the timber structure. The impact from an event is a one-time effect, and it must be determined if the material stiffness or mass distribution changes enough to significantly impact the behavior of the structure for the design acceleration spectrum. The three such parameters that are being investigated are fire, a previous seismic event, and a scheduled renovation or retrofit.

Fire

A fire event can significantly impact the structural behavior of the building. Where the fire is, how long it burnt, how much surface area was burned, and the fire resistance methods used in the design will significantly impact the way the structure behaves under seismic loading. A high-rise structure will have measures in place to prevent the fire from spreading through the whole tower, controlling it within a compartment. Thus, once

the fire has been put out, the other areas of the tower remain usable. For a timber structure, a charring layer will occur on the surfaces of the timber panels, beams, floors, or columns, reducing its weight and load carrying capacity. Thus, the impact of the burned floors on the total structure's seismic behavior must be analyzed after a burn out. Or in the initial design, it can even be pre-analyzed and designed for such that a certain amount of burnout can be considered acceptable through the various locations of the structure.

Seismic

A previous seismic event may not bring down the building but can still significantly impact the behavior of the structure in the next seismic event which occurs. As shown in the SOFIE project, damage from a seismic event includes yielding of the screws, hold-downs, or brackets, and crushing of the wood at these connections or in the floor below. This kind of behavior can be modelled in a non-linear analysis, where the overall reduction in the effective stiffness of the CLT wall can be determined. Thus, when the next earthquake occurs, the loads will be distributed in a different manner since some walls are not weaker.



Seven story test structure from the SOFIE project



Nail failures at hold-downs



Nail withdrawal at angle brackets



Wood crushing under hold-downs

Figure 3.14 Examples of damage from seismic event for CLT shear wall construction (Ceccotti et al. 2013)

Renovation

After a renovation or retrofit, the mass distribution of the structure will have significantly changed. Thus, the structural connections (which are controlling the inelastic behavior of the structure) might also need to be changed to adjust the stiffness of the structure to accommodate the new mass distribution. Preemptively analyzing the impact of a renovation later in the structure's lifetime can help to future proof the initial design.

3.5 Validation Strategies

Once the modelling strategy is designed, its accuracy and effectiveness must be validated. In previous research, modelling strategies for tall timber structures have been validated by comparing the results of the proposed model to that of previous models, simulations, or full-scale experiments. The implementation of the proposed modelling strategy might then also be demonstrated via a case study, showcasing its applicability especially if the strategy includes a new feature for analysis.

Comparative Studies

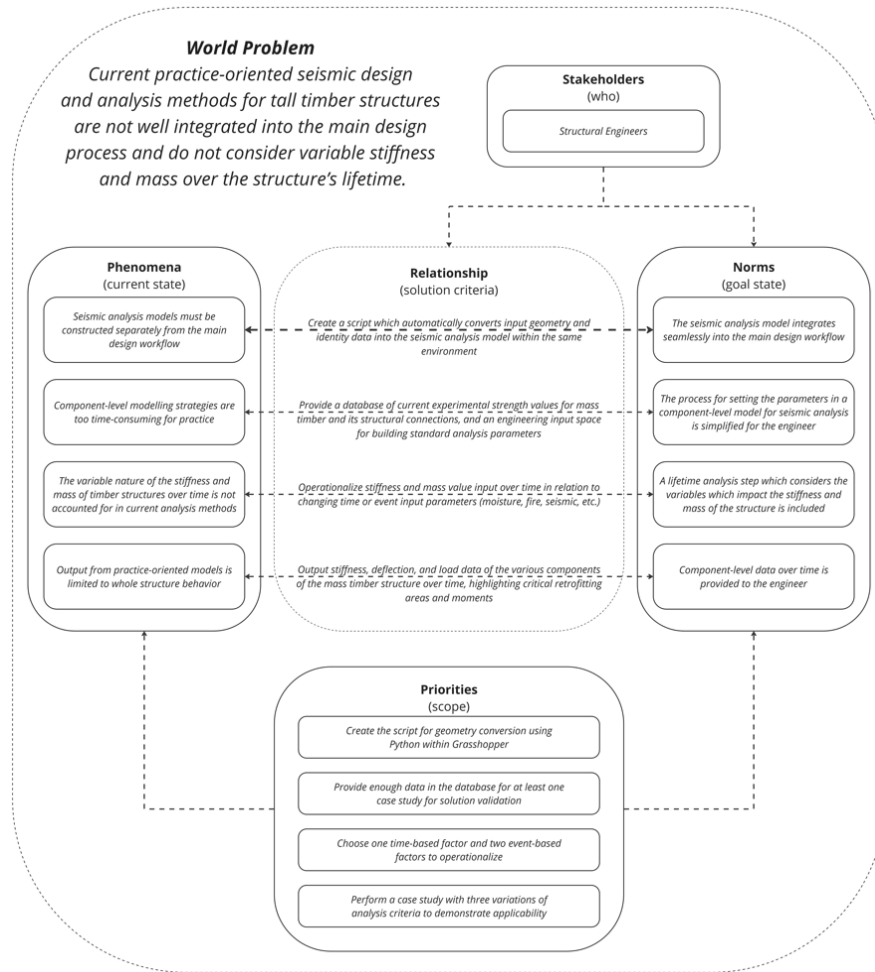
Comparative studies are often used to determine the accuracy of the model by comparing its results to that of previous models and experimental results. The modelling strategy put forth by Rinaldi et al. (2021) was first compared to previous modelling strategies to show the difference in results. With the goal of the modelling strategy being to simplify the modelling procedure of the connections while still accounting for their contribution to the overall deflection of the wall, it was first directly compared to a target model which used numerous springs to represent the connections (the more conventional modelling strategy). It was then also compared to the modelling strategy put forth by Christovasilis et al. (2020), which Rinaldi's modelling strategy was directly improving upon by including rocking deformation contribution. This three-way comparison was done by modelling the same

single- and multi-panel wall configurations with and without the rocking mechanism engaged. These models were compared by their stiffness curves from a stepped pushover analysis and further compared to the elastoplastic curve derived by the equivalent energy elastic-plastic (EEEP) method. This selection of comparisons demonstrated reasonable accuracy of the proposed modelling strategy when compared to the EEEP curve and target model pushover curve in all cases, while also demonstrating the limitations of the model proposed by Christovasilis and how Rinaldi's upgraded model addresses those.

Furthermore, Rinaldi's upgraded modelling strategy analyzed its accuracy by direct comparison to the experimental results of single story CLT wall tests done by Gavric et al. (2015). The lateral stiffness of the model was off from the experimental results by up to 25%, but was determined to be reasonably accurate because of the decidedly intrinsic randomness of the experimental results.

Case Studies

Case studies are often used to showcase the implementation of the research. The initial layout of connections for an iterative approach to seismic analysis put forth by Rinaldi et al. (2021) was demonstrated with a case study of a two-story CLT structure. The wall constructions of this new structure were assigned using their proposed method of grouping the walls based on wall length and tributary loads, and then the structure was analyzed to show the resulting seismic behavior. This case study demonstrated their method to the reader through an example, which is quite effective when a workflow or process has been developed. It was then compared to other ways of assigning wall constructions to a new design to show the impact of their implementation.



3.6 Results from Problem Investigation

Now that the initial literature review has been conducted, the factors of the world problem can be defined. As a reminder, the problem statement is also follows:

Current practice-oriented seismic analysis methods for tall timber structures are isolated from the main design process, complex to implement, and do not consider variability of parameters over the structure's lifetime.

This world problem can be defined with the following parameters:

1) **Phenomena:** (current state)

- Seismic analysis models must be constructed separately from the main design workflow
- Component-level modelling strategies are too time-consuming for practice
- The variable nature of timber structures over time is not accounted for in current analysis methods
- Output from practice-oriented models is limited to whole structure behavior

2) **Norms:** (goal state)

- The seismic analysis model integrates seamlessly into the main design workflow
- The process for setting the parameters in a component-level

model for seismic analysis is simplified for the engineer

- A lifetime analysis step which considers the variables impacting structural behavior over time is included
- Component-level data over time is provided to the engineer
- 3) **Relationships** between norms and phenomena: (solution criteria)
 - Automatically generate the analysis model from the design model in the same workspace
 - Provide a database of current experimental strength values for mass timber and its structural connections
 - Operationalize changing time and event input parameters (moisture, fire, seismic, etc.) and their impact on the structural performance
 - Output relevant data to a format which is easy to assess and use for post-processing
- 4) Stakeholders: (who)
 - Structural engineers
- 5) Priorities: (scope)
 - Create the script for geometry conversion using Python within Grasshopper
 - Provide enough data in the database for at least one case study for solution validation
 - Choose one time-based factor and two event-based factors to operationalize
 - Perform a case study with three variations of analysis criteria to demonstrate applicability of the tool and its outputted data

Now that the goals of the solution to this problem have been clearly defined, the solution design stage of the engineering cycle may begin.

4 Solution Design

This present research will develop a practice-oriented computational workflow for the seismic analysis of tall timber structures which:

- 1) Integrates the seismic analysis model seamlessly into the main design workflow
- 2) Simplifies the process for setting the parameters with a semi-component-level model for seismic analysis
- 3) Includes a lifetime analysis option which considers the variables impacting structural behavior over time
- 4) Provides the engineer with component-level data over time

This will be achieved by:

- 1) Automatically generating the analysis model from the design model in the same workspace
- 2) Providing a database of current experimental strength values for mass timber and its structural connections
- 3) Operationalizing changing time and event input parameters (moisture, fire, seismic, etc.) and their impact on the structural performance
- 4) Outputting relevant data into a format which is easy to assess and use for post-processing

Such that these goals can be achieved within the timeframe of the master's thesis, the scope of the project must be well defined.

4.1 Defining the Scope

4.1.1 Software Environment

The computational workflow will be developed within the Grasshopper environment for Rhino 8. This will provide control over the format of the building model input for automatic analysis model generation, and control over the output structure

Table 4.1 – Construction Type Scope

Height	At least 8 stories tall
Form	Rectilinear
Function	Residential
Core	Centered
Materials	CLT panels and glulam beams, concrete core and podium
Structural System	Shear-wall system
Building Standard	Eurocode (drafts and supporting research)

for the analysis. Most of the coding will occur outside of Grasshopper, and files will be called into the python components of Grasshopper as objects and functions. The Grasshopper environment will act as the user interface, simplified as much as possible for the user's view using grasshopper clusters. This way, the Grasshopper file will remain relatively small and clean, and the functions and analysis scripts will always exist in only one place. An advantage of the Grasshopper workspace is the modular nature of the workspace, which will allow the engineer to construct their own analysis workflow utilizing the components created in this project.

The various structural components of the structure will be modelled in Rhino (or Grasshopper) and act as direct input into the model generation script to create objects of defined Python classes. The mechanical properties of these objects will be sourced from the material and component properties database, the format of which will be developed in this research. The material and component properties database will be created in Excel, naming all material (physical, mechanical, characteristic) properties required for the analyses developed in this workflow.

Most of the existing software for finite element modelling is separated from the main design workflow and requires the structural engineer to reconstruct the model in this other environment. Some plug-ins or add-ons for Rhino and Grasshopper or REVIT exist, but they do not automatically generate analysis models from Rhino or Grasshopper geometry. Furthermore, the

output is limited to what the plug-in is designed to output, and the structure of it remains unclear. Thus, utilizing OpenSeesPy to generate functions which perform the analysis would provide great control over the analysis procedure and the desired output. The python component in Grasshopper for Rhino 8 was running Python 3.9.10 when this workflow was developed, thus OpenSeesPy version 3.4 is used.

4.1.2 Construction Type

To ensure that the workflow is designed such that it is applicable for most tall timber construction types, the model will be designed for the primary trends in tall timber structure as listed below:

The height of tall timber structures is defined as over 8 stories tall (above the podium). For simplicity's sake, only rectilinear forms will be considered with walls in only two perpendicular directions. The function of the building will be residential, which will matter when considering renovation designs and frequencies. The core will remain centralized, avoiding complicated eccentric forces and torsional forces. The materials database will be focused on CLT and glulam members and their connection between themselves as well as to concrete. The core and podium will be made of concrete and will be assumed as relatively rigid elements. While the most prominent structural system is the shear-frame system, existing research on how to model the behavior of this system under seismic loading is quite complex and has been determined to be too computationally heavy to fit

within the scope of this project. Thus, the structural model will be developed for a shear-wall system instead. Finally, though the current Eurocode does not have proper procedures and factors for the seismic analysis of tall CLT structures, it will be used as a basis and supporting drafts and research will be referenced to fill the knowledge gaps of the current standards. As much as is possible, the computational workflow will be designed in such a way that it can be further developed for the less prominent tall timber construction types.

4.1.3 Material and Component Database

Current computational modelling strategies rely on experimental data for the stiffnesses and strengths of timber materials and connection hardware. As will be explained later, a semi-component level modelling strategy will be used, the mechanical properties of which must be collected from current research. It will be organized in a database such that the engineer can select the hardware and timber material being used, and the appropriate experimental values will be utilized. Where possible and appropriate, equations will be used to calculate the properties of the material. These calculations will be implemented on a separate sheet within the Excel document, allowing the user to calculate their own properties for selected components (again, when possible or appropriate).

The database is designed to be expandable so that as research continues, information can be appended to the collection. Without providing a database, engineers would need to seek out existing sources themselves to utilize in the component model. This could cause inaccuracies in the analysis if the type of data that is used is not appropriate for the component-level modelling approach that the finite element analysis will be designed around. Clear instructions for the accumulation of data within this database will be

provided, to minimize inaccuracies in the analysis results.

4.1.4 Seismic Analysis Parameters Input

The seismic analysis parameters which are building standard specific are kept separate from the main analysis script so that future implementations of this computational workflow can be adjusted for different construction standards. Different standards have different means of generating the structural parameters which are used to determine the loads in the structure. Thus, the static linear analysis module will simply utilize the building period, however it was calculated, to determine the base shear, story forces, and wall forces of the structure. The significant mode shape and normalized force vectors used for static non-linear analysis will also be calculated by the seismic parameters module so that it can be used for an external static non-linear analysis (as this will not be developed in this project).

For the purposes of this research, the seismic analysis parameters follow the Eurocodes, as more than half of current tall timber structures are in Europe. This also achieves the learning goal of the present researcher to become more familiar with the Eurocodes. A design acceleration spectrum is required to test the response of the structure via static-linear analysis. Other factors specific to the Eurocode, such as the behavior factor of the structure, are also required. The behavior factor of tall-timber structures is not yet defined in the Eurocodes, but there are proposals available in research that can be used for this (Pozza et al. 2015).

4.1.5 Variable Parameters

One time-based parameter and two event-based parameters are included in the scope of this project. As an existing model for the prediction of mold growth and its impact on mechanical properties of the connections has been identified,

and given that it is closely linked to moisture, the time-based parameter that will be considered is biological deterioration. The first event-based parameter to be considered will be a low-force seismic event. This type of seismic event should cause some damage but not enough to render the building unsafe. An analysis of the structure without renovations after a small seismic event is within reason and should be relatively quick to implement as the results can be derived from the model itself. The second event-based parameter to be included in the scope of this project will be renovations and retrofit. This is because of the simplicity of the impact on the stiffness and mass of the structure, the complexity will lie in identifying the moments in time where this occurs. Fire events were not chosen to be included within the scope of this project because of the complicated fire modelling process it would require and the limited knowledge of how fire spreads through a tall CLT structure.

Biological Deterioration

The biological degradation of the timber wall will be modelled utilizing the linear regression models produced by Udele et al. (2023). The modelling strategy provided by Rinaldi et al. (2021) for determining the effective stiffness of a CLT panel considers the yield strength and stiffness of the hold-down, the stiffness of the angle brackets, and the weight of the structure. Construction specific research conducted by Udele on hold-downs and angle brackets are specific to the construction, and thus cannot be used generally in this practice-oriented model. Data from this included mass loss and hold-down and angle bracket stiffness over time. Udele's team also researched embedment strength, which can be applied to this computational workflow as it can be adapted for other dowel-type fasteners. Unfortunately, the embedment strength of the fasteners only impacts the hold-down strength within the modelling strategy, but this was the data deemed usable for this project. Furthermore, the suggestion from

Wang et al. (2020) will be implemented, and the regression model will be reduced by a factor of three to more closely represent real-world conditions for fungal growth

4.1.5.1 Previous Seismic Event

The previous seismic event will adjust the stiffnesses of specified walls to represent the damage they endured from a previous earthquake event. This will be represented as some percentage of the original stiffness; the percentage can be assigned by the engineer arbitrarily or determined via a non-linear analysis of the wall. These new stiffnesses will then impact the entire structure's behavior, which will be recalculated before being sent through another static linear analysis to determine the new force distribution through the structure.

Renovation

The renovation of the structure will be modelled by providing the engineer with several options for future renovation. These changes will include changing the wall or floor constructions, adding or removing walls, and adding new floors. The structure's parameters will then be recalculated, and the structure can be run through a static linear analysis again to determine the new force distribution.

4.2 Computational Workflow

The computational workflow will be done in a modular style which allows the engineer to pick and choose their analysis path. This set up works well in the Grasshopper environment, which utilizes a similar style for computational modelling and analysis. This work will be divided into four categories: the materials and components database, the automatic generation of the analysis model, the components for static linear analysis and lifetime analyses, and structuring the output of the data. The materials and components database will include all relevant information about the materials used in the structure. The seismic

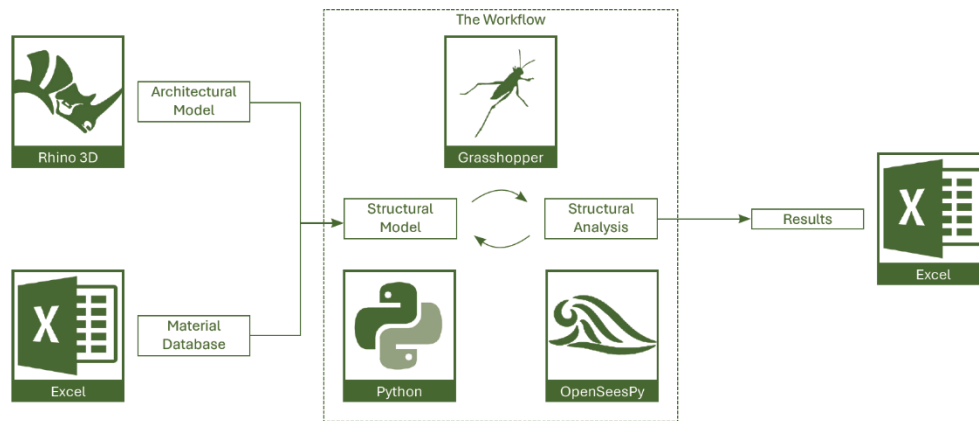


Figure 4.1 The workflow and the programs used

analysis model will be automatically generated with a Grasshopper script, following the referenced modelling strategy (Rinaldi et al. 2021). OpenSeesPy will be used as the seismic analysis library. Several analyses will be developed, first a static-linear analysis will be performed on the full structure to determine its overall behavior and loads, then the changing parameters will be applied such that the structure can be reanalyzed with the effects of fungal decay, a previous seismic event, or a proposed renovation. The output of these analyses will provide the information required for a static non-linear analysis to be performed on the walls that have entered non-linear behavior.

4.2.1 Materials and Component Database

The materials and components database will include all relevant information about the materials used in the structure. For shear walls, cross-laminated timber, angle brackets, hold-downs, and fastener properties will be required. The floors will need cross-laminated timber properties. The whole structure will need material densities for non-structural materials so that the floor and wall surface weights can be defined. Some methods have been identified for calculating the mechanical properties of CLT, this will also be included as a calculation sheet in this database.

4.2.2 Modelling the Structure

The building model will be supplied by the architect such that it is rotated in line with the existing cartesian grid in the Rhino space, with one corner of the bounding box of the structure at the origin. The walls and floors will be modelled as rectangular planes. The floors will be expected to act as rigid diaphragms between the walls. Walls with openings for windows or doors should not be considered structural for this model. Structural walls will be indexed from left to right (for walls in the y-direction), then top to bottom (for walls in the x-direction).

These structural elements (walls and floors) will be represented by Python class objects which will hold all geometry and material properties of the member to be used for structural analysis. The structural engineer will need to provide a list assigning the wall types to the walls, indexed to match the index order of the walls as produced by the script. If the engineer has not yet provided this, they will be prompted to do so. This will be done similarly with floors and floor types.

4.2.3 Analysis

The first analysis will be a pushover analysis of each wall to determine its stiffness, using the modelling strategy put forth by Rinaldi et al. (2021). Then the full structure can be analyzed via an eigen analysis to determine the fundamental period of the

structure and the significant mode shape. This will be modelled with an equivalent 1-dimensional multi-node system, using nodes with masses to represent floors and links between to represent the stiffness of each floor.

A static linear analysis will then be performed on the full structure to determine the base shear and load distribution through the structure. This analysis will require the fundamental period and behavior factor of the structure, key values from the spectral design ground acceleration graph, and other standard related factors. This will output the peak expected values at each key connection point in the system (force and deflection) and will indicate which connections have yielded and are thus behaving non-linearly under this load.

Different changing parameter options will be developed to provide analysis flexibility for the engineer. To determine the impact of biological degradation, a component of the workflow will be focused on the reduction in peak load capacity of the hold-downs, as existing models for embedment strength have been identified (Udele et al. 2024). Two different analyses will be performed using this. The first will analyze each wall individually to determine at what time (after fungal growth has begun) that the connection will not be able to withstand the expected peak load in the connection (per those determined via the static linear analysis). The second will analyze the full structure after specified walls have been experiencing fungal growth for a specified number of weeks; this will update the effective wall stiffnesses and calculate the new structural parameters to be used for the static linear analysis module. To account for a previous seismic event, a component of the workflow will edit the properties of or remove the walls which have yielded in the first seismic event before redistributing the forces through the structure via the static linear analysis method. To edit the properties of the wall, an understanding of the non-linear behavior of the full wall is required, which can be represented with

a percentage in wall stiffness reduction either arbitrarily assigned or determined via an external static non-linear analysis on the wall. To account for renovation, a component of the workflow will provide the engineer with options to add, remove, or change the properties of different structural elements, and calculate the new structural parameters to be used for the static linear analysis module.

4.3 Validation Design

The validation of the modelling strategy will be done via a comparative analysis, and the implementation will be done via case study.

Modelling Strategy

To validate the implementation of Rinaldi's modelling strategy for the wall stiffness determination, a direct comparison to the values provided by Rinaldi et al. (2020) will be made. That research team further compared its model to the experimental results of Gavric et al.'s 2015 full wall tests, which will also be done here.

Implementation

To demonstrate the full implementation of the tool, a new structure will be modelled. It will be taller than eight stories and subscribe to the prominent trends in tall timber construction as previously identified. The initial design of the structure will be analyzed via static linear analysis, which will output the peak values of the system and the walls which are yielding. The impact of biological degradation on each wall will be determined, and what its results mean by the engineer will be discussed. The impact of a previous seismic event and a planned renovation will be demonstrated and discussed similarly.

5 Implementation

The computational workflow which was developed can be summarized with four main parts: the materials and components database, the

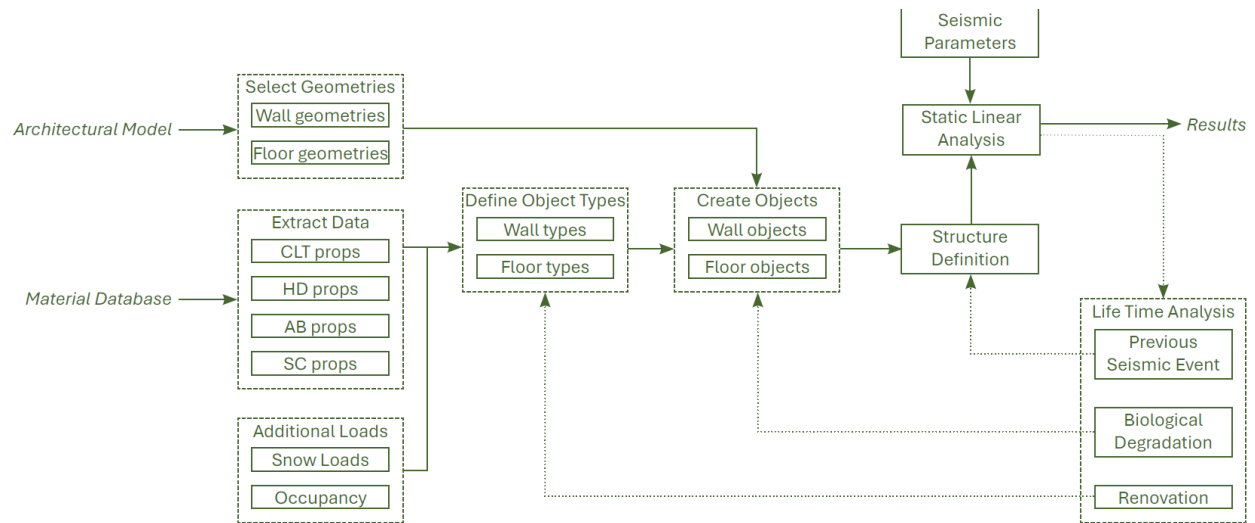


Figure 5.1 Flowchart of the developed computational workflow

automatic model generation for analysis, the static linear analysis of the structure and lifetime analysis modules, and the output structure. The database was created in Excel and includes worksheets containing the mechanical properties of the CLT panels, hold-downs, angle brackets, and splicing fasteners required for the modelling strategies used. The model is generated and analyzed using Python components within Grasshopper, each distinct step split up differently to allow for flexibility of use to the engineer and allow for integration with further developments. The results are output to Excel documents to be easily used and processed by the engineer. The theory behind each step is discussed below, and more details on use can be found in the instruction manual for this project.

5.1 Materials and Components Database

The materials and components database is an Excel document with several either listing mechanical properties of the materials or components, or are calculation sheets to be used to determine these properties. They are summarized below.

Cross-Laminated Timber (CLT) Sheet

The properties for the cross laminated timber are required for the shear walls and floors of the structure. The cross-laminated timber (CLT) sheet lists the following properties: standard-catalogue, classification, raw timber classification, number of layers (m), total thickness (t), thickness ratio (tt), modulus of elasticity of raw timber (E_0), wood species, modulus of elasticity parallel to the external grain (E_v), modulus of elasticity perpendicular to the external grain (E_h), modulus of elasticity perpendicular to the panel (E_{90}), shear modulus of the panel (G_v), the mass and weight densities (ρ), the value source (either from experimental research, straight from the catalogue, or from a calculation method), and the source citation. These cells can be filled in by the user, but the headers should remain the same as they are used by the modelling script to search and identify for properties.

Hold-down (HD) Sheet

The properties for the hold-downs are required for the shear walls of the structure. The hold-down (HD) sheet lists the following properties: hold-down type, connection type (CLT-CLT or CLT-Concrete), the yield load (F_y), the stiffness in the tensile direction (k_{up}), the stiffness in the shear direction (k_s), the yield displacement (u_y),

fastener type, number of fasteners ($fast_n$), length of fastener ($fast_L$), diameter of fastener ($fast_d$), plate thickness ($plate_t$), fastener yield strength ($fast_{yield}$), overstrength factor for connection, and the source of the values. These cells can be filled in by the user, but the headers should remain the same as they are used by the modelling script to search and identify for properties.

Angle Bracket (AB) Sheet

The properties for the angle brackets are required for the shear walls of the structure. The angle bracket (AB) sheet lists the following properties: angle bracket type, connection type (CLT-CLT or CLT-Concrete), the stiffness in the tensile direction (k_{up}), the stiffness in the shear direction (k_s), fastener type, number of fasteners ($fast_n$), length of the fastener ($fast_L$), diameter of the fastener ($fast_d$), plate thickness ($plate_t$), fastener yield strength ($fast_{yield}$), overstrength factor for connection, and the source of the values. These cells can be filled in by the user, but the headers should remain the same as they are used by the modelling script to search and identify for properties.

Screwed Joint (SC) Sheet

For multi-panel walls, the seam between CLT panels is fastened together with screws or nails and are important to include in the model of the wall. The screw joint (SC) sheet lists the following properties: screw type, panel connection (Wall-Wall or Wall-Floor), orientation (parallel or orthogonal), joint type (lap, spline, both sides, or through wall), load direction (vertical or lateral, in or out of plane), yield load (F_y), stiffness (k), and the source of the values. These cells can be filled in by the user, but the headers should remain the same as they are used by the modelling script to search and identify for properties.

Material Densities Sheet

Material densities are required for giving mass and weight to the structure. The material densities

sheet lists the following properties: material name, and density. These cells can be filled in by the user, but the headers should remain the same as they are used by the modelling script to search and identify for properties.

CLT Calculation Sheet

The CLT calculation sheet is used to determine the required properties of the cross-laminated timber panels, if the values aren't available otherwise. The input values required are:

The total thickness of each set of layers out from the core is calculated at a_i , and the coefficient k_i is calculated according to Blass and Fellmoser (2004). With this information, the effective stiffness values of the CLT can be determined. The full calculation can be reviewed in the Appendix. Additionally, the thickness ratio (tt) of the CLT panel is the ratio of longitudinal layers to the whole thickness and is required for the linear regression models for biological degradation of the timber; it is calculated here as well.

The effective shear modulus is calculated according to Bogensperger et al. (2016), which provides three different equations: a general one, one calibrated to 3-ply panels, and one calibrated to 5-ply panels. The full summary of this calculation is available in the Appendix.

5.2 Model Generation

To store all properties of each structural element, different classes of Python objects are created. Each of these classes requires the type and geometry to initiate the object. The base units are millimeters, grams, and newtons; all geometries and calculations are based on this.

Extract Material and Loads Data

The extracting material properties from the material database is done within a Grasshopper cluster, which uses the *Read Excel* component from the Lunchbox plug in (for Grasshopper). To define

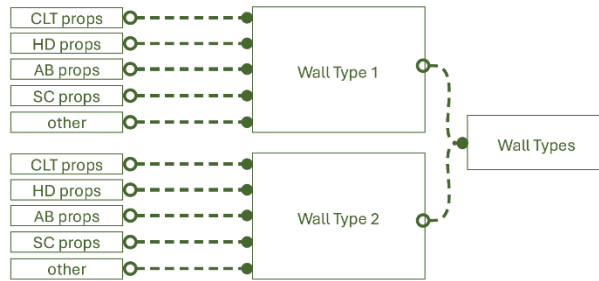


Figure 5.2 Wall type generation

the wall and floor types, the materials and their properties must be extracted and chosen. The first step is to extract the data from the Excel database into format readable by Python (using a NumPy array).

The data in the NumPy array is further parsed, by first getting the first identity category of each material or component (for the CLT sheet, that's the Standard/Catalogue, for the HD sheet it's the HD type, and so on). The user is then prompted to choose one of the options before moving to the next parsing category, and so on, until they have properly selected one material or component type.

For ease of use, the *Item Selector* component was used from the *Human* plugin for Grasshopper, allowing for a dropdown menu to be automatically populated for the user to select the identity category of the material. This extra plugin can be avoided by instead using Grasshopper default components to select the desired option (must be passed in as a text string into the next parsing cluster).

Since this research project is following the Eurocode, some percentage of variable loads must be accounted for on the floors and roofs of the structure for seismic analysis. In some cases, this includes snow loads. Thus, a final cluster can be created to include these variable loads.

Generate Object Types

Once the materials are chosen, the object types can be created. These object types will contain all property information of the structural element,

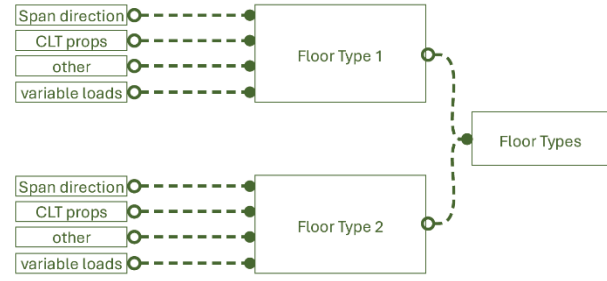


Figure 5.3 Floor type generation

before being combined with the geometry parameters of the structural element. This division of information allows the engineer to change the properties of an object type such that it impacts all class objects that type is assigned to. This will make things easier for the lifetime analysis modules.

All object id's and lists of properties are collected into NumPy arrays via the following Grasshopper cluster(s), such that it can be properly interpreted by the class objects. These will be fed into the object creation modules as input.

Create Wall Objects

The *Create Wall Objects* cluster assigns the wall properties to the wall geometries, creating a list of wall class objects as defined by the *Wall_Class.py* script. A more detailed description of the *Wall* object class is available in the instruction manual.

If the wall types are not yet set, the component can be run such that the walls are sorted and named based on their direction, floor, gridline, and location along their gridline. Then the wall types can be assigned as a list of integers corresponding to the list of sorted walls initially outputted by the component. The engineer can copy this list of names into an excel sheet for ease of editing or can directly write the list of *wall_type_ids* in a Grasshopper panel.

Create Floor Objects

The *Create Floor Objects* cluster assigns the floor properties to the floor geometries, creating a list of floor class objects as defined by the *Floor_Class.py*

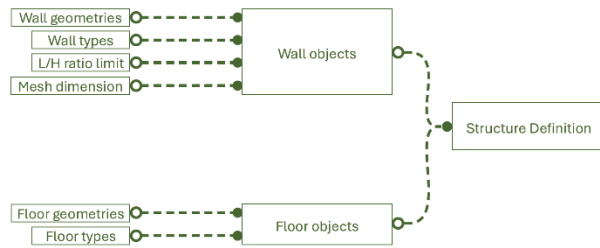


Figure 5.4 Wall object, floor object, and structure definition generation

script. A more detailed description of the *Floor* object class is available in the instruction manual.

Full structure Definition

If the wall and floor objects are defined properly as described above, the *Full Structure Definition* cluster can be initiated. This Grasshopper cluster will automatically generate an analysis model per the referenced modelling strategy (Rinaldi et al. 2021), where the CLT shearwalls will be modelled as two-dimensional elements with horizontal strips representing the connection zone and the floor properties. Equivalent stiffnesses are calculated for the wall elements to include effects from both sliding and rocking deformation from the connections into the overall wall behavior. Friction contribution is neglected, which is a conservative approach (friction helps reduce deflections). Please refer to the appropriate appendix section for more diagrams and equations for this modelling strategy.

When initiating the *Full Structure Definition* cluster, several attributes of the wall and floor objects which depend on one another will be updated. For example, the floor weight on top of each wall, or the total story mass. Once these properties are updated, the *Full Structure Definition* cluster then is used to determine the effective stiffness of each wall and the required structure specific seismic analysis parameters in each direction. The effective stiffness is determined with a load-controlled pushover analysis (using the Openseespy library). The natural building period and significant mode shape are determined through an eigen analysis of a simplified one-dimensional model of the full

structure, with a single node representing each total story-mass and links representing total story-stiffness in each direction. The natural building period will be used to perform the static linear analysis on the full structure, and the significant mode shape will be used to perform a static non-linear analysis on specific walls of interest.

5.3 Analysis

The analysis portion of this workflow is split up into several modules, allowing the engineers to build their own analysis workflow. The first step is the static linear analysis of the original structure, then the lifetime analysis modules account for two biological degradation analysis methods, a static linear analysis of the structure after a previous seismic event, and a static linear analysis of the structure after a renovation.

5.3.1 Static Linear Analysis

A static linear analysis is first performed on the structure, to determine the structure's base shear, the forces and deflection in each wall throughout the structure, identify which walls exhibit rocking behavior, and determine which walls are yielding. This cluster requires multiple input variables for the site-specific seismic parameters. The values from the spectral acceleration graph (S_α and S_β) can be retrieved from the appropriate resources for the region. For this research, the hazard maps provided by the European Facilities for Earthquake Hazard and Risk (EFERHR) were referenced at their online platform, <http://hazard.efehr.org>. The behavior factor (q) is specific to the structural system and materials used, and this is not defined by the current Eurocodes, but several studies

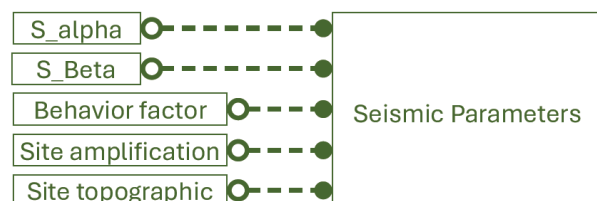


Figure 5.5 Seismic parameters cluster

suggest setting $q = 3.0$, thus this is the default value. The topographic factor (F_T) and the site amplification factor (F_β) can be found in EN 1998, but their default values are set as $F_T = 1.0$ and $F_\beta = 4.0$.

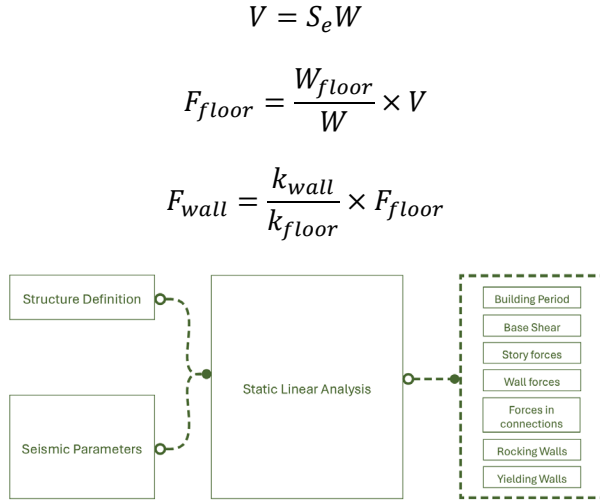


Figure 5.6 Static linear analysis cluster

5.3.2 Lifetime Analysis

Biological Deterioration over time

In an ideal design, the CLT would always be properly protected from biological damage, thus predicting when it will happen is not a reasonable thing to assess. However, if a structure is already built and is presenting with evidence of fungal decay, modelling how the mechanical properties of the structure will change can help inform the engineer of the urgency of renovation needs.

This phenomenon was implemented utilizing the equations from the Udele et al. (2023) study, which provides several linear regression models modelling the reduction in embedment strength of dowel like fasteners in CLT members for different wood species and mold types (summarized in Appendix J). The grasshopper cluster defaults to using the worst-case value calculated by these linear regression models if the wood species or mold type is not known. Furthermore, these linear regression models were calibrated to experimental

values in laboratory conditions, which are not necessarily representative of real-world conditions, thus these regression models were reduced by a factor of three as suggested by Wang et al. (2020).

Two different grasshopper clusters (or analysis modules) were created to represent this phenomenon, one which allows the engineer to model the impact of mold on the wall properties over time, and another which calculates and applies this reduced embedment strength at one instance in time (as defined by the user). The former provides the engineer with information on how the various wall properties (such as the hold-down strength, angle bracket strength, and overall wall stiffness) changes over time, which is useful for determining which walls are most susceptible to loss in strength and stiffness in the structure (for example). The latter provides the engineer with the properties of the whole structure when specified walls have experienced a level of fungal decay. In this, the engineer can either input information after biological decay has been identified on the structure, or the engineer could specify walls which might be susceptible to moisture infiltration and model the impact that this would have on the structure. Then the overall structural parameters are calculated (building period, significant modal shape, etc.) and the new structure is ready for the static linear analysis module. With this information, the engineer could adjust the design to minimize this impact by changing the CLT type, the fasteners in the hold downs or angle brackets, or by selecting a different wood species.

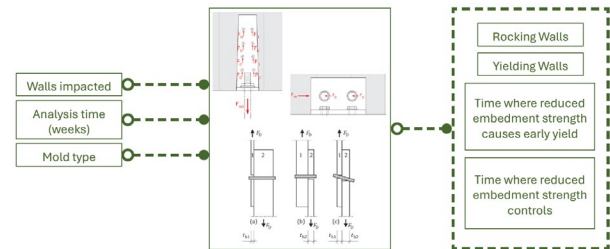


Figure 5.7 Biological degradation of structure at time t cluster

Previous Seismic Event

Knowing how a structure would respond to a secondary earthquake after one has already hit can be useful when future-proofing your design. This phenomenon was implemented such that the stiffness of specified walls (perhaps those which were determined to yield in the initial static linear analysis module) can be reduced by some percentage factor. This percentage factor could come from a non-linear analysis (not included in this project) or can be assumed by the engineer, such as a 50% loss in strength. Then the overall structural parameters are calculated (building period, significant modal shape, etc.) and the new structure is ready for the static linear analysis module. With this information, the engineer could preemptively adjust their design to future proof the structure a bit, by providing extra strength or ductility in the structure to account for loss in stiffness after the first earthquake.

Renovation

As mentioned previously, since timber structures are relatively lightweight, any changes in the façade, floor, or ceiling constructions can drastically impact the weight distribution of the structure and thus its overall performance and behavior. Understanding the impact of this early on can help the engineer futureproof the initial structure against renovations later down the line. Providing extra strength in the structure now might make it easier to transition the structure from a residential building to an office space or allow for a top up structure to be added later or allow for a heavier façade to be implemented.

The renovation module implements this phenomenon by allowing the engineer to adjust a copy of the original structure in several ways. The options provided are to change the properties of the walls based on wall types, changing the geometry of the wall, adding or removing walls, changing the properties of the floors based on floor types, or adding additional floors on top of

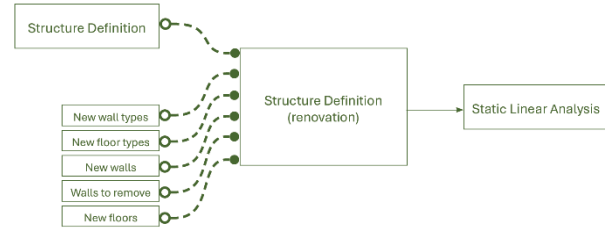


Figure 5.9 Renovation cluster

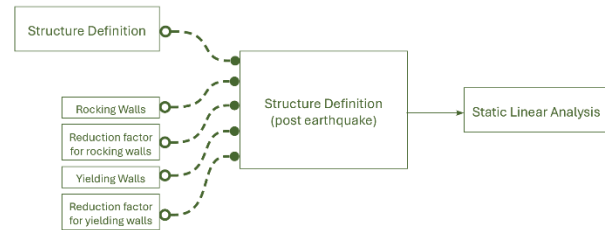


Figure 5.8 Previous seismic event cluster

the structure. Then the overall structural parameters are calculated (building period, significant modal shape, etc.) and the new structure is ready for the static linear analysis module. With this module, the engineer can begin designing a renovation or can future proof their original design to accommodate future renovations.

5.4 Outputting Data to Excel

The data which is exported to excel varies based on the type of analysis that was performed on the structure. Each version of the structure is exported to its own unique file, from which comparison charts can be created. For ease of use and to avoid overwriting data, a timestamp can be included in the file naming convention by utilizing the boolean feature. A more detailed explanation of the outputted data structure can be found in the instruction manual.

5.5 Other User Features

Printing Object Properties

To help the user with identifying issues, the *Print Properties* clusters can help for getting the object's attributes.

Table 5.1 – Comparative analysis results for implementation of Rinaldi modelling strategy

	Number of panels	E_{strip} (MPa)			G_{strip} (MPa)			Stiffness (N/mm)		
		Value	Rinaldi	% Diff.	Value	Rinaldi	% Diff.	Value	Rinaldi	% Diff.
Wall I.1	1	324.00	371.92	-12.88	3.14	3.13	+0.32	3487	3490	-0.09
Wall I.2		254.00	253.61	+0.15	6.27	6.25	+0.32	6324	5490	+15.19
Wall I.3		129.00	128.70	+0.23	6.27	6.25	+0.32	6288	4620	+36.1
Wall II.1	2	-	-	-	3.67	3.66	+0.27	4068	4360	-6.7
Wall III.1					3.11	3.10	+0.32	3501	3770	-7.14
Wall III.2					3.11	3.10	+0.32	3501	3770	-7.14
Wall III.3					3.11	3.10	+0.32	3501	3770	-7.14
Wall III.4					2.12	2.11	+0.47	2454	2670	-8.09

* mesh size of 100 mm

Selecting Walls or Floors

The wall and floor selection module allows the engineer to quickly select components of the structure without having to name them. The two ways to select walls and floors are by their representative Rhino or Grasshopper geometries, or by a specified wall or floor type. This is useful for the several lifetime analysis modules that require the specification of wall or floor objects that have seismic damage, fungal damage, or are subject to renovations.

The accuracy of the implementation of the Rinaldi model was tested through a comparative analysis of stiffness values determined by this research's implementation of the model to that of the Rinaldi research team for similar wall constructions. The results of this comparative analysis are available in the table below, and more detailed information of the wall properties can be found in the appendix. A variance in calculated wall stiffness varied from 5 – 40% across all tested wall configurations, all comparatively conservative values. This discrepancy has been attributed to potential unknown assumptions made within the SAP2000 software used by the Rinaldi team that were not applied within this implementation using Python and OpenSeesPy, since all other properties and

5.6 Evaluation of Implementation

5.6.1 Comparative Study of FE Modelling Strategy

Table 5.2 – Comparative analysis of stiffnesses with varied mesh dimensions

Mesh dim.	No.	R.	Stiffness (N/mm)									
	-	50	%	100	%	112.5	%	125	%	150	%	
Wall I.1	1	3490	2888	-17.25	3487	-0.09	3159	-9.48	2825	-19.05	2367	-32.18
Wall I.2		5490	5316	-3.17	6324	+15.19	5780	+5.28	5216	-4.99	4428	-19.34
Wall I.3		4620	5285	+14.39	6288	+36.1	5751	+24.48	5192	+12.38	4410	-4.55
Wall II.1	2	4360	3376	-22.57	4068	-6.7	3688	-15.41	3299	-24.33	2767	-36.54
Wall III.1		3770	2898	-23.13	3501	-7.14	3169	-15.94	2831	-24.91	2369	-37.16
Wall III.2		3770	2898	-23.13	3501	-7.14	3169	-15.94	2831	-24.91	2369	-37.16
Wall III.3		3770	2898	-23.13	3501	-7.14	3169	-15.94	2831	-24.91	2369	-37.16
Wall III.4		2670	2021	-24.31	2454	-8.09	2215	-17.04	1973	-26.01	1645	-38.39

functions are identical. Particularly since the stiffnesses were conservative, the implementation was considered good enough to continue the project. **With** more time, further trouble shooting and investigating the possible causes for variance between models is recommended.

Better accuracy could possibly be achieved by calibrating the mesh dimension of the model, see comparison below in Table 5.2. Through this calibration process, Wall 1.2 and Wall 1.3 have consistently higher percentage difference values, the way that these walls were modelled should be further investigated. Smaller mesh sizes theoretically give higher accuracy, but they take

longer to analyze the stiffness of the wall because of the many more elements within the model.

5.6.2 Case Study of Implementation

The case study was used to test the implementation of the workflow on the design of a tall timber structure. The structure was a residential building, 10 stories tall with a shear wall structural system and a centralized CLT core. The structure was modelled in Rhino, and the walls and floors were split into layers depending on the wall or floor type that they would be assigned to. Non-structural walls and glass were included to aid in the calculation of additional mass from non-structural members in the structure. The floors are

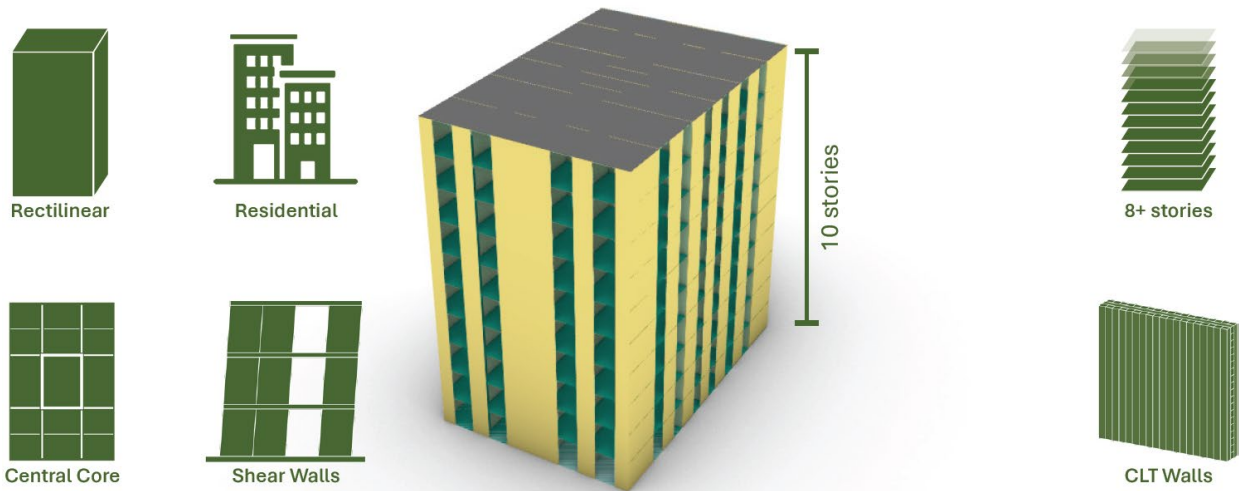


Figure 5.10 Case study parameters

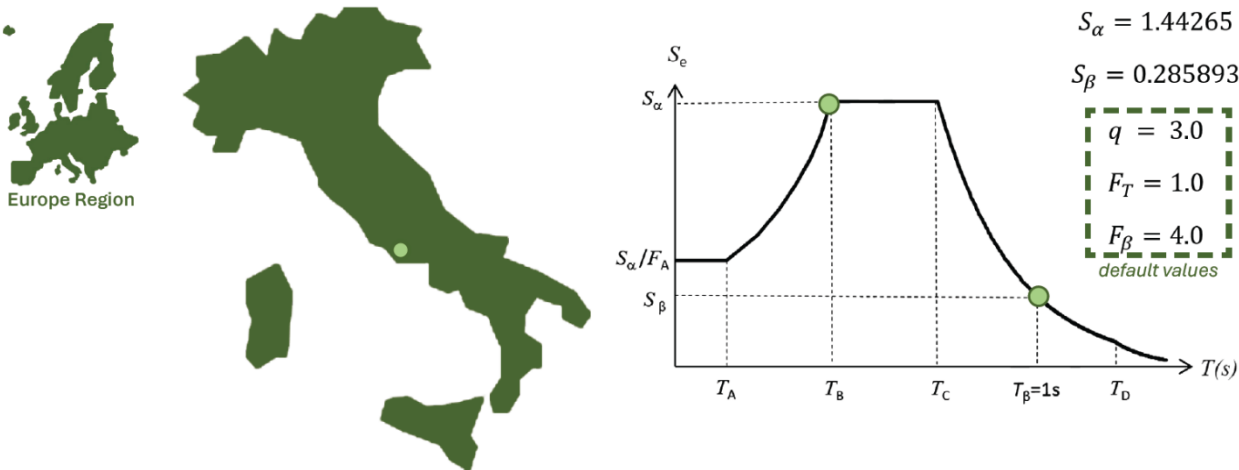


Figure 5.11 Location parameters

to be modelled as rigid diaphragms and span in the east-west direction of the structure. The general layout of the walls is based on the SOFIE project floor plan for the 6-story test structure, however this floor plan was expanded upon.

Three different wall types were used and assigned according to the method laid out by Rinaldi et al. (2021); by splitting the walls into three groups based on relative load. Since the floors span in the east-west direction, the east-west walls have relatively little gravity load acting on them; these make up the small loads group. The exterior north-south walls have roughly half of the gravity loads acting on them compared to the interior north-south walls, thus these will make up the medium loads and large loads groups (respectively). There was a total of 420 walls defined in the structure (42 per floor). The two floor types were assigned based on whether the level was a floor or a roof. The site was set at the base of the mountains behind Rome, Italy, where higher seismicity is expected. The spectral data used is summarized in the instruction manual's example.

Initial Static Linear Analysis

This initial design of the structure was analyzed, where upon the static linear analysis revealed 28 walls to be rocking, and 32 walls to be yielding in this configuration, or 14% of the total walls. These rocking and yielding walls were limited to the upper two stories, which indicates that the lateral loads at the top floors were large enough to initiate rocking behavior due to low gravity loads on the walls. When the data was further review, it was seen the yielding in the walls was at the angle brackets, not at the hold-downs, and only on walls in the east-west direction.

Secondary Seismic Event

Then the stiffnesses of the rocking and yielded walls were reduced for a secondary seismic analysis, where upon more different walls yielded now that the loads were redistributed through the structure. The stiffness of the rocking walls was

reduced to 80%, and the yielded walls to 50%. Interestingly, more walls exhibited rocking behavior (42 walls) and less exhibited yielding (18). No walls that had previously yielded in the first earthquake yielded further on the top (tenth) story, but several new walls yielded on the ninth story and previously yielded walls yielded further. This is to be expected because the relative stiffness of the rocking and yielded walls decreased, so in the secondary seismic event less load went to the weaker walls. Larger loads were distributed to stronger walls, which then cause them to begin yielding. Furthermore, with the reduced stiffnesses, the structure's natural period and base shear was reduced.

Biological Degradation Over Time

Next the exterior walls of the original structure were analyzed to determine the critical points in time after biological degradation begins that the wall's structural performance will weaken significantly. This is two different points in time; the first is where the embedment strength of the angle bracket or hold-down connections become the weak point in the connection (ie. the embedment strength is less than the connection component's strength), the second is where the connection will yield under the analyzed loading conditions (based on the first static linear analysis). The exterior walls were focused on as these are most at risk for moisture penetration, and the analysis was run for a year (52 weeks). The results showed that 259 walls weakened at the angle brackets after 19-24 weeks of exposure to fungal decay, and 10 walls weakened enough between 8-42 weeks that these would yield under the current loading conditions. The results show that the hold-down would weaken after 1 week of fungal exposure, but that's an indication of the overstrength factor not being properly accounted for in the calculation, which is discussed further in the conclusion.

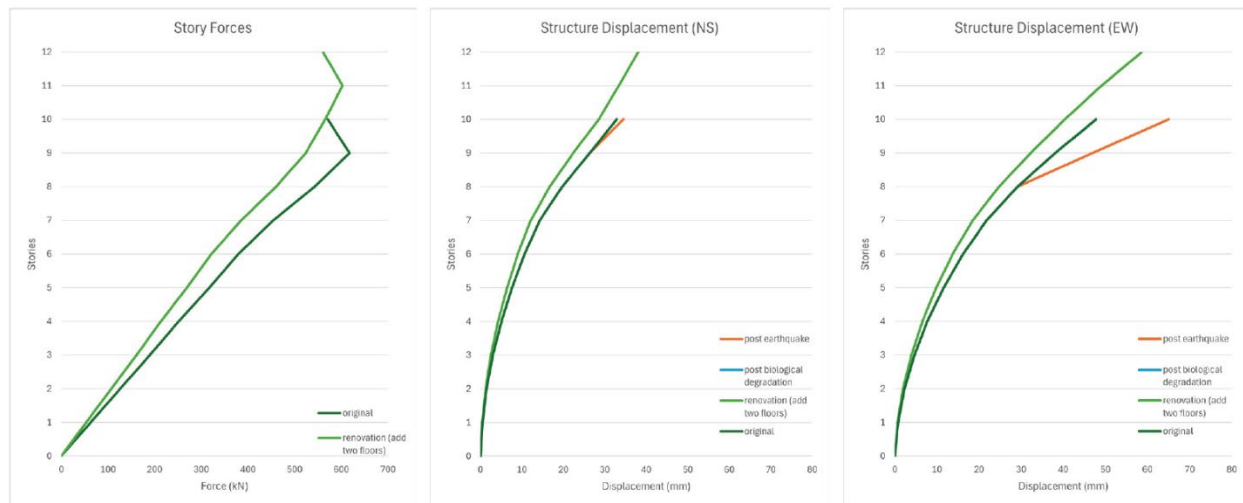


Figure 5.12 Comparison between structure story forces and deflections

Biological Degradation after 52 weeks

The structure was then analyzed, if 52 weeks of fungal growth was present on the exterior walls, to see how the overall structure would be affected. Now 35 walls would yield under the seismic loading, 2 of which are on the eighth floor, and 27 walls would be rocking (but not yet yielded). When analyzed in more detail, most walls yield at the angle brackets but some do yield at the hold-downs. The fundamental period and base shear of the structure don't change significantly, but the structural parameters required for non-linear analysis (the significant modal shape) does, making a non-linear analysis of this structure important now.

Renovation

The modular layout of this workflow allows events to be easily stacked upon each other, which is especially useful for the renovation component. The renovation tested on this case study is the addition of two extra floors on top of the structure, changing it to a 12-story residential structure. If no earthquake has hit prior to this renovation, the rocking and yielding walls would be limited to the top two floors, the natural period would decrease (higher natural frequency), and the base shear would increase. If this top up were to occur after a

previous earthquake and no other renovations had occurred, yielding walls extend three floors down.

6 Conclusions and Reflection

This research project aims to advance knowledge in the field of seismic analysis for tall timber structures by developing a practice-oriented computational workflow which integrates the seismic analysis model seamlessly into the main design workflow, simplifies the process for setting the parameters in a component-level model for seismic analysis, includes a lifetime analysis option which considers the variables which impact the overall behavior of the structure, and provides the engineer with component-level data. It will increase the timeframe of analysis that the engineer can perform on tall timber structures such that the initial structural design can be informed by future predicted events. The computational workflow developed by this project addresses these goals appropriately.

The materials and components database helps collect all existing and relevant data into one usable space. The exact parameters required for the modules in this workflow are in the database, and are presented in a format that can be

expanded upon (using Excel). Existing calculation strategies were implemented into the database so that the mechanical properties of CLT panels can be quickly calculated and added to the materials database. Furthermore, this database stores information about how the values were determined, whether via calculation, experiment, or from a catalogue. This information is important when understanding what kind of model each component can be used for.

The computational workflow is modular, providing flexibility and control to the engineer over what analysis steps he or she wishes to take. This came naturally when implementing the workflow into Grasshopper, which uses components to step through design steps already. Furthermore, the modular approach allows for the impact of several events to be stacked on one another, as was demonstrated with the renovation module in the case study. This modularity also allows the engineer to further develop the workflow, or combine this with other existing tools or plugins as they find useful, allowing for a customizable analysis process.

The model is automatically generated using geometries and type information. The use of class objects within the Python space made accessing and updating the wall, floor, and structure parameters simple and kept the script well organized. The geometries used to define the structure are directly linked to the analysis script, allowing for instant analysis when the design changes. The overall structural behavior and parameters (such as the natural period, modal shape, and base shear) are instantly updated, and the static linear analysis is performed, and any other lifetime analysis.

The importance of considering lifetime variable parameters was demonstrated in this workflow. The biological deterioration of the walls showed a clear change in structure behavior, with different walls engaging in rocking behavior or experiencing

plastic deformations (yielding). The impact of a previous seismic event was also clear, with several yielding walls shifting from the top story to the story below. And the renovation impact, adding two whole floors to the structure, greatly impacted the structure's performance. All this information gives the engineer the ability to adjust the initial design such that yielding walls are less prominent even after one earthquake has already occurred, or fungus has begun to grow, or both. They are able to test for events in the future, allowing for more resilient structures to be designed.

Finally, the outputted data to the excel sheet help the engineer to transfer the data to other tools or software for post-processing of the results. This would be useful for performing the non-linear analyses on the walls, or for comparing the results of several designs, or creating charts or visuals to represent the data.

There are currently several limitations on the application of this workflow as it stands. The structure must be rectilinear with a shear wall system. The CLT shear wall construction is limited to multi-or single panel walls with standard hold-downs at the corners and angle brackets along the bottom. The workflow currently assumes a rigid diaphragm for load distribution through the system. The floors must also be structural made of CLT. Concrete and hybrid structures are currently not able to be used with this developed script for structure definition and analysis. The biological deterioration model only considers embedment strength, which only effects the effective stiffness of the wall at the hold-down strengths, due to the modelling strategy used to determine the effective stiffness. It also does not account for mass lost in the CLT or changes in stiffness due to wetting and redrying effects. Furthermore, the calculation of the embedment strength used for the biological degradation analyses seems to be significantly off from experimental research. This is why the hold-downs appeared to reduce in strength significantly after one week of fungal decay in the model, when

in actuality the initial calculated embedment is already lower than the teste yield strength of the hold-down connection. The workflow remains relatively open and easy to edit and add on to, so some of these limitations could be addressed.

Some suggested future improvements include first implementing a non-linear analysis module. This was not completed in this project due to the time frame of the research. The modellings strategy used for determining the effective stiffness of the CLT walls (provided by Rinaldi et al. 2021) is only applicable for static linear analysis, thus a different modelling strategy would need to be implemented. This would greatly improve the workflow. Different options for the model generation would be nice to develop as well. First, a relatively simple improvement, would be providing an analysis path for a timber structure with a flexible diaphragm. Next, it would be useful to include concrete components as part of the structure, as nearly all tall timber structures are positioned on top of a concrete podium, and many have concrete cores. Ultimately, it would be ideal for the shear-frame system to become a modelling option for this workflow, as this is the most prominent structural system for tall timber structures. With this, walls on the top floors would not yield as quickly because the frame will help resist the large deformations at the top. This would require the implementation of column and beam objects in addition to wall and floor objects. Finally, the user interface could be improved upon. Currently, the modules are contained in grasshopper clusters, which works but might be a bit raw and intimidating for those unfamiliar with certain terms.

Overall, the project successfully improves upon the existing practice-oriented seismic analysis process of tall timber structures. It utilizes a modular approach to simplify the process and is well integrated into the main design workspace. It also includes a lifetime analysis portion, allowing for the inclusion of multi-disciplinary factors such as

moisture control into the seismic analysis process. The effect of these lifetime variable parameters was shown to be useful to the engineer via a case study. These interdisciplinary considerations align closely with the core values of the Building Technology program. Finally, the modular nature of this workflow is adaptable; it allows for future developments or other tools or software to be easily integrated with the modules of this workflow, making the workflow itself, future-proof.

7 Resources

Blass, H., and Peter Fellmoser. "Design of Solid Wood Panels with Cross Layers," 2004. <https://www.semanticscholar.org/paper/Design-of-solid-wood-panels-with-cross-layers-Blass-Fellmoser/0ac31e3f0a8923666100baa6e19f6a87c91f7a1a>.

Bogensperger, Thomas, Thomas Moosbrugger, and Gregor Silly. "Verification of CLT-Plates under Loads in Plane," June 2, 2016.

Christovasilis, I. P., L. Riparbelli, G. Rinaldin, and G. Tamagnone. "Methods for Practice-Oriented Linear Analysis in Seismic Design of Cross Laminated Timber Buildings." *_Soil Dynamics and Earthquake Engineering_* 128 (January 1, 2020): 105869. <https://doi.org/10.1016/j.soildyn.2019.105869>.

Dong, Weiqun, Zhiqiang Wang, Jianhui Zhou, Hao Zhang, Yue Yao, Wei Zheng, Meng Gong, and Xinyi Shi. "Embedment Strength of Smooth Dowel-Type Fasteners in Cross-Laminated Timber." *_Construction and Building Materials_* 233 (February 2020): 117243. <https://doi.org/10.1016/j.conbuildmat.2019.117243>.

- "EN1995-1-1 General - Common Rules and Rules for Buildings - DRAFT 2023." In *Eurocode 5: Design of Timber Structures*, 2023. 1263. <https://doi.org/10.3390/buildings12081263>.
- Flaig, M, and H J Blaß. "Shear Strength and Shear Stiffness of CLT-Beams Loaded in Plane," 2013.
- Foster, R.M., and Michael H. Ramage. "Tall Timber." *Nonconventional and Vernacular Construction Materials*, 2020, pp. 467–490, <https://doi.org/10.1016/b978-0-08-102704-2.00017-2>.
- Gavric, Igor, Massimo Fragiaco, and Ario Ceccotti. "Cyclic Behaviour of Typical Metal Connectors for Cross-Laminated (CLT) Structures." *Materials and Structures* 48, no. 6 (June 2015): 1841–57. <https://doi.org/10.1617/s11527-014-0278-7>.
- Gavric, Igor, Massimo Fragiaco, and Ario Ceccotti. "Cyclic Behavior of Typical Screwed Connections for Cross-Laminated (CLT) Structures." *European Journal of Wood and Wood Products* 73, no. 2 (March 2015): 179–91. <https://doi.org/10.1007/s00107-014-0877-6>.
- Gavric, Igor, Massimo Fragiaco, and Ario Ceccotti. "Cyclic Behavior of CLT Wall Systems: Experimental Tests and Analytical Prediction Models." *Journal of Structural Engineering* 141, no. 11 (November 2015): 04015034. [https://doi.org/10.1061/\(ASCE\)ST.1943-541X.0001246](https://doi.org/10.1061/(ASCE)ST.1943-541X.0001246).
- González-Retamal, Marcelo, Eric Forcael, Gerardo Saelzer-Fuica, and Mauricio Vargas-Mosqueda. "From Trees to Skyscrapers: Holistic Review of the Advances and Limitations of Multi-Storey Timber Buildings." *Buildings* 12, no. 8 (August 2022): 1263. <https://doi.org/10.3390/buildings12081263>.
- Ilgin, Hüseyin Emre. "Analysis of the Main Architectural and Structural Design Considerations in Tall Timber Buildings." *Buildings* 14, no. 1 (December 22, 2023): 43. <https://doi.org/10.3390/buildings14010043>.
- Izzi, Matteo, Daniele Casagrande, Stefano Bezzi, Dag Pasca, Maurizio Follesa, and Roberto Tomasi. "Seismic Behaviour of Cross-Laminated Timber Structures: A State-of-the-Art Review." *Engineering Structures* 170 (September 1, 2018): 42–52. <https://doi.org/10.1016/j.engstruct.2018.05.060>.
- Laguarda Mallo, M. F., & Espinoza, O. (2015). Awareness, perceptions and willingness to adopt cross-laminated timber by the architecture community in the United States. *Journal of Cleaner Production*, 94, 198–210. <https://doi.org/10.1016/j.jclepro.2015.01.090>.
- Kennedy, S., A. Salenikovich, W. Munoz, and M. Mohammad. "Design Equations for Dowel Embedment Strength and Withdrawal Resistance for Threaded Fasteners in CLT." *Proceedings of the World Conference on Timber Engineering*, 2014, Quebec, Canada.
- Mitchell, H., Kotsovinos, P., Richter, F., Thomson, D., Barber, D., & Rein, G. (2022). Review of fire experiments in mass timber compartments: Current understanding, limitations, and research gaps. *Fire and Materials*, 47(4), 415–432. <https://doi.org/10.1002/fam.3121>.

- Phillion, Ethan, et al. "Structural fire modeling strategies for exposed mass timber compartments and experimental gaps for model validation." *Journal of Performance of Constructed Facilities*, vol. 36, no. 6, 2022, [https://doi.org/10.1061/\(asce\)cf.19435509.0001761](https://doi.org/10.1061/(asce)cf.19435509.0001761).
- Pozza, Luca, Marco Savoia, Luca Franco, Anna Saetta, and Diego Talledo. "Effect Of Different Modelling Approaches On The Prediction Of The Seismic Response Of Multi-Storey CLT Buildings," 2017. <https://www.witpress.com/elibrary/cmем-volumes/5/6/1930>.
- Pozza, Luca, Roberto Scotta, Davide Trutalli, and Andrea Polastri. "Behaviour Factor for Innovative Massive Timber Shear Walls." *Bulletin of Earthquake Engineering* 13, no. 11 (November 1, 2015): 3449–69. <https://doi.org/10.1007/s10518-015-9765-7>.
- Puettmann, M. E., & Wilson, J. (2005). Life-cycle analysis of wood products: cradle-to-gate LCI of residential wood building materials. *Wood and Fiber Science*, 37, 18–29.
- Rinaldi, Vincenzo, Daniele Casagrande, Catia Cimini, Maurizio Follesa, and Massimo Fragiaco. "An Upgrade of Existing Practice-Oriented FE Design Models for the Seismic Analysis of CLT Buildings." *Soil Dynamics and Earthquake Engineering* 149 (October 1, 2021): 106802. <https://doi.org/10.1016/j.soildyn.2021.106802>.
- Schmidt, Evan, and Mariapaola Riggio. "Monitoring Moisture Performance of Cross-Laminated Timber Building Elements during Construction." *Buildings* 9, no. 6 (June 2019): 144. <https://doi.org/10.3390/buildings9060144>.
- The Efficient Engineer. (2021, April 27). *Understanding the Finite Element Method* [Video]. YouTube. <https://www.youtube.com/watch?v=GHjo pp47vvQ>.
- Udele, Kenneth Emamoke, Jeffrey J. Morrell, Anthony Newton, and Arijit Sinha. "Evaluation of Dowel Bearing Strength of Fungal-Decayed Cross-Laminated Timber." *Wood Material Science & Engineering* 19, no. 3 (May 3, 2024): 564–72. <https://doi.org/10.1080/17480272.2023.269392>.
- Udele, Kenneth Emamoke, Jeffrey J. Morrell, Jed Cappellazzi, and Arijit Sinha. "Characterizing Properties of Fungal-Decayed Cross Laminated Timber (CLT) Connection Assemblies." *Construction and Building Materials* 409 (December 2023): 134080. <https://doi.org/10.1016/j.conbuildmat.2023.134080>.
- Uibel, T., and H.J. Blab. "Joints with Dowel Type Fasteners in CLT Structures." *Focus Solid Timber Solutions—European Conference on Cross Laminated Timber (CLT)*, COST Action FP1004, 2013, pp. 119–134. Graz, Austria.
- Viitanen, Hannu, and Tuomo Ojanen. "Improved Model to Predict Mold Growth in Building Materials." *Thermal Performance of the Exterior Envelopes of Whole Buildings X—Proceedings CD*, 2007.
- Viitanen, Hannu, Juha Vinha, Kati Salminen, Tuomo Ojanen, Ruut Peuhkuri, Leena Paajanen, and Kimmo Lähdesmäki. "Moisture and Bio-Deterioration Risk of Building Materials and Structures." *Journal of Building Physics* 33, no. 3 (January 1,

- 2010): 201–24.
<https://doi.org/10.1177/1744259109343511>.
- Wang, Wei. “Research on Seismic Design of High-Rise Buildings Based on Framed-Shear Structural System.” *_Frontiers Research of Architecture and Engineering_* 3, no. 3 (December 14, 2020): 87–90.
<https://doi.org/10.30564/rae.v3i3.2670>.
- Wang, X., Q. Xu, X. Wang, J. Guo, W. Cao, and C. Xiao. “Strength Degradation of Wood Members Based on the Correlation of Natural and Accelerated Decay Experiments.” *Journal of Renewable Materials* 8, no. 5 (2020): 565–577.
<https://doi.org/10.32604/jrm.2020.09020>.
- Wieringa, R. J., and J. M. G. Heerkens. “The Methodological Soundness of Requirements Engineering Papers: A Conceptual Framework and Two Case Studies.” *Requirements Engineering* 11, no. 4 (September 2006): 295–307.
<https://doi.org/10.1007/s00766-006-0037-6>.
- Yan, Luyue, Yi Li, Wen-Shao Chang, and Haoyu Huang. “Seismic Control of Cross Laminated Timber (CLT) Structure with Shape Memory Alloy-Based Semi-Active Tuned Mass Damper (SMA-STMD).” *_Structures_* 57 (November 1, 2023): 105093.
<https://doi.org/10.1016/j.istruc.2023.105093>.

8 Appendix

8.1 Appendix A

Summary of modelling strategy from Rinaldi et al. 2021

The modelling strategy is a semi-component approach, utilizing representative equations to capture the deformation effects from the connections in the overall wall behavior. This style helps to reduce computational power and time required to create the model. It is an upgraded version of the model proposed by Christovasilis et al. (2020), now including the effects from rocking. This modelling strategy has slightly different equations for single panel vs multi-panel shear walls, because rocking behavior for multi-panel walls is considered negligible.

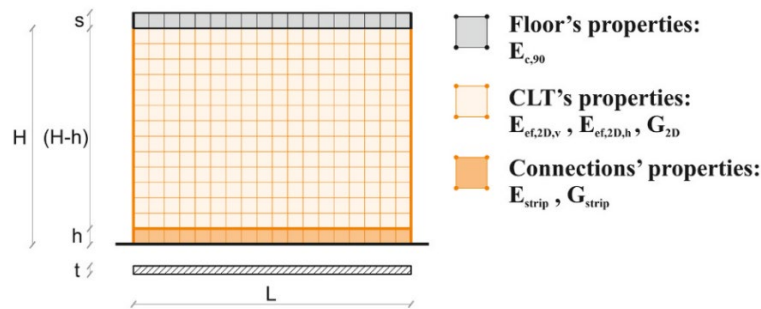


Figure __ – CLT shear wall modelling strategy, 2D elements (Rinaldi et al. 2021)

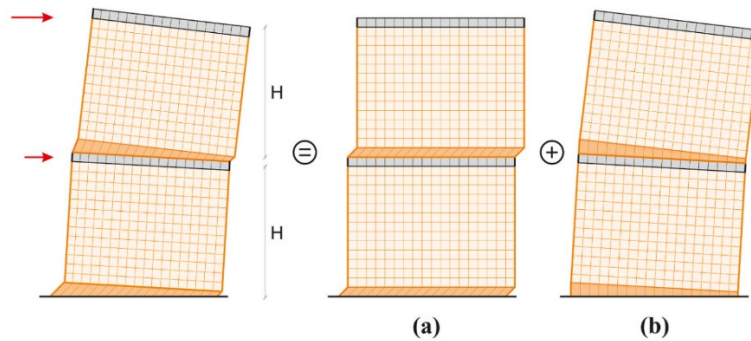


Figure __ – Multi-story wall deformation, contributions from (a) sliding and (b) rocking (Rinaldi et al. 2021)

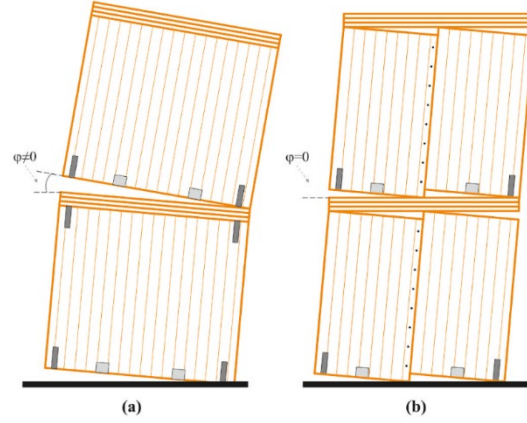


Figure __ – The deformation from rocking behavior for (a) single-panel walls vs (b) multi-panel walls (Rinaldi et al. 2021)

Equivalent properties for bottom strip

Rocking Stiffness

$$K_r = \frac{M_{0.4HD,y}}{d_{0.4HD,y}H}$$

Sliding Stiffness

$$K_s = n_{AB}k_{AB,s} + n_{HD}k_{HD,s}$$

Single-panel walls

Equivalent Shear Modulus

$$G_{strip} = K_s \frac{h}{Lt}$$

Equivalent Modulus of Elasticity

$$E_{strip} = \begin{cases} K_r \frac{12H^2h}{L^3t} \leq E_{ef,2D,v}, & \text{where } M_{stab} = \frac{wL^2}{2} < M_{0.4HD,y} \\ E_{ef,2D,v}, & \text{where } M_{stab} = \frac{wL^2}{2} \geq M_{0.4HD,y} \end{cases}$$

Overturning Moment

$$M_{HD,y} = L \left[F_{y,HD,up} + \frac{u_{HD,y}k_{AB,up}}{L^2} \sum_0^{n_{AB}} x_i^2 + \frac{wL}{2} \right]$$

Lateral Displacement @ 40% the Overturning Moment

$$d_{0.4HD,y} = \frac{M_{0.4HD,y} - 0.5wL^2}{L^2 k_{HD,up} + k_{AB,up} \sum_0^{n_{AB}} x_i^2} H$$

Multi-panel walls

Equivalent Shear Modulus

$$G_{strip} = \begin{cases} \left(\frac{1}{K_r} + \frac{1}{K_s} \right)^{-1} \frac{h}{Lt} \leq K_s \frac{h}{Lt}, & \text{if } M_{stab} = \frac{mwb_{clt}^2}{2} < M_{0.4HD,y} \\ K_s \frac{h}{Lt}, & \text{if } M_{stab} = \frac{mwb_{clt}^2}{2} \geq M_{0.4HD,y} \end{cases}$$

Equivalent Modulus of Elasticity

$$E_{strip} = E_{ef,2D,v}$$

Overturning Moment

$$M_{HD,y} = b_{CLT} \left[F_{y,HD,up} \left(1 + \frac{1}{b_{CLT}^2} \frac{k_{AB,up}}{k_{HD,up}} \sum_0^{n_{AB}} x_i^2 \right) + (m-1)n_{SC}F_{y,SC} + \frac{wmb_{CLT}}{2} \right]$$

Lateral Displacement @ 40% the Overturning Moment

$$d_{0.4HD,y} = \frac{M_{0.4HD,y} - 0.5wb_{CLT}^2 m}{b_{CLT}^2 \left[k_{HD,up} + (m-1)n_{SC}k_{SC} + \frac{k_{AB,up}}{b_{CLT}^2} \sum_0^{n_{AB}} x_i^2 \right]} H$$

where:

$E_{ef,2D,v}$ is the effective modulus of elasticity of the CLT along the vertical direction

$F_{y,HD,up}$ is the hold-down yield tensile strength

$F_{y,SC}$ is the shear strength of each fastener

$M_{0.4HD,y}$ is 40% of the overturning moment capacity at the holddown yielding

$M_{HD,y}$	is the overturning moment capacity at the holddown yielding
M_{stab}	is the stabilizing moment
b_{CLT}	is the length of each CLT panel
$d_{0.4HD,y}$	is the lateral top displacement related to $M_{0.4HD,y}$
$k_{AB,s}$	is the angle bracket stiffness along horizontal (shear) direction
$k_{AB,up}$	is the angle-bracket stiffness along vertical (tensile) direction
$k_{HD,s}$	is the hold-down stiffness along horizontal (shear) direction
$k_{HD,up}$	is the hold-down stiffness along vertical (tensile) direction
k_{SC}	is the stiffness of each fastener along the vertical joint
n_{AB}	is the number of angle brackets
n_{HD}	is the number of hold-downs
n_{SC}	is the number of fasteners along the vertical joint
$u_{HD,y}$	is the yield displacement of hold-down along vertical (tensile) direction
x_i	is the distance of the angle bracket i-th from the centre of rotation of the CLT panel
h	is the height of the horizontal bottom strip
H	is the height of the shearwall panel
L	is the length of the shearwall
m	is the number of panels
t	is the thickness of the CLT panel
w	is the vertical load per unit length

8.2 Appendix B

Summary of CLT property calculations via Blass and Fellmoser (2004)

Blass and Fellmoser (2004) put forth a method of calculating the modulus of elasticity various loading cases based on the material properties of the timber pieces which make up the panel. These are summarized in the tables below. This method for calculating the stiffness of the CLT panels has been tested repeatedly by various researchers against experimental values for CLT panels and has been used in various analytical modelling verifications.

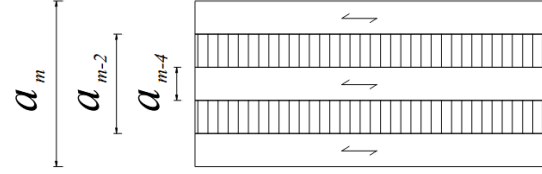


Figure B.1 – Build-up and terms of solid wood panel with cross layers (with $m = 5$)

Table B.1 - Summary of compositions factors k_i for solid wood panels with cross layers

Loading diagrams	k_i
	$k_1 = 1 - \left(1 - \frac{E_{90}}{E_0}\right) \frac{\alpha_{m-2}^3 - \alpha_{m-4}^3 + \dots \pm \alpha_1^3}{\alpha_m^3}$
	$k_2 = \frac{E_{90}}{E_0} + \left(1 - \frac{E_{90}}{E_0}\right) \frac{\alpha_{m-2}^3 - \alpha_{m-4}^3 + \dots \pm \alpha_1^3}{\alpha_m^3}$
	$k_3 = 1 - \left(1 - \frac{E_{90}}{E_0}\right) \frac{\alpha_{m-2} - \alpha_{m-4} + \dots \pm \alpha_1}{\alpha_m}$
	$k_4 = \frac{E_{90}}{E_0} + \left(1 - \frac{E_{90}}{E_0}\right) \frac{\alpha_{m-2} - \alpha_{m-4} + \dots \pm \alpha_1}{\alpha_m}$

Table B.2 - Effective values of strength and stiffness for solid wood panels with cross layers

Loading type	To the grain	Effective strength value	Effective stiffness value
Perpendicular to plane loading			
Bending	Parallel	$f_{m,0,ef} = k_1 f_{m,0}$	$E_{m,0,ef} = k_1 E_0$
	Perpendicular	$f_{m,90,ef} = k_2 f_{m,0} (\alpha_m / \alpha_{m-2})$	$E_{m,90,ef} = k_2 E_0$
In plane loading			
Bending	Parallel	$f_{m,0,ef} = k_3 f_{m,0}$	$E_{m,0,ef} = k_3 E_0$
	Perpendicular	$f_{m,90,ef} = k_4 f_{m,0}$	$E_{m,90,ef} = k_4 E_0$
Tension	Parallel	$f_{t,0,ef} = k_3 f_{t,0}$	$E_{t,0,ef} = k_3 E_0$
	Perpendicular	$f_{t,90,ef} = k_4 f_{t,0}$	$E_{t,90,ef} = k_4 E_0$
Compression	Parallel	$f_{c,0,ef} = k_3 f_{c,0}$	$E_{c,0,ef} = k_3 E_0$
	Perpendicular	$f_{c,90,ef} = k_4 f_{c,0}$	$E_{c,90,ef} = k_4 E_0$

Example of CLT property calculation

The properties required for this seismic analysis model include:

$$E_{90} = E_{m,0,ef} = k_1 E_0$$

$$E_v = E_{m,0,ef} = k_3 E_0$$

$$E_h = E_{m,90,ef} = k_4 E_0$$

For a 5-layer CLT panel with lay-up pattern 40-20-40-20-40 made of C24 timber with $E_0 = 11,000$ MPa and $E_{90} = 370$ MPa, the modulus of elasticity in each direction is calculated as:

$$\alpha_5 = 40 + 20 + 40 + 20 + 40 = 160 \text{ mm}$$

$$\alpha_3 = 20 + 40 + 20 = 80 \text{ mm}$$

$$\alpha_1 = 40 \text{ mm}$$

$$k_1 = 1 - \left(1 - \frac{370}{11000}\right) \frac{80^3 - 40^3}{160^3} = 0.894$$

$$k_3 = 1 - \left(1 - \frac{370}{11000}\right) \frac{80 - 40}{160} = 0.758$$

$$k_4 = \frac{370}{11000} + \left(1 - \frac{370}{11000}\right) \frac{80 - 40}{160} = 0.275$$

$$E_{90} = k_1 E_0 = 0.894(11000) = 9837 \text{ MPa}$$

$$E_v = k_3 E_0 = 0.758(11000) = 8343 \text{ MPa}$$

$$E_h = k_4 E_0 = 0.275(11000) = 3028 \text{ MPa}$$

8.3 Appendix C

Summary of CLT shear modulus calculations via Bogensperger et al. 2016

The research done by Bogensperger et al. (2016) has been used to calculate the effective shear modulus of CLT panels. It was determined that if the timber boards in each layer were glued together along the narrow face, the shear stiffness of the CLT panel would be equivalent to that of the individual timber boards. If this is not the case, the effective shear stiffness for the CLT panel would be a ratio of that of the timber boards. This method has been referenced repeatedly by other researchers and has been tested and peer-reviewed thoroughly.

$$G^* = \frac{G_{0,mean}}{1 + 6\alpha_{FE-FIT,ortho} \left(\frac{t}{a}\right)^2}$$

where:

- $G_{0,mean}$ is the shear modulus of the
- $\alpha_{FE-FIT,ortho}$ is the correction function
- t is the average board thickness
- a is the average board width

Three versions of the correction function were developed by the research team, a general one, one calibrated for 3-layer CLT panels, and one calibrated for 5-layer CLT panels.

$$\alpha_{FE-FIT,ortho} = 0.3117 \left(\frac{t}{a}\right)^{-0.7474}$$

$$\alpha_{FE-FIT,ortho,3} = 0.5345 \left(\frac{t}{a}\right)^{-0.7947}$$

$$\alpha_{FE-FIT,ortho,5} = 0.4253 \left(\frac{t}{a}\right)^{-0.7941}$$

Example of CLT shear modulus calculation

For a 5-layer CLT panel with lay-up pattern 40-20-40-20-40 made of C24 timber with $G_{0,mean} = 690 \text{ MPa}$, and an average board width of 76.5 mm, the shear modulus is calculated as:

$$t = \frac{40 + 20 + 40 + 20 + 40}{5} = 32 \text{ mm}$$

$$\alpha_{FE-FIT,ortho,5} = 0.4253 \left(\frac{32}{76.5}\right)^{-0.7941} = 0.8497$$

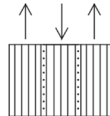
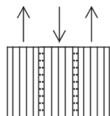
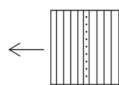

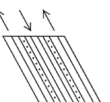

$$G^* = \frac{690}{1 + 6(0.8497) \left(\frac{32}{76.5} \right)^2} = 416 \text{ MPa}$$

8.4 Appendix E

Summary of connection and full wall tests conducted by Gavric et al. 2015

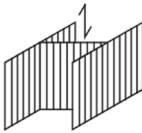
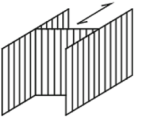
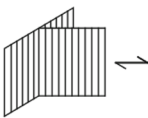
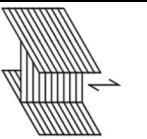
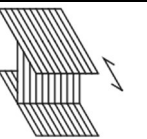
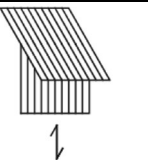
8.4.1 E.1 Cyclical behavior of screwed connections in CLT

Table E.1 – Mechanical properties of parallel panel–panel screwed CLT connections

												
Test	1		2		3		4		11		12	
Loading Direction	Lateral parallel		Lateral parallel		Lateral perpendicular		Lateral perpendicular		Lateral parallel		Lateral perpendicular	
	(lap joint)		(splice joint)		(lap joint)		(splice joint)		(lap joint)		(lap joint)	
Type and number of screws	HBS $\phi 8 \times 80 \text{ mm}$		HBS $\phi 8 \times 80 \text{ mm}$		HBS $\phi 8 \times 80 \text{ mm}$		HBS $\phi 8 \times 80 \text{ mm}$		HBS $\phi 10 \times 140 \text{ mm}$		HBS $\phi 10 \times 140 \text{ mm}$	
	2x2 screws		2x4 screws		2 screws		2x2 screws		2x2 screws		2 screws	
	\bar{x}_{mean}	COV	\bar{x}_{mean}	COV	\bar{x}_{mean}	COV	\bar{x}_{mean}	COV	\bar{x}_{mean}	COV	\bar{x}_{mean}	COV
k_{el} (kN/mm)	1.24	18.5 9	0.84	16.2 8	1.25	29.6 5	0.94	17.0 2	1.27	20.6 7	0.83	6.98
k_{pl} (kN/mm)	0.11	20.0 1	0.1	39.8 1	0.21	29.6 5	0.16	17.0 2	0.21	20.6 7	0.14	6.98
F_y (kN)	3.23	11.9 5	4.85	17.6 7	2.91	17.6 4	3.23	7.02	6.67	10.2 3	6.91	9.36
v_y (mm)	2.55	11.9 9	5.7	22.7 5	2.34	24.1 7	3.13	20.0 5	5.39	26.9 1	7.3	14.7 8
F_{max} (kN)	5.25	13.1 8	7.33	11.8 9	4.91	24.4 1	6.4	4.96	10.1	4.28	9.83	11.7 5
$F_{max(3rd)}$ (kN)	3.69	14.9 3	5.24	12.6 1	4.07	23.9 2	5.62	5.77	7.39	8.8	7.75	22.9 3
v_{max} (mm)	23.5	9.81	34.3 7	17.4	17.5 1	28.8 4	39.4	8.9	29.8 3	0.12	31.5 9	28.2 2
F_u (kN)	4.2	13.1 8	5.86	11.8 9	3.93	24.4 2	5.12	4.94	8.08	4.29	7.87	11.7 5

v_u (mm)	31.5 5	2.48	37.6 6	8.79	23.7 6	17.7 9	50.5 2	16.2 8	33.5 9	18.6 6	41.1 7	15.6 1
D	12.8 1	10.3 4	7.15	21.2	10.7 1	31.6 9	16.3 6	14.1 8	6.58	10.2 3	5.74	23.8 5
D_{mon}	15.9 8	-	14.4 3	-	20.9 7	-	15.6 6	-	13.4 4	-	8.99	-
F_{30} (kN)	4.61	15.9 8	7.81	12.5 9	-	-	6.02	2.82	9.44	13.3 1	9.16	15.7 8
D_{30}	12.1 2	11.0 1	7.3	21.4 9	-	-	9.91	20.1 9	6.14	21.7 3	4.2	16.8 7
ΔF_{1-3} (%)	29.6 1	17.6 7	28.3 7	16.1 2	13.9 3	14.1	10.4 4	5.73	26.7 3	24.5 4	13.1 7	13.0 4
$v_{eq(1st)}$ (%)	14.5 2	6.71	14.7 2	10.4 8	5.98	10.5 6	5.81	9.41	22.2	4.12	8.58	13.7 3
$v_{eq(3rd)}$ (%)	9.12	23.3 7	11.2 7	14.8 6	2.97	19.3	3.3	13.9 3	15.1 7	7.63	2.49	12.1 6
$F_{0.05}$ (kN)	3.81	-	5.62	-	2.64	-	5.23	-	9.13	-	7.3	-
$F_{0.95}$ (kN)	7.14	-	8.56	-	8.67	-	7.45	-	11.1 6	-	13.0 8	-
γ_{Rd}	1.88	-	1.52	-	3.28	-	1.42	-	1.22	-	1.79	-

Table E.2 – Mechanical properties of orthogonal panel–panel screwed CLT connections

Test												
	5		6		7		8		9		10	
Loading Direction	Lateral parallel		Lateral perpendicular		Withdrawal		Lateral parallel		Lateral perpendicular		Withdrawal	
Type and number of screws	HBS φ10x180mm 2x2 screws		HBS φ10x180mm 2x2 screws		HBS φ10x180mm 4 screws		HBS φ10x260mm 2x2 screws		HBS φ10x260mm 2x2 screws		HBS φ10x260mm 4 screws	
	x_{mean}	COV	x_{mean}	COV	x_{mean}	COV	x_{mean}	COV	x_{mean}	COV	x_{mean}	COV
k_{el} (kN/mm)	1.49	21.1 1	1.3	21.3 6	2.9	6.21	1.45	22.4 4	0.97	13.6	4.08	11.7 6
k_{pl} (kN/mm)	0.25	21.1 1	0.22	21.3 6	0.19	14.1 3	0.24	22.4 4	0.16	13.6	0.23	15.3
F_y (kN)	5.25	6.96	5.29	22.2 3	4.66	13.0 3	5.04	16.9 6	5.84	8.97	5.08	18.6 3
v_y (mm)	3.44	13.3 6	4.22	23.4 5	1.75	15.7 5	3.59	26.8 3	5.95	18.8 6	1.3	23.5 1
F_{max} (kN)	7.54	6.82	7.92	16.4 7	7.83	7.27	7.87	13.8 9	8.53	7.13	8.1	7.78
$F_{max(3rd)}$ (kN)	5.95	9.12	6.14	19.0 2	6.55	8.27	6.22	17.2 5	6.93	9.84	6.41	5.39
v_{max} (mm)	23.1	22.6 4	27.3	13.7 9	28.0	15.2 4	27.1	16.7 6	28.5	10.4 8	18.5	10.3 6
F_u (kN)	6.03	6.81	6.34	16.4 5	6.27	7.27	6.3	13.8 9	6.82	7.11	6.52	7.4
v_u (mm)	31.9	3.27 4	31.8	0.61 2	49.5	14.3 8	32.2	2.72 5	48.2	18.5 7	28.9	17.1 6
D	9.65	16.7 7	10.8	25.0 1	28.7	16.8 5	10.0	33.9 5	8.9	23.6 6	23.8	35.5 3

D_{mon}	17.2 7	-	16.3 5	-	21.8 5	-	30.6 1	-	21.5 7	-	27.7 4	-
F_{30} (kN)	6.67	3.18	7.46	15.4	7.66	8.32	7.26	13.6 8	8.17	7.12	-	-
D_{30}	9.04	15.4 3	10.3 4	24.0 2	17.5 2	14.1 7	8.92	37.4 7	5.57	17.9 3	-	-
ΔF_{1-3} (%)	19.5 3	28.5 2	20.2 2	27.7 6	10.5 4	24.5 6	20.8 6	23.8 1	18.7	20.5	14.9 4	20.3 3
$v_{eq(1st)}$ (%)	17.3 1	4.38	18.2	9.51	8.25	10.0 6	17.7 5	6.44	15.0 5	9.09	9.17	6.74
$v_{eq(3rd)}$ (%)	13.2 9	4.68	12.4 1	21.6 6	1.32	7.62	13.8 7	8.18	11.0	14.4 6	2.15	8.49
$F_{0.05}$ (kN)	6.41	-	5.27	-	6.59	-	5.59	-	7.16	-	6.75	-
$F_{0.95}$ (kN)	8.83	-	11.6 3	-	9.27	-	10.9 1	-	10.1 1	-	9.67	-
γ_{Rd}	1.38	-	2.21	-	1.41	-	1.95	-	1.41	-	1.43	-

8.4.2 E.2 Cyclical behavior of typical metal connectors in CLT

Table E.3 – Mechanical properties of orthogonal panel–panel screwed CLT connections

	Metal connector	Nails no.	Connection type	Loading direction	Cyclic test no.	No. of cycles	F_{max} (kN)	$F_{max(3rd)}$ (kN)
1	Hold-down WHT540	12	CLT– foundation	Tension	6	3	48.33	41.33
2	Hold-down WHT440	9	CLT–CLT	Tension	6	3	36.21	31.27
3	Hold-down WHT540	12	CLT– foundation	Shear	6	3	9.98	9.17
4	Hold-down WHT440	9	CLT–CLT	Shear	6	3	7.88	6.85
5	Angle bracket BMF 90 × 116 × 48 × 3	11	CLT– foundation	Tension	6	3	23.47	18.59
6	Angle bracket BMF 100 × 100 × 90 × 3	8	CLT–CLT	Tension	6	3	12.57	10.96

7	Angle bracket BMF 90 × 116 × 48 × 3	11	CLT– foundation	Shear	6	3	26.85	18.8
8	Angle bracket BMF 100 × 100 × 90 × 3	8	CLT–CLT	Shear	6	3	19.91	14.26

Table E.4 – Mechanical properties of hold-down connections^a

Test	1		2		3		4	
	x_{mean}	COV	x_{mean}	COV	x_{mean}	COV	x_{mean}	COV
k_{el} (kN/mm)	4.51	14.31	2.65	19.27	3.4	33.25	1.56	16.2
k_{pl} (kN/mm)	0.75	14.24	0.44	19.13	0.28	7.27	0.21	5.43
F_y (kN)	40.46	8.11	32.21	4.52	3.61	35.59	2.72	28.13
v_y (mm)	8.81	21.76	11.91	19.83	1.13	42.3	1.71	17.23
F_{max} (kN)	48.33	5.37	36.21	5.45	-	-	-	-
$F_{max(3rd)}$ (kN)	41.33	7.53	31.27	7.68	-	-	-	-
v_{max} (mm)	20.3	14.17	21.52	11.0	-	-	-	-
F_u (kN)	38.79	5.31	30.22	12.8	-	-	-	-
v_u (mm)	23.75	13.82	22.99	9.51	-	-	-	-
D	2.76	16.21	1.97	13.75	-	-	-	-
F_{30} (kN)	-	-	-	-	9.98	7.03	7.88	4.78
D_{30}	-	-	-	-	31.26	43.5	18.73	20.0
ΔF_{1-3} (%)	15.9	34.59	66.3	9.05	12.45	25.48	10.98	20.18
$v_{eq(1st)}$ (%)	8.5	5.7	8.11	9.98	19.84	13.91	21.38	6.93
$v_{eq(3rd)}$ (%)	2.78	17.29	3.6	24.4	14.63	17.79	16.09	14.86
$F_{0.05}$ (kN)	42.4	-	31.59	-	8.48	-	7.04	-
$F_{0.95}$ (kN)	54.95	-	41.4	-	11.7	-	8.8	-
γ_{Rd}	1.3	-	1.31	-	1.38	-	1.25	-

^a according to EN 12512 with overstrength factors (γ_{Rd})**Table E.5 – Mechanical properties of angle bracket connections^a**

Test	5		6		7		8	
	x_{mean}	COV	x_{mean}	COV	x_{mean}	COV	x_{mean}	COV

k_{el} (kN/mm)	2.53	9.72	2.98	22.05	2.09	16.41	1.1	12.34
k_{pl} (kN/mm)	0.42	10.11	0.5	22.01	0.35	16.56	0.18	11.95
F_y (kN)	19.22	2.73	11.12	9.69	22.98	5.19	16.61	7.46
v_y (mm)	7.26	9.04	3.97	28.12	11.74	5.87	13.73	7.27
F_{max} (kN)	23.47	4.32	12.57	7.71	26.85	3.15	19.91	6.95
$F_{max(3rd)}$ (kN)	18.59	9.72	10.96	7.8	18.8	10.25	14.26	9.75
v_{max} (mm)	17.69	9.62	7.1	10.62	28.51	14.75	29.09	7.01
F_u (kN)	18.74	4.32	10.06	7.68	21.48	3.15	15.86	7.59
v_u (mm)	23.19	6.14	20.01	46.39	31.86	0.33	52.26	2.21
D	3.21	6.86	5.4	54.2	2.63	6.03	3.97	10.81
ΔF_{1-3} (%)	22.85	32.43	9.26	9.32	32.59	9.31	28.2	6.79
$v_{eq(1st)}$ (%)	12.33	5.43	7.4	11.71	22.75	5.93	17.49	5.59
$v_{eq(3rd)}$ (%)	7.07	19.17	1.74	10.9	14.01	6.84	11.17	14.15
$F_{0.05}$ (kN)	21.16	-	10.45	-	24.89	-	16.8	-
$F_{0.95}$ (kN)	26.0	-	15.05	-	28.93	-	23.49	-
γ_{Rd}	1.23	-	1.44	-	1.16	-	1.4	-

^a according to EN 12512 with overstrength factors (γ_{Rd})

8.4.3 E.3 Cyclical behavior of full scale CLT walls

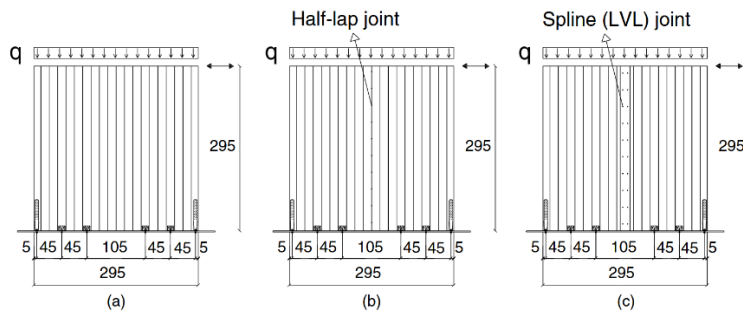


Figure E.1 – Wall panel test configurations: (a) configuration I—single walls; (b) configuration II—coupled walls with half-lap joint; (c) configuration III—coupled walls with spline (LVL) joint (measures in cm)

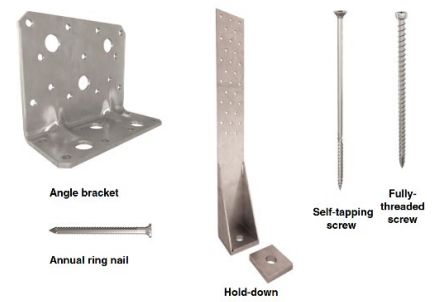


Figure E.2 – Metal connectors and fasteners used in CLT wall tests

Table E.6 – Wall configurations tested

	I.1	I.2	I.3	I.4 ^a	II.1	II.2 ^a	II.3	II.4
No. of hold-downs	2	2	2	2	2	2	2	4
No. of angle brackets	2	4	4	4	4	4	4	4
No. of screws in vertical joints	—	—	—	—	20	20	10	5
Vertical load (kN/m)	18.5	18.5	9.25	18.5	18.5	18.5	18.5	18.5
	III.1	III.2	III.3	III.4	III.5	III.6	III.7	III.8 ^b
No. of hold-downs	2	2	4	2	2	2	2	2
No. of angle brackets	4	4	4	4	4	4	4	4
No. of screws in vertical joints	2 × 20	2 × 10	2 × 5	2 × 10	2 × 10	2 × 10	2 × 10	2 × 10
Vertical load (kN/m)	18.5	18.5	18.5	18.5	18.5	0.0	18.5	18.5

^a Nails were positioned in lower holes of hold-downs

^b Screws in the vertical joint were doubly inclined (35° in vertical direction and 35° in horizontal direction)

Table E.7 – Mechanical properties of tested CLT wall panels^a

	I.1	I.2	I.3	I.4	II.1	II.2	II.3	II.4
k_{el} (kN/mm)	4.69	4.78	4.97	3.86	5.77	5.28	4.48	4.4
k_{pl} (kN/mm)	0.78	0.8	0.83	0.64	0.96	0.88	0.75	0.73
F_y (kN)	50.0	87.4	79.0	97.4	69.2	65.5	65.4	69.2
v_y (mm)	10.0	17.0	14.8	23.6	11.0	11.7	13.7	14.6
F_{max} (kN)	70.7	104.2	100.5	106.7	97.2	92.3	84.4	93.1
$F_{max(3rd)}$ (kN)	50.4	87.0	83.4	91.8	79.9	70.4	72.3	81.9
v_{max} (mm)	38.7	57.3	42.8	46.7	56.2	45.1	46.9	54.3

F_u (kN)	56.5	83.4	80.4	85.4	77.8	73.8	67.5	74.5
v_u (mm)	39.0	57.3	56.6	56.7	73.3	65.4	76.0	73.7
D	4.0	3.4	3.9	2.5	6.7	5.6	5.7	5.1
ΔF_{1-3} (%)	28.5	14.8	14.3	13.3	14.9	18.8	14.2	11.5
E_d (kJ)	12.9	23.8	20.2	27.9	25.5	23.8	28.1	27.8
$v_{eq(1st)}$ (%)	19.6	16.2	16.8	17.0	16.3	16.4	15.7	13.9
$v_{eq(3rd)}$ (%)	18.0	11.5	9.7	13.3	14.3	15.7	10.6	8.9
	III.1	III.2	III.3	III.4	III.5	III.6	III.7	III.8
k_{el} (kN/mm)	5.17	3.5	4.32	3.13	3.77	2.82	4.84	3.84
k_{pl} (kN/mm)	0.86	0.58	0.72	0.52	0.63	0.47	0.81	0.64
F_y (kN)	72.1	67.6	80.4	61.7	68.1	46.5	60.0	64.9
v_y (mm)	12.8	17.6	17.4	17.8	16.8	15.3	11.6	15.9
F_{max} (kN)	102.5	91.8	102.9	82.4	86.4	63.4	84.6	79.3
$F_{max(3rd)}$ (kN)	89.7	79.5	88.6	71.1	72.4	53.3	70.3	66.5
v_{max} (mm)	56.4	66.0	56.0	76.3	59.6	55.7	57.4	37.5
F_u (kN)	82.0	73.5	82.3	65.9	69.1	50.7	67.7	63.4
v_u (mm)	76.4	76.1	75.7	76.2	79.6	75.2	77.4	77.4
D	6.0	4.4	4.3	4.3	4.7	4.9	6.7	5.0
ΔF_{1-3} (%)	12.0	11.6	13.5	11.7	14.9	15.9	15.4	14.8
E_d (kJ)	38.0	29.3	29.3	26.0	31.6	12.1	26.8	26.1
$v_{eq(1st)}$ (%)	15.3	13.9	14.4	13.4	15.8	13.3	14.7	15.7
$v_{eq(3rd)}$ (%)	11.5	10.1	9.3	9.5	11.0	7.9	9.7	9.7
^a according to EN 12512								

Table E.8 – Contribution of Deformability Components to Total Lateral Deflection of Walls (δ_{tot})

I.1	I.2	I.3	I.4	II.1	II.2	II.3	II.4
-----	-----	-----	-----	------	------	------	------

[illegible]

8.5 Appendix F

Summary of reviewed and proposed models for CLT embedment strength per Dong et al. 2020

Dong et al. (2020) reviewed four different calculation models of embedment strengths for dowel-type fasteners CLT. This was done by using the calculation models to predict the embedment strength of 33 different CLT configurations, and these values were then compared to the experimental results of these same configurations. Twenty replicas of each configuration type were tested, and then the research team created their own calculation model to address the discrepancies found in the four models they reviewed. Overall, the calculation models follow the format of the Hankinson formula:

$$f_{\theta} = \frac{f_0 f_{90}}{f_0 \sin^2(\theta) + f_{90} \cos^2(\theta)}$$

where:

- f_0 the embedment strength parallel to the grain
- f_{90} the embedment strength perpendicular to the grain
- θ the angle of the load to the grain of face layer

For the following calculation models, the variables used are defined as:

- $f_{\theta,avg}$ average embedment strength (MPa)
- $f_{\theta,k}$ characteristic embedment strength (MPa)
- d fastener nominal diameter (mm)
- θ loading angle relative to the grain of face layer (°)
- ρ_{12} measured density based on volume and mass at 12% moisture content (g/cm³)
- $\rho_{12,k}$ characteristic density based on volume and mass at 12% moisture content (g/cm³)
- G_0 measured relative density for the species or species group based on oven-dry mass and volume
- G mean relative density for the species or species group based on oven-dry mass and volume

8.5.1 F.1 Design equations by Uibel and Blaß (2013)

Uibel and Blass (2013) developed two different calculation models for smooth dowels inserted into the face of a CLT panel. The validity of this study is limited to the maximum layer thickness of 40 mm and the ratio of thickness of the longitudinal and transverse layers being between 0.95 and 2.1.

The first is general and independent of panel layout type:

$$f_{\theta,avg,UB1} = \frac{105.7(1 - 0.015d)\rho_{12}^{1.16}}{1.1\sin^2\theta + \cos^2\theta}$$

The second accounts for panel layout:

$$f_{\theta,avg,UB2} = 111.7(1 - 0.016d)\rho_{12}^{1.16} \times \left[\frac{\sum_{i=1}^n t_{0,i}}{t(1.2\sin^2\theta + \cos^2\theta)} + \frac{\sum_{j=1}^{n-1} t_{90,j}}{t(1.2\cos^2\theta + \sin^2\theta)} \right]$$

where:

- t the total thickness of CLT
- $t_{0,i}$ the thickness of individual longitudinal layer
- $t_{90,j}$ the thickness of individual transverse layer

Finally, the characteristic embedment strength of dowels in CLT (based on the first equation) is reduced to:

$$f_{\theta,k,UB} = \frac{93.6(1 - 0.015d)\rho_{12,k}^{1.16}}{1.1\sin^2\theta + \cos^2\theta}$$

When compared to the experimental tests conducted by Dong et al. (2013), it was found that over 80% of the calculated values for both equations predicting average embedment strength were overestimating the test values. This was similarly true for the estimation of the characteristic value for embedment strength.

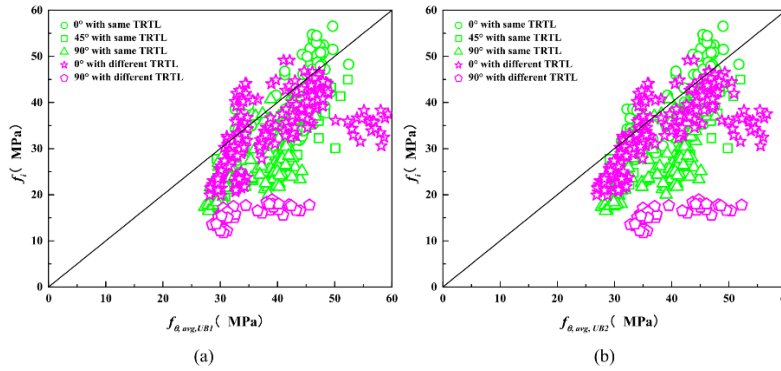


Figure F.1 – Comparisons between test values (f_i) and predicted values: (a) $f_{\theta,avg,UB1}$ and (b) $f_{\theta,avg,UB2}$

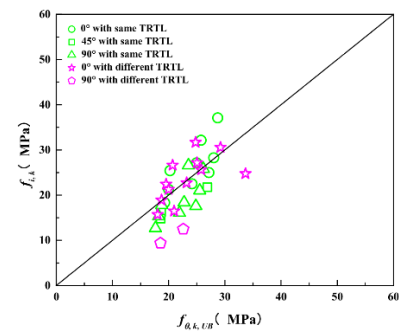


Figure F.2 – Comparison of characteristic embedment strength between test data ($f_{i,k}$) adjusted to standard load duration and predicted values ($f_{\theta,k,UB}$)

8.5.2 F.2 Design equations by Kennedy et al. (2014)

Kennedy et al. (2014) conducted 720 embedment tests with lag screws and 360 embedment tests with self-drilling screws in Canadian CLT with diameters ranging from 6.0-19.1 mm. A non-linear regression model independent of panel layup and fastener diameter was developed:

$$f_{\theta,avg,Ken} = \frac{80(\rho_{12} - 0.12)^{1.11}}{1.07(\rho_{12} - 0.12)^{-0.07} \sin^2 \theta + \cos^2 \theta}$$

The characteristic embedment strength of dowels in CLT is reduced to:

$$f_{\theta,k,Ken} = \frac{41(\rho_{12} - 0.12)^{1.11}}{1.07(\rho_{12} - 0.12)^{-0.07} \sin^2 \theta + \cos^2 \theta}$$

When compared to the experimental tests conducted by Dong et al. (2013), it was found that over 70% of the calculated values predicting the average embedment strength were underestimating the test values. Similarly, the characteristic equation provide conservative values.

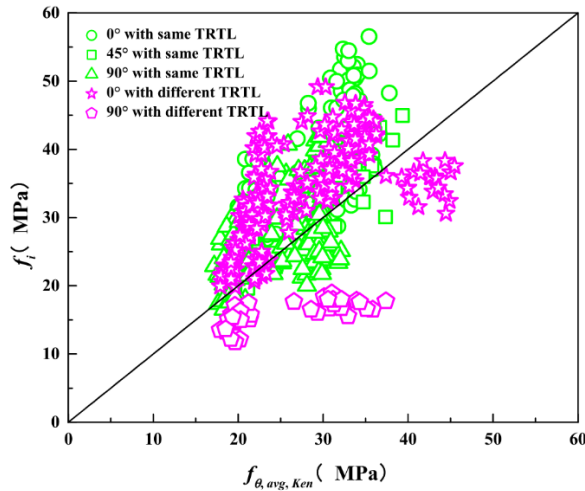


Figure F.3 – Comparisons between test values (f_i) and predicted values ($f_{\theta,avg,Ken}$)

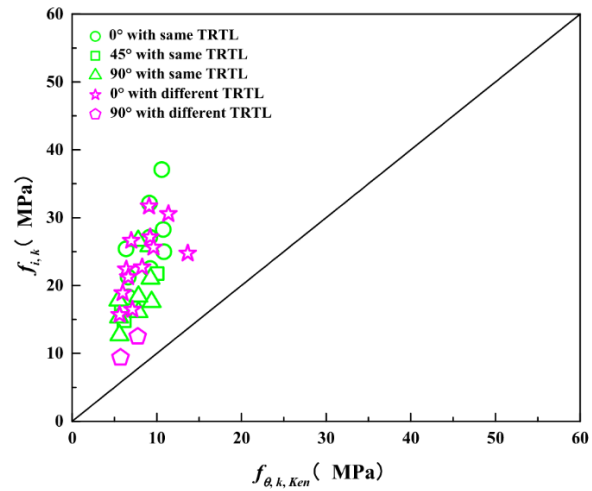


Figure F.4 – Comparison of characteristic embedment strength between test data ($f_{i,k}$) adjusted to standard load duration and predicted values ($f_{\theta,k,Ken}$)

8.5.3 F.3 Design equations provided by the National Design Specification

The National Design Specification for Wood Construction (NDS) presents a design model for the embedment strengths of dowel-type fasteners in CLT, considering its layup characteristics. According to its model, the embedment strength of the face layer is associated with the “effective” bearing length of the fastener, which is adjusted in proportion to the embedment strengths of the cross layer and parallel layer. If applied directly to the embedment strength of the CLT, this model is expressed as:

$$f_{\theta,CLT} = \frac{l_0 f_{\theta} + l_{90} f_{90-\theta}}{l_p}$$

where:

- l_0 the fastener bearing length in parallel layer(s)
- l_{90} the fastener bearing length in cross layer(s)
- l_p the total bearing length of fastener in CLT panel
- f_{θ} the embedment strength of parallel layer(s)
- $f_{90-\theta}$ the embedment strength of cross layer(s)

The average and characteristic value equations for the embedment strength of an individual layer parallel and perpendicular to the grain are:

$$f_{avg} = \begin{cases} f_{0,avg} = 77G_0 \\ f_{90,avg} = 212G_0^{1.45}d^{-0.5} \end{cases}$$

$$f_k = \begin{cases} f_{0,k} = 44G \\ f_{90,k} = 105G^{1.45}d^{-0.5} \end{cases}$$

Thus, the average and characteristic value equations at any loaded angle for CLT is:

$$f_{\theta,avg,NDS} = \frac{l_0}{l_p} \frac{77G_0}{0.36G_0^{-0.45}d^{0.5}\sin^2\theta + \cos^2\theta} + \frac{l_{90}}{l_p} \frac{77G_0}{0.36G_0^{-0.45}d^{0.5}\cos^2\theta + \sin^2\theta}$$

$$f_{\theta,k,NDS} = \frac{l_0}{l_p} \frac{44G_0}{0.42G_0^{-0.45}d^{0.5}\sin^2\theta + \cos^2\theta} + \frac{l_{90}}{l_p} \frac{44G_0}{0.42G_0^{-0.45}d^{0.5}\cos^2\theta + \sin^2\theta}$$

When compared to the test results, the predicted average embedment strengths had a better correlation than that of the Uibel and Blass model. The characteristic embedment strengths are conservative, but less conservative than that of the Kennedy model.

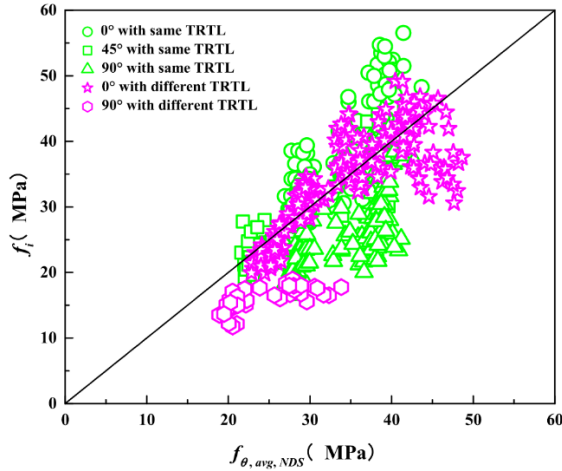


Figure F.5 – Comparisons between test values (f_i) and predicted values ($f_{\theta, avg, NDS}$)

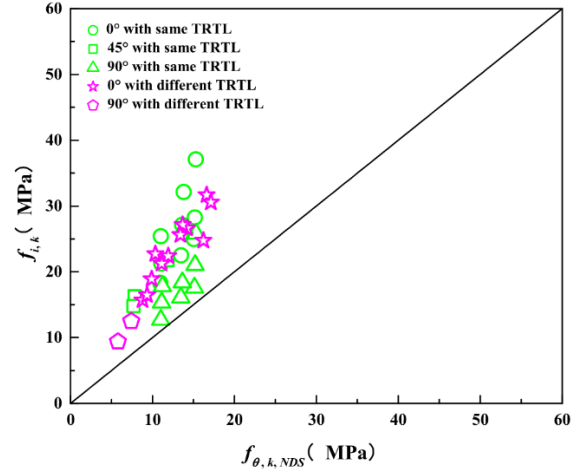


Figure F.6 – Comparison of characteristic embedment strength between test data ($f_{i,k}$) adjusted to standard load duration and predicted values ($f_{\theta, k, NDS}$)

8.5.4 F.4 Design equations in CSA O86

In the CSA O86 for Engineering design in wood, the model for the embedment strength of the parallel layer in CLT uses an adjustment factor J_x of 0.9. All other cases, J_x is equal to 1.0. The average and characteristic value equations for the embedment strength of the parallel and perpendicular to grain of the face layer:

$$f_{avg} = \begin{cases} f_{0, avg} = 82\rho_{12}(1 - 0.01d)J_x \\ f_{90, avg} = 36\rho_{12}(1 - 0.01d) \end{cases}$$

$$f_k = \begin{cases} f_{0, k} = 50G(1 - 0.01d)J_x \\ f_{90, k} = 22G(1 - 0.01d) \end{cases}$$

The average and characteristic value equations at any loading angle for CLT when calculated via the Hankinson formula are:

$$f_{\theta, avg, CSA} = \frac{0.9 \times 82\rho_{12}(1 - 0.01d)}{0.9 \times 2.27\sin^2\theta + \cos^2\theta}$$

$$f_{\theta, k, CSA} = \frac{0.9 \times 50G(1 - 0.01d)}{0.9 \times 2.27\sin^2\theta + \cos^2\theta}$$

When compared to the test results, 75% of the predicted average embedment strengths were lower than the tested values. The characteristic embedment strengths are conservative.

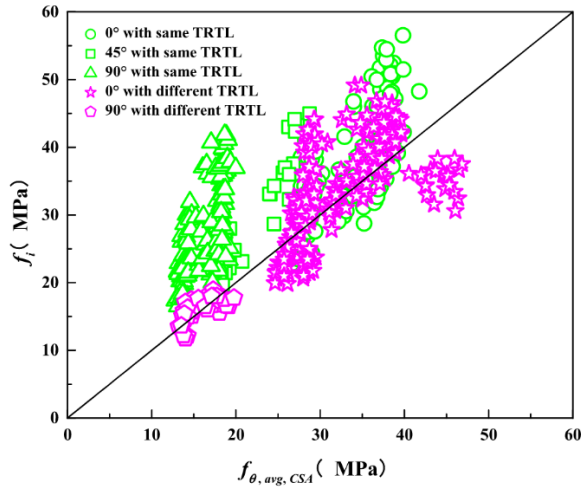


Figure F.7 – Comparisons between test values (f_i) and predicted values ($f_{\theta, avg, CSA}$)

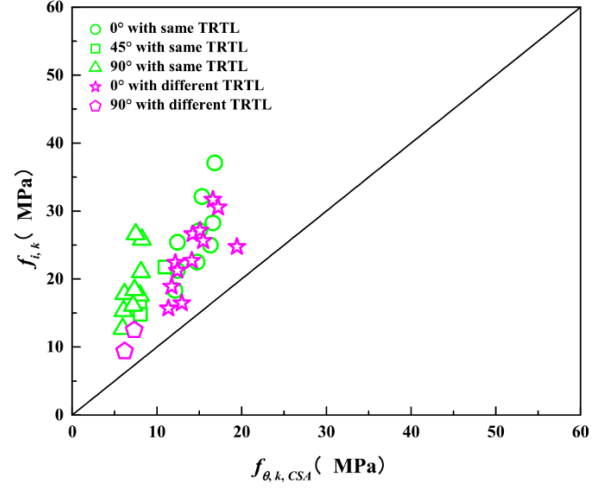


Figure F.8 – Comparison of characteristic embedment strength between test data ($f_{i, k}$) adjusted to standard load duration and predicted values ($f_{\theta, k, CSA}$)

8.5.5 F.5 Modified design equations developed by Dong et al. (2020)

Dong et al. (2020) developed a predictive equation for CLT dowel embedment strength dependent upon wood density, dowel diameter, loading angle, and the layer thickness ratio based on the tested specimen. The new modified design equations for average and characteristic values are:

$$f_{\theta, avg, Mod} = 336.4(0.45 - 0.02d)\rho_{12} \times \left(\frac{tt}{1.41\cos^2\theta + \sin^2\theta} + \frac{1 - tt}{1.41\sin^2\theta + \cos^2\theta} \right)$$

$$f_{\theta, k, Mod} = 257.5(0.45 - 0.02d)\rho_{12} \times \left(\frac{tt}{1.41\cos^2\theta + \sin^2\theta} + \frac{1 - tt}{1.41\sin^2\theta + \cos^2\theta} \right)$$

where:

tt the thickness ratio of transverse layer to the total thickness of CLT panel

When tt is 0 or 1, the equation can be used to calculate the embedment strength of glue-laminated timber parallel or perpendicular to the grain. This modified equation is most applicable for three-layer CLT, and provides relatively accurate average embedment strength and less conservative characteristic values than the reviewed models. The predicted values of the modified model versus the tested values are charted below:

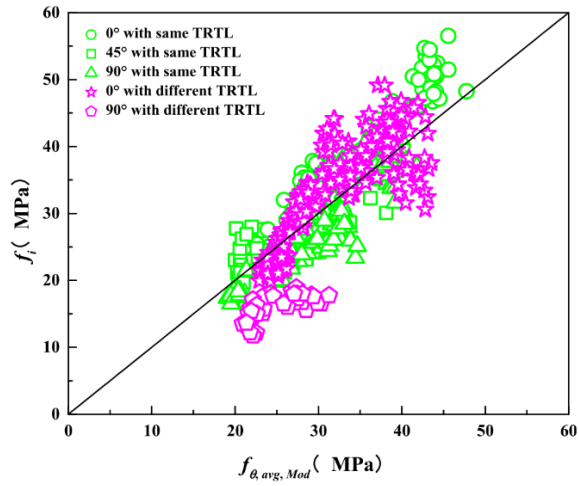


Figure F.9 – Comparisons between test values (f_i) and predicted values ($f_{\theta, avg, Mod}$)

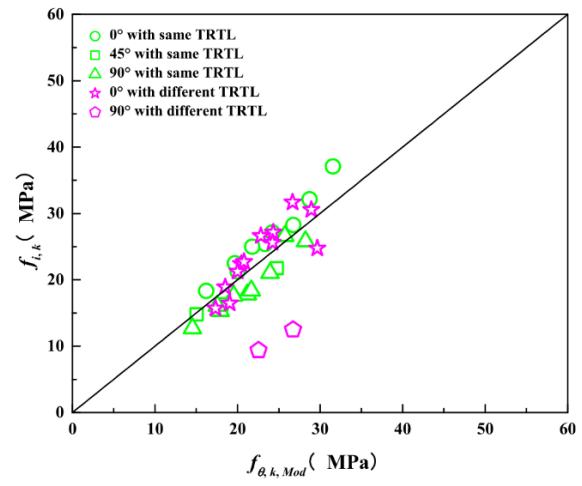


Figure F.10 – Comparison of characteristic embedment strength between test data ($f_{i,k}$) adjusted to standard load duration and predicted values ($f_{\theta, k, Mod}$)

8.6 Appendix G

Summary of determining the lateral resistance of a fastener via EN 1995

8.6.1 G.1 Determining the lateral resistance of a fastener (EN 1995-1-1 § 11.2.3)

The characteristic lateral resistance per shear plane of a single fastener ($F_{v,k}$) should be taken as:

$$F_{v,k} = F_{D,k} + F_{rp,k}$$

where:

$F_{D,k}$ the characteristic dowel-effect contribution per shear plane

$F_{rp,k}$ the characteristic rope-effect contribution

For a single shear connection (between two members) there are six failure modes for the fastener connection that must be accounted for in the calculation, the least of which is the characteristic dowel-effect contribution to the shear connection. The failure modes and their calculation equations are summarized below:

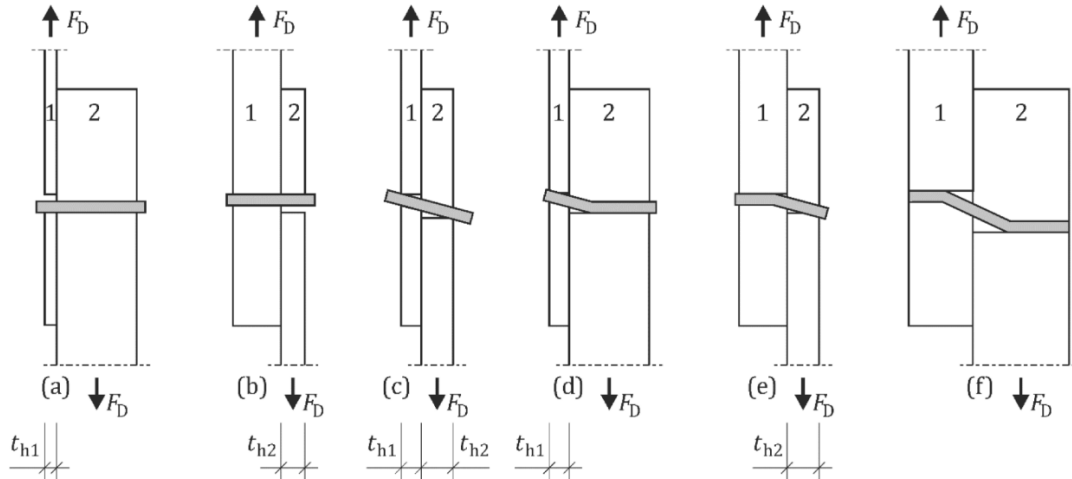


Figure G.1 – Possible failure modes (a) – (f) for a fastener loaded in single shear

$$F_{D,k} = \min \begin{aligned} & f_{h,1,k} t_{h1} d & (a) \\ & f_{h,2,k} t_{h2} d & (b) \end{aligned}$$

$$\left\{ \begin{array}{l} \frac{f_{h,1,k} t_{h1} d}{1+\beta} \left[\sqrt{\beta + 2\beta^2 \left[1 + \frac{t_{h2}}{t_{h1}} + \left(\frac{t_{h2}}{t_{h1}} \right)^2 \right] + \beta^3 \left(\frac{t_{h2}}{t_{h1}} \right)^2} - \beta \left(1 + \frac{t_{h2}}{t_{h1}} \right) \right] \quad (c) \\ 1.05 \frac{f_{h,1,k} t_{h1} d}{2+\beta} \left[\sqrt{2\beta(1+\beta) + \frac{4\beta(2+\beta)M_{y,k}}{f_{h,1,k} d t_{h1}^2}} - \beta \right] \quad (d) \\ 1.05 \frac{f_{h,2,k} t_{h2} d}{1+2\beta} \left[\sqrt{2\beta^2(1+\beta) + \frac{4\beta(2+\beta)M_{y,k}}{f_{h,2,k} d t_{h2}^2}} - \beta \right] \quad (e) \\ 1.15 \sqrt{\frac{2\beta}{1+\beta}} \sqrt{2M_{y,k} f_{h,1,k} d} \quad (f) \end{array} \right.$$

with:

$$\beta = \frac{f_{h,2,k}}{f_{h,1,k}}$$

where:

$f_{h,1,k}, f_{h,2,k}$ the characteristic embedment strengths for members 1 and 2

t_{h1}, t_{h2} the embedment depths of members 1 and 2

$M_{y,k}$ the characteristic yield moment of the fastener

d the diameter of the fastener

For predrilled steel plates:

$$f_{h,k} = k_{pl} 600$$

where:

$k_{pl} = 1.0$ for inner steel plates

$k_{pl} = 0.5$ for $d/t \leq 0.5$ for outer steel plates

$k_{pl} = 1.0$ for $d/t > 1.0$ for outer steel plates

with interpolation for intermediate ratios d/t .

For dowel-type fasteners:

$$M_{y,k} = 0.3 f_{y,k} d^{2.6}$$

with:

$d = d_1$ (equivalent tensile stress diameter) for rods with metric thread approximately $0.86d$

$d = d_1$ for screws and rods with wood screw thread with $3.5 \leq d \leq 22$ with the following ratios for outer diameter d to inner thread diameter d_1 :

d	$3.5 \leq d \leq 10$	$10 < d \leq 14$	$14 < d \leq 22$
d_1/d	0.65	0.60	0.75

where:

d diameter or side length in mm

d_1 inner thread diameter in mm

$f_{y,k}$ characteristic yield strength of the dowel in MPa

The characteristic embedment strength of CLT members has no standard calculation method per the Eurocode, but several studies have been conducted to develop such a model; these are summarized in Appendix F. There are several caveats for including the characteristic rope-effect contribution ($F_{rp,k}$) in the lateral resistance equation, and it is conservative to leave it out for dowel-type fasteners.

8.7 Appendix I

Wall Class Object Definition, Attributes and Functions

The wall class stores all relevant information about the wall for the required analyses of the computational workflow. To initiate a *Wall* object, it requires the following input variables:

Wall(*np_node_coords*, *LH_limit*, *mesh_dimension*, *wall_type_props*, *wall_type_id*)

where:

Input	Type	Description
<i>np_node_coords</i>	NumPy Array	coordinates of wall corners in a NumPy array
<i>LH_limit</i>	Number	
<i>mesh_dimension</i>	Integer	
<i>wall_type_props</i>	rhinoscriptsyntax	the <i>wall_type_props_np</i> output from the Collect Wall Types cluster
<i>wall_type_id</i>	Integer	the <i>wall_type_ids</i> corresponding to the wall

Below is a list of the class attributes and where they come from when the walls are initialized:

Attribute	Type	Description
<i>mesh_dimension</i>	Float	the <i>mesh_dimension</i> input variable
<i>corners</i>	NumPy Array	the <i>np_node_coords</i> input variable
<i>direction</i>	String	can be either 'EW' or 'NS', from a function using the <i>corners</i> attribute
<i>location</i>	Float	gives the location of the wall related to the origin in the perpendicular direction, from a function using the <i>corners</i> attribute
<i>elevation</i>	Float	gives the elevation of the top of the wall, from a function using the <i>corners</i> attribute
<i>midx</i>	Float	gives the y-coordinate (for 'NS' walls) or the x-coordinate (for 'EW' walls) of the midpoint of the bottom of the wall, from a function using the <i>corners</i> attribute
<i>grid_line</i>	Integer	the <i>location</i> of the wall, divided by 1000

L	Float	gives the length of the wall, from a function using the <i>corners</i> attribute
H	Float	gives the height of the wall, from a function using the <i>corners</i> attribute
h	Float	the average height of the mechanical connectors of the wall, 6.8% of the height (<i>H</i>)
b_CLT	Float	dimension of the panels in a multi-panel wall, using the <i>LH_limit</i>
m	Integer	number of the panels in a multi-panel wall, using the <i>LH_limit</i>
node_coords	NumPy Array	the coordinates of the nodes of the wall for the 2D Rinaldi FE model, via the <i>discretization</i> function using the <i>mesh_dimension</i> input
element_coords	NumPy Array	the nodes of each element in the wall for the 2D Rinaldi FE model, via the <i>discretization</i> function using the <i>mesh_dimension</i> input
wall_type_id	Integer	the <i>wall_type_id</i> input variable
t	Float	the thickness of the CLT wall, from the <i>wall_types_props</i> list for the specified wall type
E0	Float	the modulus of elasticity of the timber in the CLT wall, from the <i>wall_types_props</i> list for the specified wall type
Ev	Float	the vertical modulus of elasticity of the CLT wall, from the <i>wall_types_props</i> list for the specified wall type
Eh	Float	the horizontal modulus of elasticity of the CLT wall, from the <i>wall_types_props</i> list for the specified wall type
E90	Float	the modulus of elasticity of the CLT wall into the plane, from the <i>wall_types_props</i> list for the specified wall type
Gv	Float	the effective shear modulus of the CLT wall, from the <i>wall_types_props</i> list for the specified wall type
p	Float	the density of the CLT wall, from the <i>wall_types_props</i> list for the specified wall type
other_mass	Float	the total area mass of other non-structural materials of the wall, from the <i>wall_types_props</i> list for the specified wall type

mass	Float	the total wall mass, multiplying the CLT density (ρ) by thickness (t) and adding the additional mass (<i>other_mass</i>), and multiplying by the wall dimensions (L and H)
weight	Float	the wall mass divided by the gravity constant ($g = 101.97 \text{ g}/N$)
I	Float	moment of inertia of the wall for in-plane bending ($I = \frac{tL^3}{12}$)
Fy_HD	Float	the yield load of the hold-down connection, from the <i>wall_types_props</i> list for the specified wall type
k_HDup	Float	the tensile stiffness of the hold-down connection, from the <i>wall_types_props</i> list for the specified wall type
k_HDs	Float	the shear stiffness of the hold-down connection, from the <i>wall_types_props</i> list for the specified wall type
u_HDy	Float	the yield displacement of the hold-down connection, from the <i>wall_types_props</i> list for the specified wall type
n_HD	Integer	the number of hold-downs for the wall, from the <i>wall_types_props</i> list for the specified wall type
k_ABup	Float	the tensile stiffness of the angle bracket connection, from the <i>wall_types_props</i> list for the specified wall type
k_ABs	Float	the shear stiffness of the angle bracket connection, from the <i>wall_types_props</i> list for the specified wall type
n_AB	Integer	the number of angle brackets for the wall, from the <i>wall_types_props</i> list for the specified wall type
xi	Float (list)	the location of the angle brackets along the length of the wall, via the <i>_get_xis</i> function
Fy_SC	Float	the yield load of the fastener for the connection between panels of multi-panel walls, from the <i>wall_types_props</i> list for the specified wall type
k_SC	Float	the stiffness of the fastener for the connection between panels of multi-panel walls, from the <i>wall_types_props</i> list for the specified wall type
sp_SC	Float	the spacing between fasteners for the connection between panels of multi-panel walls, from the <i>wall_types_props</i> list for the specified wall type

n_SC	Integer	the number of fasteners for the connection between panels of multi-panel walls, calculated from the spacing (sp_SC) and the wall height (H)
floor	Integer	the floor level the wall is supporting, determined once all wall objects are initialized
trib_width	Float	the tributary width of floor supported by the wall, determined once all wall objects are initialized
n	Integer	the location of the wall along its gridline in relation to other walls on the same gridline, determined once all wall objects are initialized
name	String	the name of the wall, determined once all wall objects are initialized

Properties updated in *Full Structure Definition* cluster:

Attribute	Type	Description
floor_Eh		
floor_E90		
floor_Ev		
floor_Gv		
floor_t		
w		
E_strip		
G_strip		
stiffness		

Properties updated after the Static Linear Analysis is performed:

Attribute	Type	Description
s		
displacement		

force

node_forces

node_disps

HD_force

AB_force

SC_force

behavior
